SEISMIC RESPONSE SPECTRA – REFINEMENT

WA-RD 333.1

Final Technical Report
December 1994

Washington State
Department of Transportation

Washington State Transportation Commission
Planning and Programming Service Center
in cooperation with the U.S. Department of Transportation
Federal Highway Administration

TECHNICAL REPORT STANDARD TITLE PAGE

1. REPORT NO.	2. GOVERNMENT ACCESSION NO.	3. RECIPIENT'S CATALOG NO.
WA-RD 333.1		

4. TITLE AND SUBTITLE	5. REPORT DATE
Seismic Response Spectra - Refinement	December 1994
	6. PERFORMING ORGANIZATION CODE
7. AUTHOR(S)	8. PERFORMING ORGANIZATION REPORT NO.
Carlton L. Ho and Khaled M. Shawish	
9. PERFORMING ORGANIZATION NAME AND ADDRESS	10. WORK UNIT NO.
Washington State Transportation Center (TRAC) Civil and Environmental Engineering; Sloan Hall, Room 101 Washington State University Pullman, Washington 99164	11. CONTRACT OR GRANT NO. T9234-04
12. SPONSORING AGENCY NAME AND ADDRESS	13. TYPE OF REPORT AND PERIOD COVERED
Washington State Department of Transportation Transportation Building, MS 7370 Olympia, Washington 98504-7370	Final Report, 8/91-12/94
	14. SPONSORING AGENCY CODE

15. SUPPLEMENTARY NOTES

This study was conducted in cooperation with the U.S. Department of Transportation, Federal Highway Administration.

16. ABSTRACT

Design response spectra were developed for the Washington State Department of Transportation (WSDOT) for nine soil groups representative of deposits that can be found in Washington State. These response spectra differ from the spectra developed for and adopted by the Applied Technology Council (ATC). Unlike the ATC spectra, the WSDOT spectra are based on the subduction zone setting that dominates Pacific Northwest seismicity. Both sets of spectra are based on numerical studies using SHAKE. The new response spectra were developed using new dynamic moduli curves for cohesive soils which have been accepted as more representative of the properties of the soils in the region. SHAKE tends to attenuate high frequencies. SHAKE based analysis compared well with analysis based on a nonlinear finite element code. The basis of most recent ATC attenuation maps is outlined, and found to be based on similar assumptions and methodology as the original ATC attenuation maps and not compatible with Washington State seismicity.

17. KEY WORDS	18. DISTRIBUTION STATEMENT
Response spectra, earthquake, seismic, subduction zone, attenuation	No restrictions. This document is available to the public through the National Technical Information Service, Springfield, VA 22616

19. SECURITY CLASSIF. (of this report)	20. SECURITY CLASSIF. (of this page)	21. NO. OF PAGES	22. PRICE
None	None	137	

Final Technical Report

Research Project TR-9234, Task 04
Update Seismic Response Spectra for Washington State Earthquakes

UPDATE SEISMIC RESPONSE SPECTRA FOR WASHINGTON STATE EARTHQUAKES

by

Carlton L. Ho
Associate Professor of Civil and Environmental Engineering
Washington State University

Khaled Shawish
Graduate Research Assistant
Washington State University

Washington State Transportation Center (TRAC)
Civil and Environmental Engineering; Sloan Hall, Room 101
Washington State University
Pullman, Washington 99164

Washington State Depratment of Transportation
Technical Monitors

M. Lwin
Bridge and Structures Engineer

A. Walley
Bridge and Structures Engineer

Prepared for

Washington State Transportation Commission
Department of Transportation
and in cooperation with
U.S. Department of Transportation
Federal Highway Administration

December 1994

DISCLAIMER

The contents of this report reflect the views of the authors, who are responsible for the facts and the accuracy of the data presented herein. The contents do not necessarily reflect the official views or policies of the Washington State Department of Transportation or the Federal Highway Administration. This report does not constitute standard specification or regulation.

TABLE OF CONTENTS

LIST OF TABLES

LIST OF FIGURES

UPDATE SEISMIC RESPONSE SPECTRA FOR WASHINGTON STATE EARTHQUAKES

SUMMARY

The Washington State Department of Transportation (WSDOT) used, until recently, seismic design guidelines of highway bridges originally developed by the Applied Technology Council (ATC) for the general use in the United States and based on research done on California earthquakes which are different in nature from the earthquakes usually occurring in Washington State. Design response spectra for Washington State were recently developed for nine typical soil groups representative of statewide locations. The spectra are based on a Magnitude 7.5 design earthquake. The computer code SHAKE and soil modulus and damping curves developed in the 1970's were used to produce the spectra.

Recently, new dynamic moduli curves for cohesive soils were reported [1]. These curves have been accepted as more representative of the properties of the soils in the region. Also, the computer code SHAKE attenuates high frequency components producing low frequency biases in the response spectra.

A significant problem in the previous study was the lack of rock records for subduction zone events. One such record has been identified for a magnitude M 5.5 event. The objective of this study is to develop new design response spectra for the same nine soil groups used in the previous study and representative of a design earthquake of the Puget Sound region. A check on SHAKE results is provided by examining the

response of several soil profiles to actual rock record and by using a nonlinear finite element code in the analysis. Finally, the background of developing the 1991 AASHTO maps of severity coefficient and the map currently used by WSDOT is discussed in a separate section.

CONCLUSIONS AND RECOMMENDATIONS

Soil amplification factors for 123 actual sites in Washington State were developed in this study. These new curves along with the base spectrum chosen are believed to be more representative of the earthquakes and soils of Washington State.

Washington State Earthquakes are unique and different in nature from the California earthquakes upon which most of the research in the field of seismicity is based. Also, soils in Washington State are very diverse. This fact justifies the use of nine soil groups rather than the three soil categories used in the AASHTO guidelines.

Newer data about the shear modulus reduction relationships for cohesive soil were used in the analysis. This was justified by the results of the sensitivity studies which showed that the shear modulus is the most dominant factor in the modeling parameters for response analysis.

Non-linear time domain modeling of the problem was compared with the linear frequency domain modeling. The response spectra produced by the two models were close. The only discrepancy was in the high frequency response for two of the sites. This discrepancy can be attributable to a characteristic of modeling method.

Improving the results for future research would require more accurate information about the soil properties in the profiles used and a precise determination of the depths of the profiles. This would involve performing laboratory tests and taking downhole velocity measurements.

Washington State contains large proportions of silty soils. Because of the

difficulties in sampling and testing these soils, little field or laboratory investigation of the dynamic properties of silt has been done. An investigation into the dynamic properties of silt and a method of defining its properties by simple field tests would be valuable.

The analysis in this study dealt only with soils and ignored any effects the structure would have on underlying soil layers. To get a better idea of the effect of the earthquake on a structure, soil foundation interaction should be considered. WSDOT is sompleting conducting this study soil-structure interaction problem.

INTRODUCTION

The Puget Sound region of western Washington State is one of the most seismically active areas in the United States. This region has experienced major earthquakes in the recent history including the 1949 magnitude 7.1 Olympia earthquake and the 1965 magnitude 6.5 Seattle earthquake. These events, along with many other smaller events, have caused severe structural damage in the area [2,3]. The high seismicity of the region requires that seismic forces be considered when designing highway bridges [4]. Figure 1 shows the principal earthquakes that affected Puget Sound in recent history [5].

STATEMENT PROBLEM

In the past, the Washington State Department of Transportation (WSDOT) used seismic design guidelines for highway bridges originally developed by the Applied Technology Council (ATC) for general use in the United States. These spectra are based on research done on California earthquakes which are different in nature from the earthquakes usually occurring in Washington State [4]. These guidelines were updated by Kornher [6] for the use in Washington State.

In an attempt to develop design response spectra for Washington State bridges that reflects the unique seismicity and geology of the region, Kornher [6] developed design response spectra for nine typical soil groups (columns) representative of statewide locations. The spectra were based on M 7.5 design earthquake using the computer code

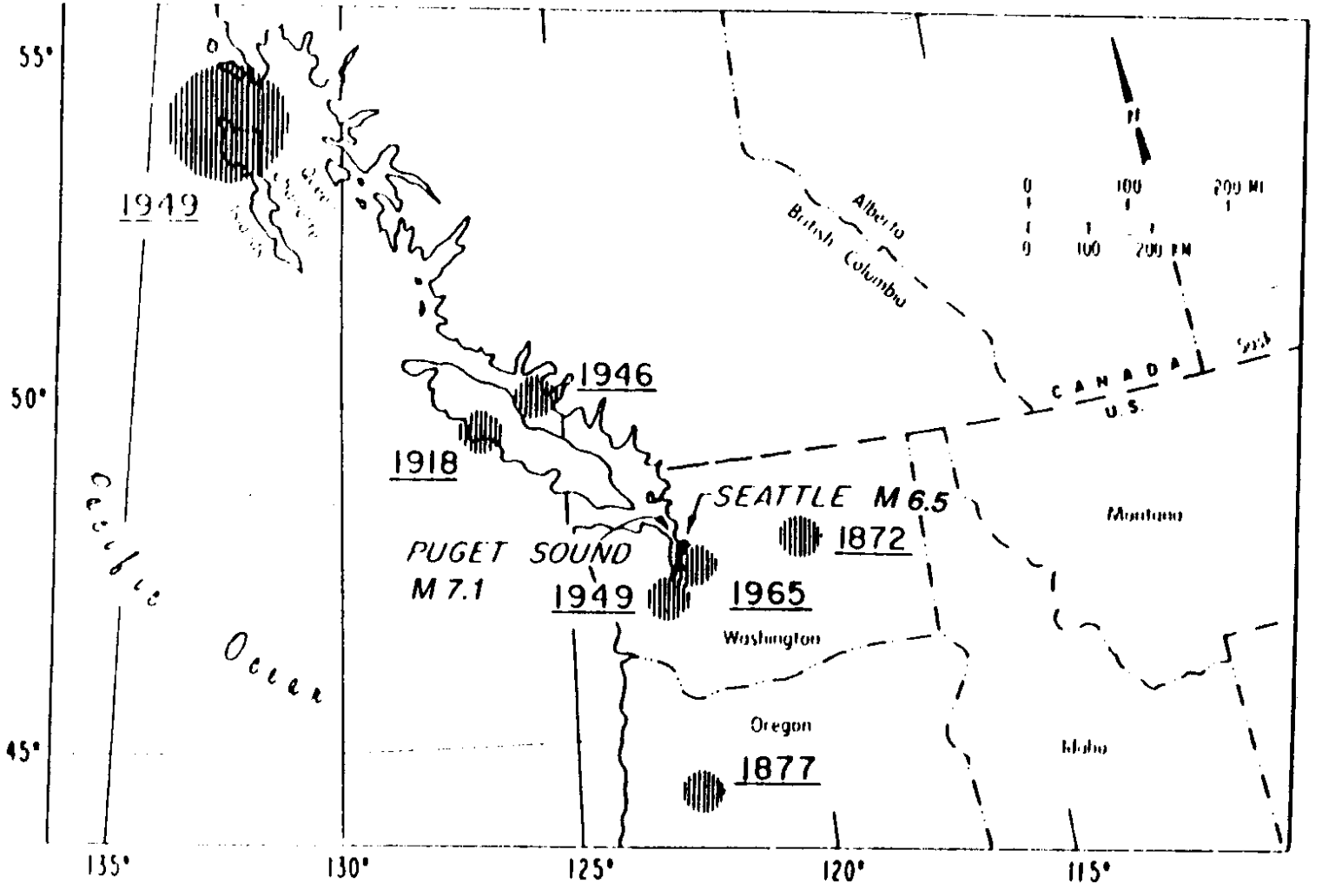

FIGURE 1. Principal earthquakes that affected Puget Sound in recent history [1].

SHAKE [7] (a computer program for linear earthquake response analysis for horizontally layered sites), and soil modulus and damping curves developed in the 1970's. The soil parameters were correlated to Standard Penetration Test data (SPT) from 123 actual boring logs from all around Washington State.

Recently, new dynamic moduli curves for cohesive soils were developed [1]. These curves have been accepted as more representative for the soil in the region. Also the computer code SHAKE, a frequency domain program, tends to attenuate high frequency components producing low frequency biases in the response spectra. New computer codes have been developed to work on the time domain; DYNA1D [8], a computer program for nonlinear seismic site response analysis, is used in this study to verify the results obtained by SHAKE.

A significant problem in developing response spectra in Kornher's study was the lack of earthquake records at rock sites for subduction zone events. One such record was identified for a magnitude M 5.0 to M 5.5 event. Strong motion accelerations resulting from the Pender Island, British Colombia earthquake of May 1976 were recorded at the Lake Cowichan telecommunications station [9]. There are also several strong motion records for smaller earthquakes than the M 7.5 design earthquake. The unique data from these records can be used to evaluate the deconvolution technique to synthesize base accelerograms.

The objective of this study is to develop new responses for the same nine soil groups used in the previous study, representative of a design earthquake of M 7.5 for the Puget Sound region. The new dynamic moduli for cohesive soils is used. A Check on

the SHAKE results is provided by the use of DYNA1D code.

ORGANIZATION OF THE REPORT

This report is divided into five main sections. The INTRODUCTION contains material about the problem statement and the research objectives and approach. The second section contains BACKGROUND material about the earthquake phenomenon, and the geology and seismicity of the Puget Sound. The third section contains details about the MODEL AND ANALYSIS and includes description of the programs SHAKE and DYNA1D. Soil modeling for both codes and the associated input parameters are also included in this section. The fourth section contains the FINDINGS AND INTERPRETATIONS. Soil amplification spectra for nine soil groups are presented in this section along with the base spectrum. Results of sensitivity study are presented in this section. Comparisons between the results of the linear analysis and the non-linear analysis are also presented along with comparisons with the current codes. The fifth section presents a comparison between the MAPS OF SEVERITY COEFFICIENT found in the AASHTO and WSDOT seismic design guidelines. Appendix A presents soil profiles used in the analysis and Appendix B contains curve ordinates developed in this study.

RESEARCH APPROACH

This research uses procedures followed by Gates [10] in developing soil amplification factors for California Department of Transportation (CalTrans). First, the

peak rock acceleration is determined from the seismologist's studies of fault activity and attenuation data as gathered from past events. In developing the seismogenic zones of the Pacific Northwest, Perkins et al. [11] used an approach relying on two different methods: the first method depends predominantly on historic seismic activity to develop a zoning rationale; the second method addresses the ongoing problem from a geological point of view. The use of geological evidence can identify currently seismic areas as areas of potential activity if they lie along or within structural trends that have historic seismicity. Figure 2 shows a map of acceleration on rock with a 90% probability of not being exceeded in 50 years developed by Perkins et al. (1980) [11].

The base spectrum developed in the previous study [6] was adopted for this study. Kornher selected a base spectrum based on anticipated ground shaking from the subduction zone earthquakes expected in Washington State. Various methods of finding an appropriate base motion were investigated. The Seed et al. stiff curve [12] was selected in Kornher's study to be appropriate as a target response spectrum in generating input motion for SHAKE. Figure 3 shows the base spectrum used in this study with the AASHTO base spectrum for comparison.

The soil amplification factors of the nine soil groups are developed using the computer codes SHAKE and DYNA1D [7,8]. SHAKE and DYNA1D were used to obtain the five percent damped acceleration response of the ground surface for the nine soil groups. Soil amplification spectra are then obtained by dividing surface response by the response of the time history at a rock outcropping. Figure 4 schematically shows how the soil amplification factors were developed. The input model for SHAKE includes

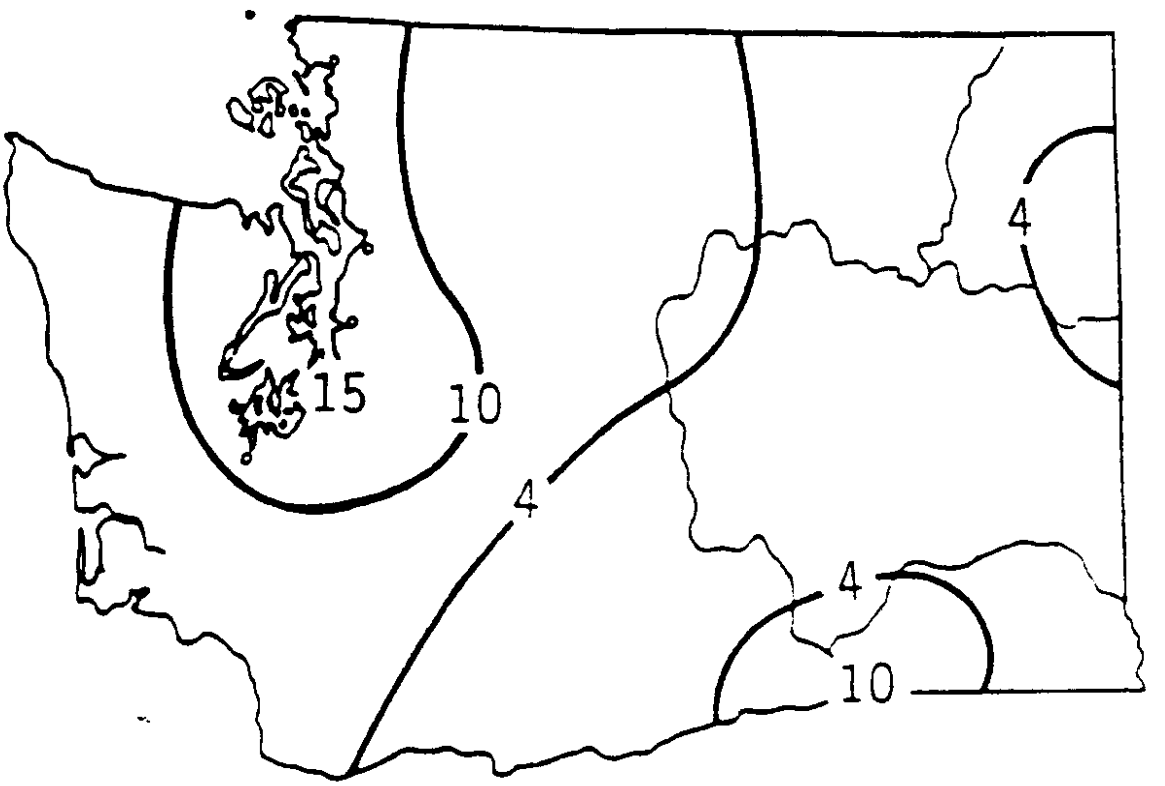

FIGURE 2. Acceleration on rock with 90% probability of not being exceeded in 50 years developed by Perkins et al. in 1980 [6].

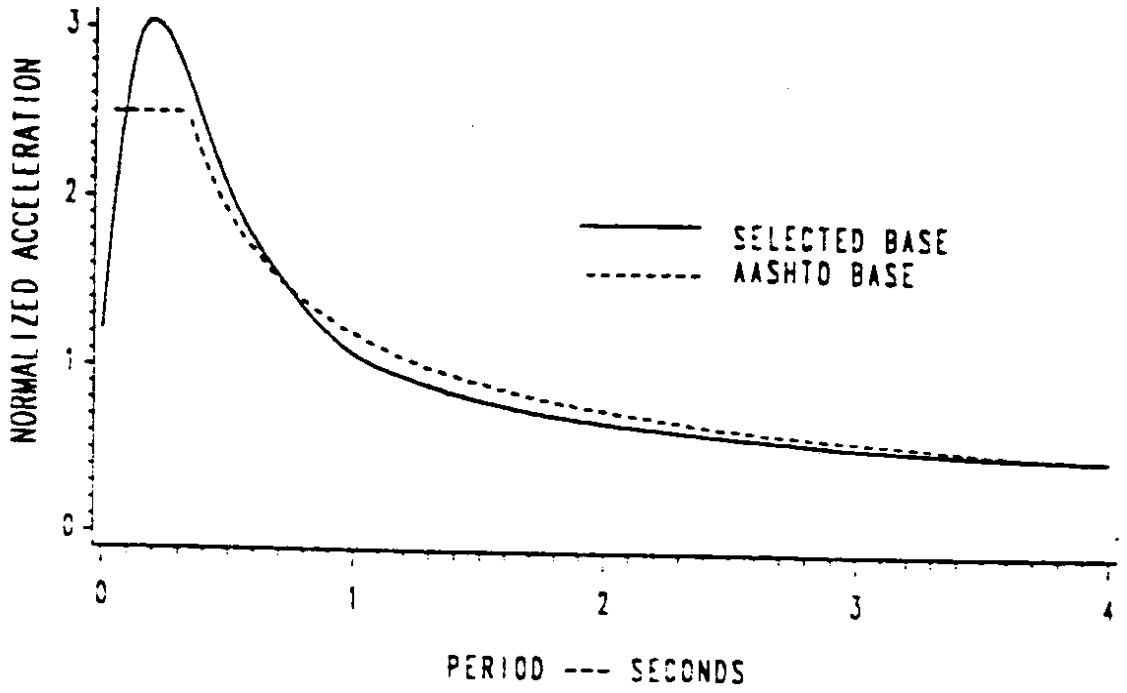

FIGURE 3. Base spectrum used in this study and the AASHTO type I curve [6].

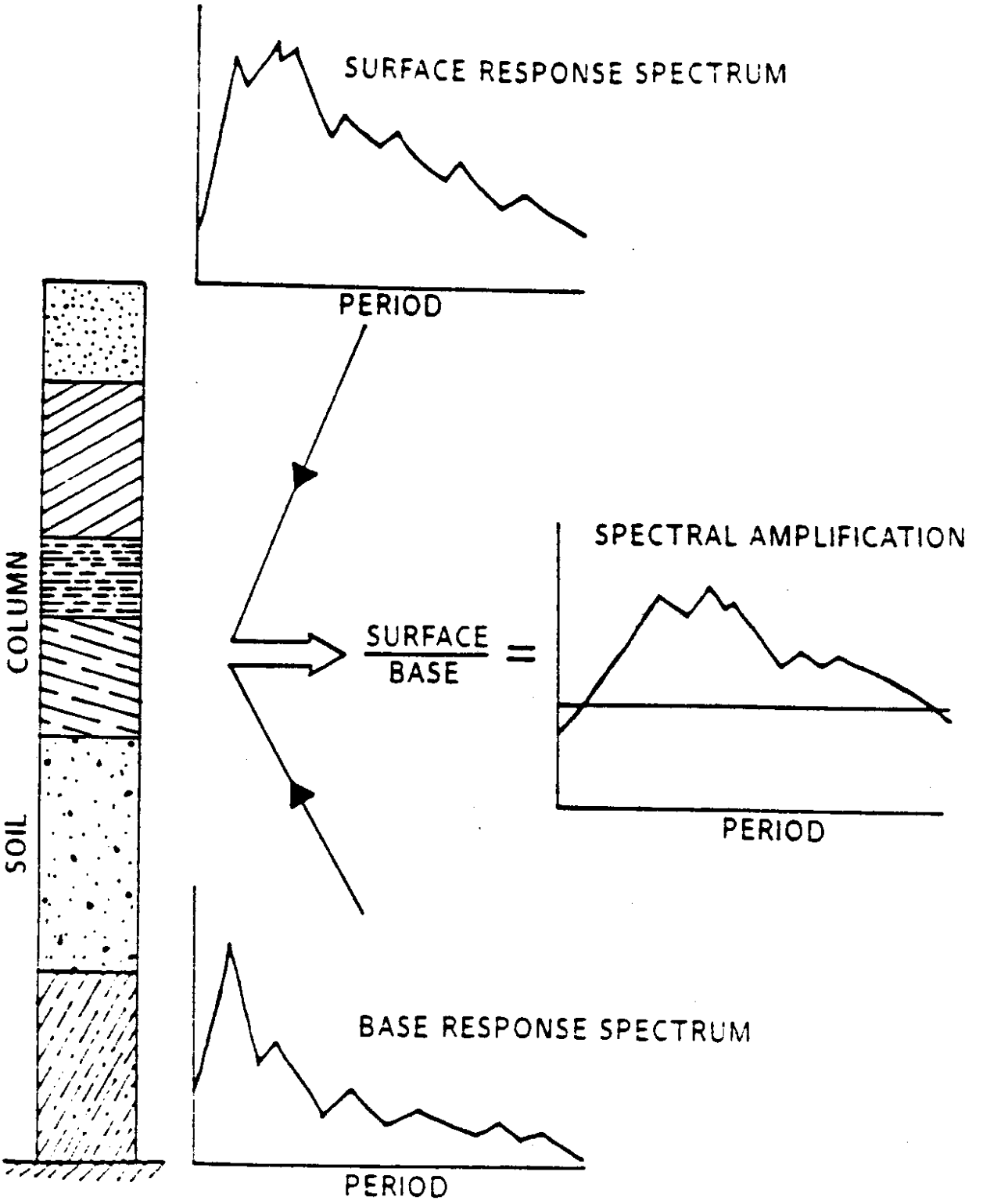

FIGURE 4. Development of soil amplification factors [6].

description of the soil profile in terms of depths of different layers, type of soil, properties of each layer, strain dependent damping and moduli curves of soils, and an acceleration time history at the base of the profile. The input model for DYNA1D includes finite element modeling of soil layers in the profile, degrees of freedom on nodes, soil properties, and an acceleration time history at the base of the profile. The same nine soil groups used in the previous study are used in this study. The use of the program DYNA1D provides a good check on the results obtained by SHAKE.

BACKGROUND

Earthquake induced ground vibrations resulted in several incidents of structural damage in the past. Earthquakes are believed to originate from the rupture of faults at varying depths within the earth [13]. When lithospheric rocks that have been subjected to deformational stress fail suddenly, they rebound rapidly toward their unstressed positions, generating shock waves at the site of the break (called the focus or hypocenter) [14]. Shock waves propagate outward from the focus through the body of the earth and along its surface. The nature of ground vibration resulting from an earthquake results from the upward transmission of the stress waves from rock to the softer soil layers. Figure 5 shows some earthquake related terms.

Magnitude is a measure of the size of an earthquake, based on the amplitude of elastic waves it generates. The magnitude scale presently in use was first developed by Richter and modified by others [13]. Richter's earthquake magnitude is represented by the equation:

$$Log_{10} E = 11.4 + 1.5 M \qquad (1)$$

where E is the energy released in ergs and M is the magnitude (Figure 6). From the above equation it can be seen that the increase in the magnitude, M, by one unit will generally correspond to about 30-fold increase in the energy released, E, by the earthquake.

Gutenberg and Richter [15] estimated the predominant periods of accelerations developed in rock for California earthquakes. Using results given by Gutenberg and

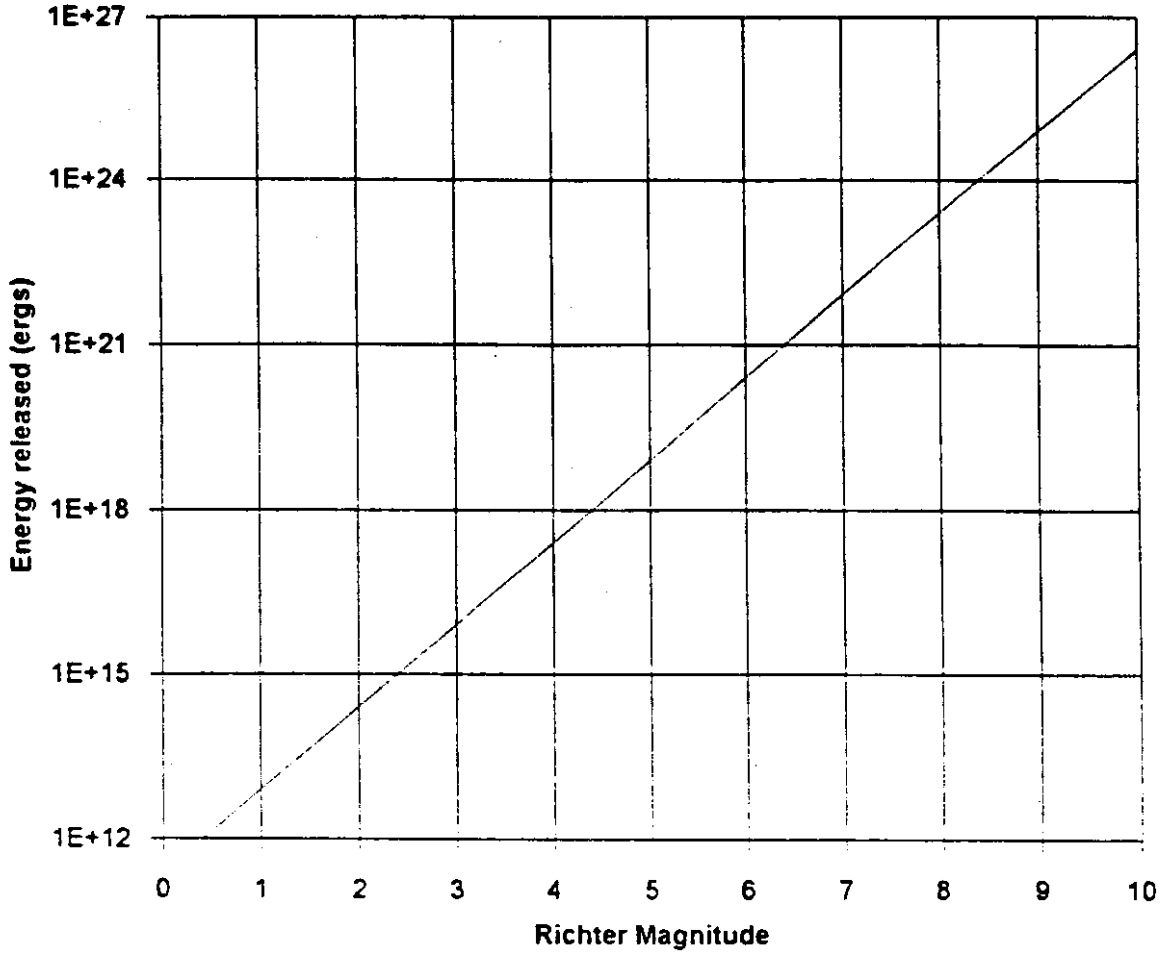

FIGURE 5. Energy as a function of Richter magnitude.

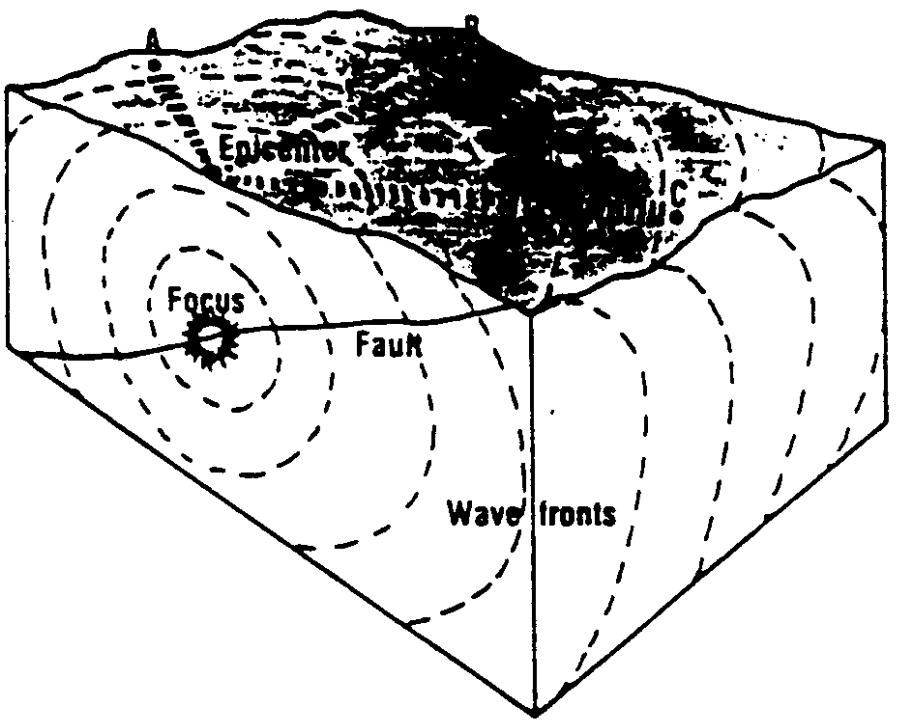

FIGURE 6. Some of seismicity related concepts [14].

Richter, Seed et al. [16] developed a chart for the average predominant periods of accelerations for various earthquakes as a function of the distance from the causative fault. This chart is shown in Figure 7 Seed et al. [16] also developed attenuation relationships for values of maximum acceleration as functions of earthquake magnitude and distance from the causative fault. These relationships are shown in Figure 8. Attenuation relationships have also been developed by others. Most of these relationships are based upon data collected from California earthquakes.

Earthquake-induced ground motion is a function of the source mechanics and the dynamic characteristics of the propagation media. The local geological and topographical conditions strongly affect the temporal and spatial behavior of the ground motion. Although it is accepted that ground motion reflects the geodynamic characteristics of the underlying soil layers, the significance of this influence has been a controversial issue in earthquake engineering and strong ground motion seismology [17]. Theoretical calculations of the influence of the local soil conditions have been successfully correlated with strong ground motion or other macroseismic data from many locations where the local subsoils are soft (e.g., Mexico City, Caracas, San Francisco and several locations in Japan including Tokyo). However, it has also been shown that ,except for data recorded on deep and soft soil deposits, the peaks of ground motion spectra do not show any correlation with the ground characteristics.

Seismic forces tend to dissipate or attenuate as they radiate outward from the causative fault; the peak ground acceleration varies as a function of the magnitude of the earthquake and the distance from the causative fault [14]. The peak ground acceleration

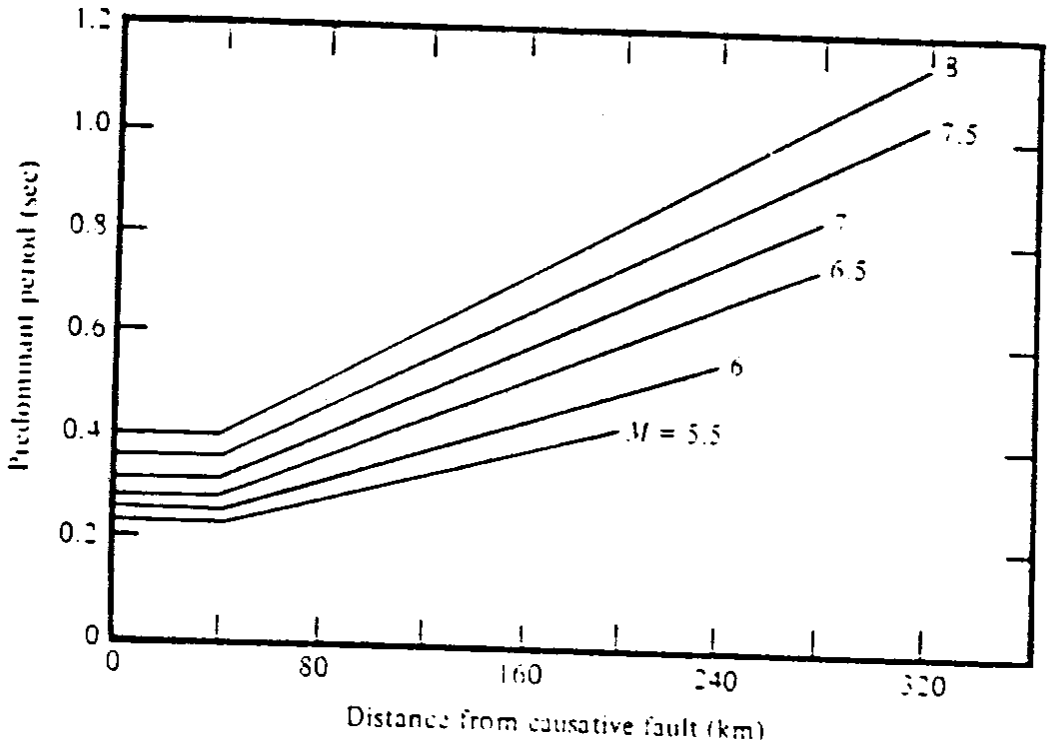

FIGURE 7. Average predominant periods of acccelerations for various earthquakes as a function of the distance from the causative fault developed by Seed et al. [13].

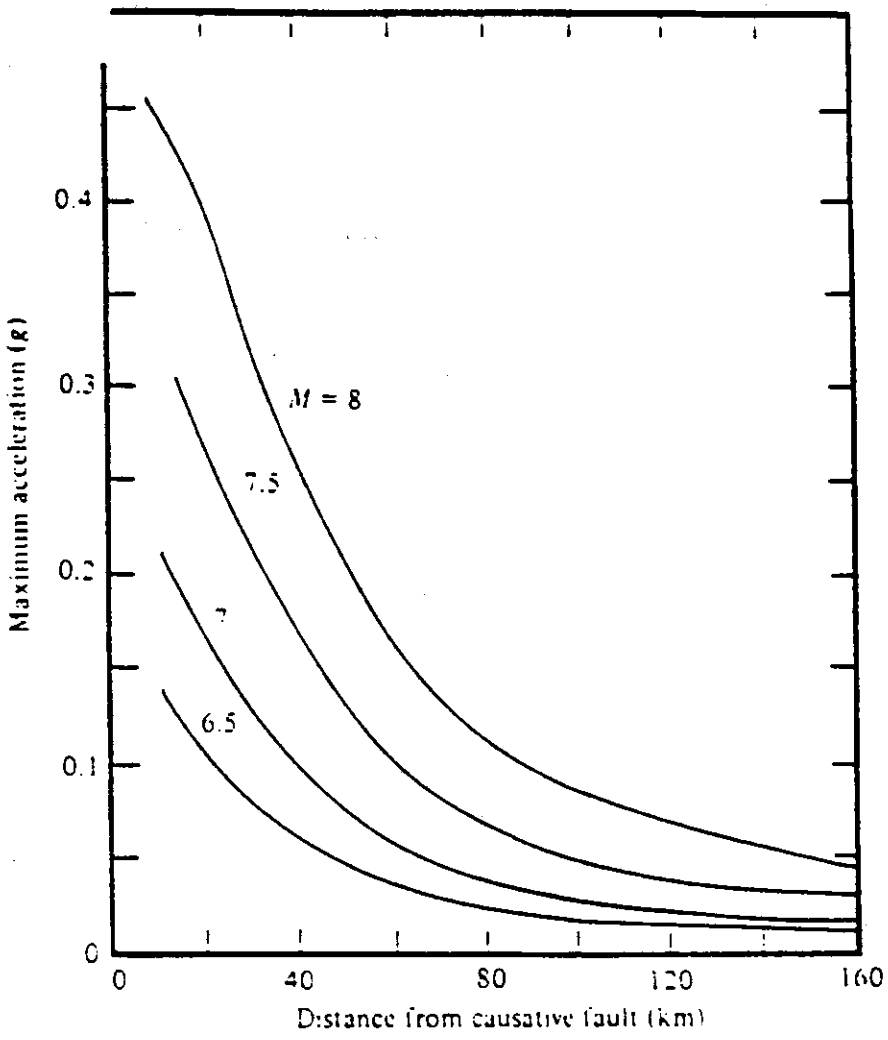

FIGURE 8. Maximum acceleration as a function of magnitudes of earthquakes and distances from causative faults developed by Seed et al. [13].

alone does not completely define the rock accelerations at a site. The dynamic response of a system of simple single degree-of-freedom pendulums (response spectrum) is usually used to indicate the frequency content of a seismic event. The shape of the response spectrum in rock is primarily controlled by the predominant period of spectra, which is the period of maximum spectral response.

In 1978 Paiwardan et al. [18] used ground motion data recorded during a number of earthquakes to develop attenuation relationships for peak acceleration, peak velocity and spectral ordinates at several periods for two categories of earthquakes: shallow-focus earthquakes, such as California earthquakes and those that occurred in parts of Japan; and subduction zone earthquakes such as those that occured offshore of Japan, South America, and the Puget Sound. Typically shallow-focus earthquakes occurred at depths less than 15 km. Records obtained during earthquakes which occurred in subduction zones typically occurred at depths greater than 25 km.

Another study by Idriss [19] showed that the peak acceleration and spectral ordinates at short periods (less than 0.4 or 0.5 seconds) can be significantly higher for the subduction zone earthquakes than for the shallow-focus earthquakes. At longer periods (longer than 1.5 or 2 seconds), the spectral ordinates for the shallow-focus earthquakes can be significantly higher than those for the subduction zone earthquakes. These trends can be partially attributed to the fact that for deeper earthquakes, the dynamic stress drop must be greater than for shallower earthquakes. A higher dynamic stress drop results in higher peak acceleration. This illustrates the importance of recognizing whether a certain

event falls in the shallow-focus category or the subduction zone category.

One of the most important factors in specifying earthquake ground motion is knowledge of seismic wave attenuation from the source in various geographic regions. One of the procedures followed for defining the seismic attenuation functions of an area is the use of observed strong ground motion acceleration-attenuation curves [20]. Such a family of acceleration attenuation curves applicable for sites in the western United States were developed by Schnabel and Seed in 1973. Each site is assumed to be located on rock material having a shear wave velocity of at least 760 m/s at low strain levels. These curves are somewhat controversial in terms of whether or not they underestimate the peak ground acceleration inside 20 km range. In spite of this they are still used at the present time in many applications.

In regional hazard analysis, zones of some severity coefficient, such as peak ground acceleration or intensity, are usually mapped [6]. The severity coefficient is used to scale a base response spectrum to represent the various strengths of earthquakes expected to occur. Seismic source zones are defined based on the best available information regarding the seismicity of the region, relation of the seismicity to geology and tectonics, the physical and temporal characteristics of earthquake source zones, ground motion attenuation, and influence of local site conditions [21].

The first national earthquake zonation map was published in 1948. It divided the United States into zones numbered 0 to 3, where 3 indicates the greatest damage potential. In 1976, Algermissen and Perkins [22] published a national seismic zonation map which presented peak acceleration values with 90 percent probability of nonexceedance in a 50

year period. The previous maps were based on a maximum intensity scale.

In 1978, the Applied Technology Council (ATC) produced two new ground shaking maps. These maps are based largely on the map developed by Algermissen and Perkins. Two separate ground motion parameters; Effective Peak Acceleration (EPA) and Effective Peak Velocity (EPV), were defined based on spectral acceleration and on spectral velocity rather than actual peak accelerations and velocities [23]. The Algermissen and Perkins approach was used in the AASHTO specifications for seismic design of highway bridges to produce contour maps for an acceleration coefficient which shows the relative severity of ground shaking. The acceleration coefficient is a response spectrum scaling factor for different ground shaking conditions [4,6]. Figure 9 shows AASHTO's map of acceleration coefficient.

In 1976, Gates [10] developed seismic design guidelines for the California Department of Transportation (CalTrans). These guidelines used base spectra developed by studies on California earthquakes and with peak ground acceleration as a severity coefficient. A maximum elastic spectrum (5% damped) on rock can be obtained by multiplying the maximum expected bedrock acceleration by the ordinate of the normalized rock spectrum curve. Soil amplification factors were developed based on computer studies (SHAKE) and by actual recorded data. The design guidelines currently used in the AASHTO codes are based on Gates' procedures.

GEOLOGY OF PUGET SOUND

The Puget Sound region of western Washington State lies in a north-trending

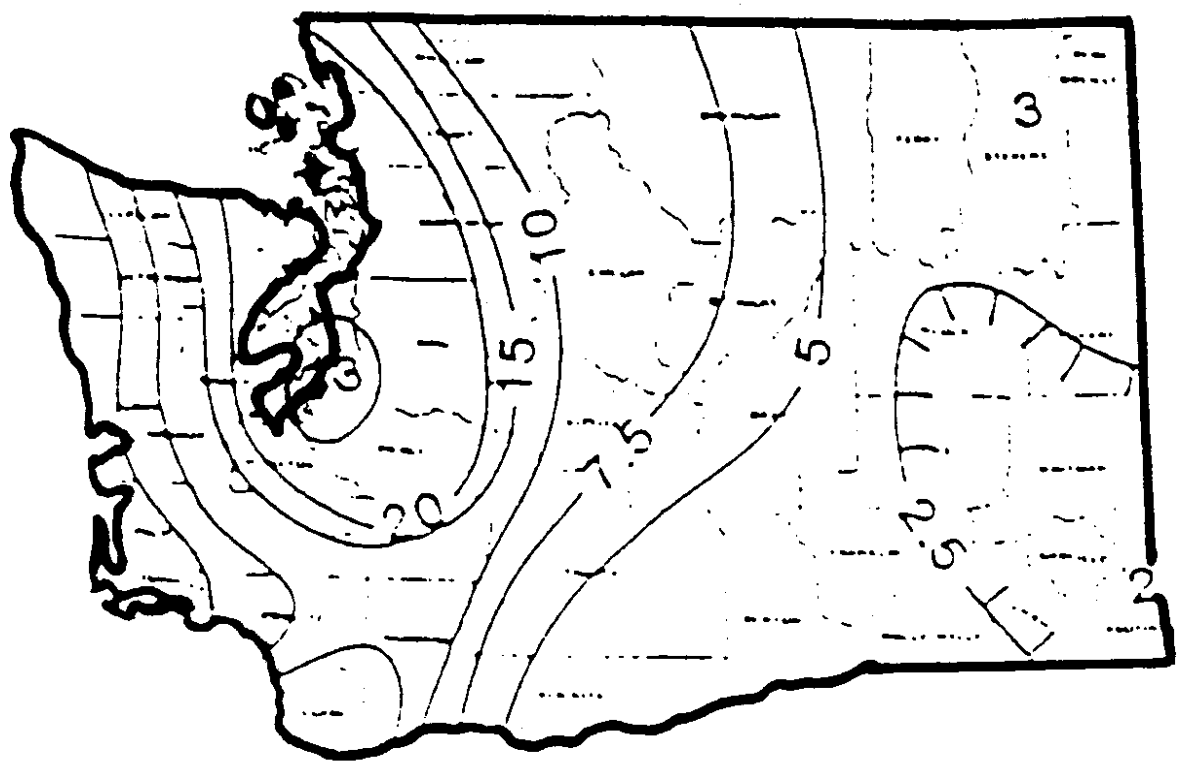

FIGURE 9. AASHTO's map of acceleration coefficient [6].

structural and topographic through between the Olympic Mountains on the west and the Cascade Range on the east. Geological structure in the basin is poorly characterized because of thick accumulations of glacial deposits which mask the underlying bedrock structure [24].

Development of the crustal structure of western North America began more than 300 million years ago, but the structural identity of the Puget Lowland was established only as recently as 20 to 40 million years ago [14]. Once the large-scale structure of the Puget Lowland was established, the detailed, small-scale surface topography was shaped. This was accomplished primarily by surfacial processes. The most prominent process was glaciation during the ice age of only a few tens of thousands of years ago.

About 350 million years ago there was a reorganization of the existing boundary on the oceanic plate somewhere west of the American Continent. This was the earliest decipherable event in the structural evolution of the western edge of the Americas, including the Puget Sound. This event marked the first addition of new crustal material against the western margin of the continent and represented the beginning of convergent plate boundary processes that have continued to this day. Figure 10 is a schematic diagram of the evolution of the western North American boundary. The several advances and retreats of glaciers have reshaped the Puget Sound [21]. The current shape of the Puget Sound is the result of scour during the glacial advancement from the north and deposition of glacial sediments during subsequent recession periods. Because of repeated glaciation, most of the sediments are highly overconsolidated. Recent studies have estimated the sediment thickness as high as 1.3 km. Figure 11 shows the glacial

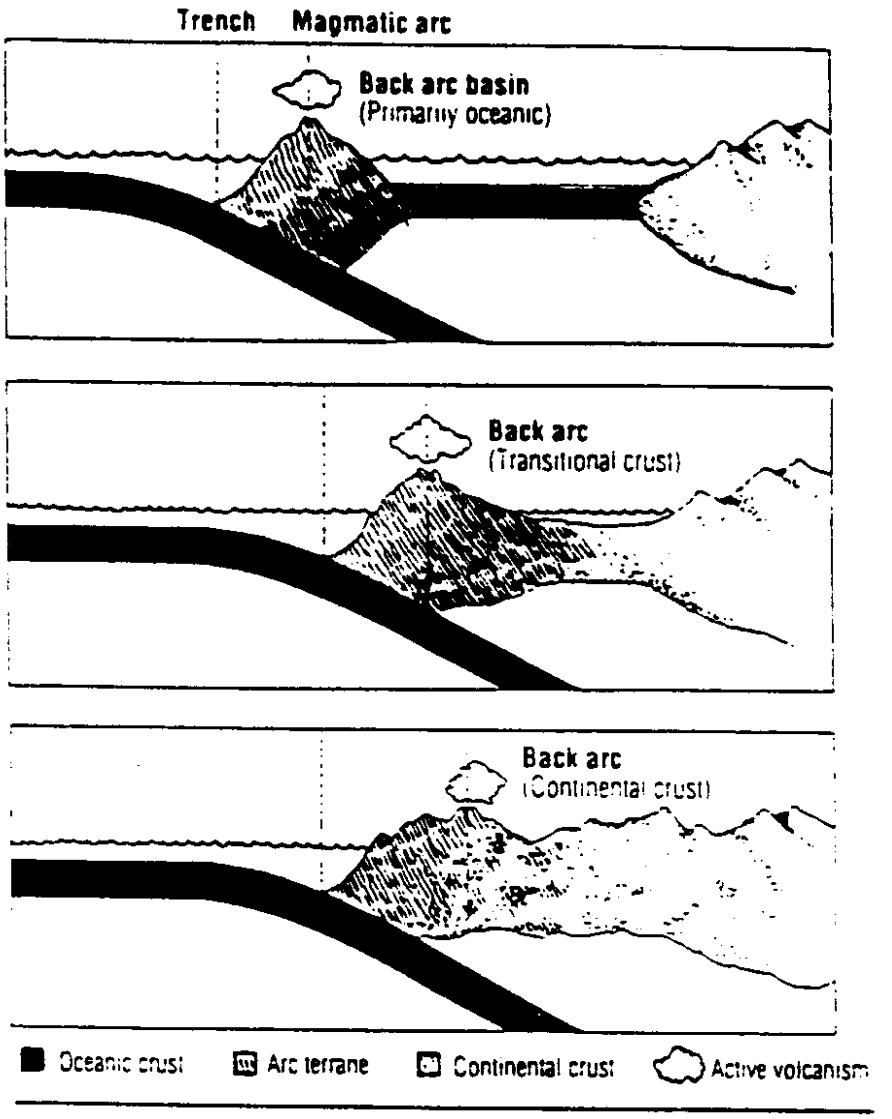

FIGURE 10. Evolution of the western North American boundary [14].

FIGURE 11. Glacial advancement that affected the Puget Sound [14].

advancement that affected the Puget Sound.

The underlying bedrock geology is thought to consist of Paleozoic and Mesozoic sedimentary and pre-Devonian crystalline rocks in the northern parts with Tertiary continental and marine sedimentary and volcanic rocks to the south.

SEISMICITY OF PUGET SOUND

Historically the Puget Sound basin is the most seismically active area of Washington State. Two destructive earthquakes occurred there within the last forty years: the April 13, 1949 event,with a magnitude of 7.1 and epicenter near Olympia, and the April 29, 1965 event, with a magnitude of 6.5 and centered near Seattle [24]. The primary cause of the seismicity of the entire western United States, including the Puget Sound, is the motion differential between the North American and the Pacific plates [5]. Figure 12 schematically illustrates the primary tectonic elements that interact in the northeast Pacific and western North America.

Earthquakes originating within the Puget Sound area can be classified into two categories according to the focal depth: shallow-focus earthquakes with focal depths at approximately 20-30 km, and deeper focus earthquakes with focal depths between 40 and 70 km. The subduction of the Juan de Fuca plate is currently active. The largest earthquakes occurring in the area are deep focus events associated with this subduction process [6]. However, most of the smaller earthquakes in Puget Sound occur at shallower depths and are associated with the existence of the Puget Sound depression. Figure 13 shows how the subduction process might be occurring.

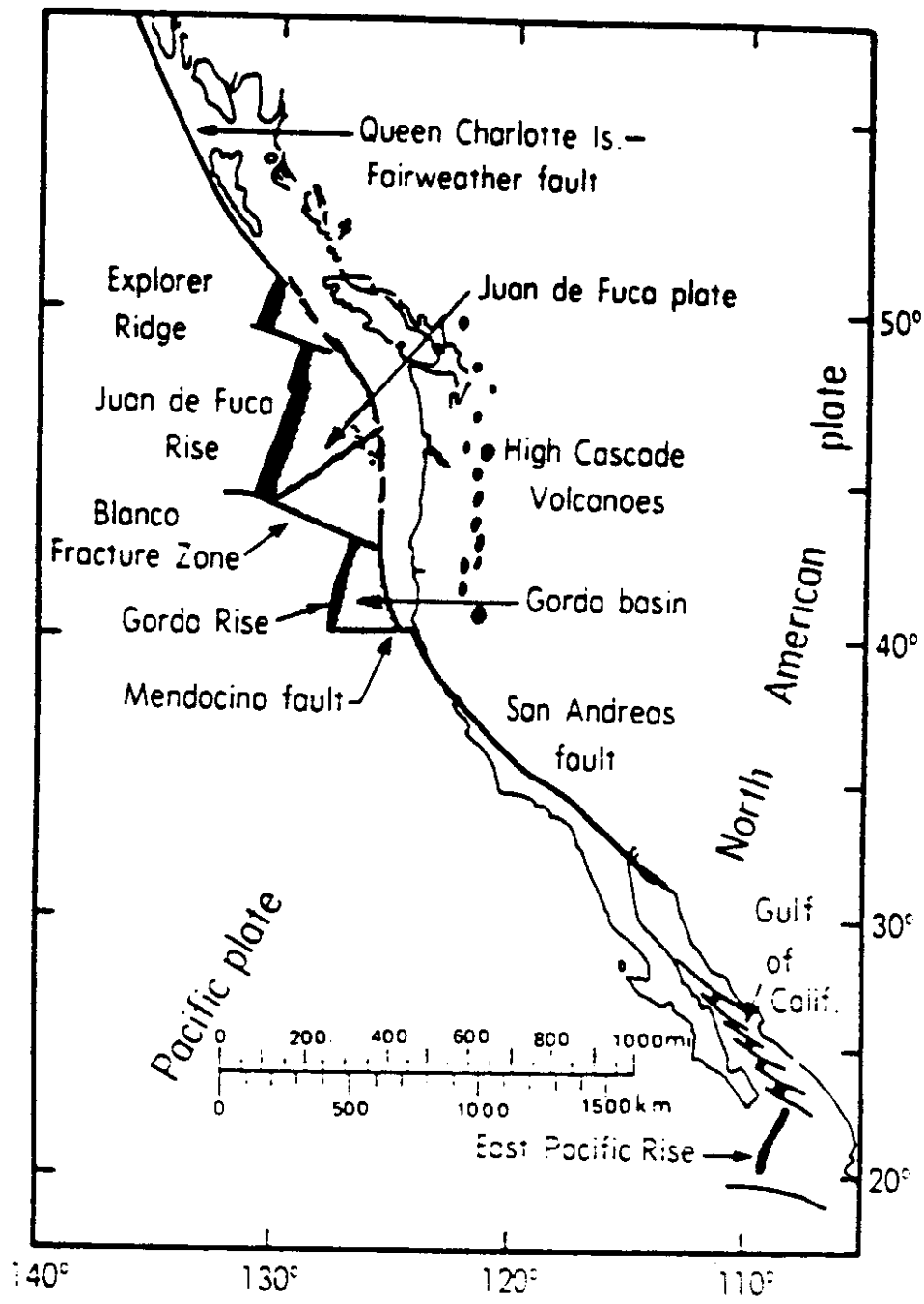

FIGURE 12. Primary tectonic elements that interact in the northeast Pacific and western North America [1].

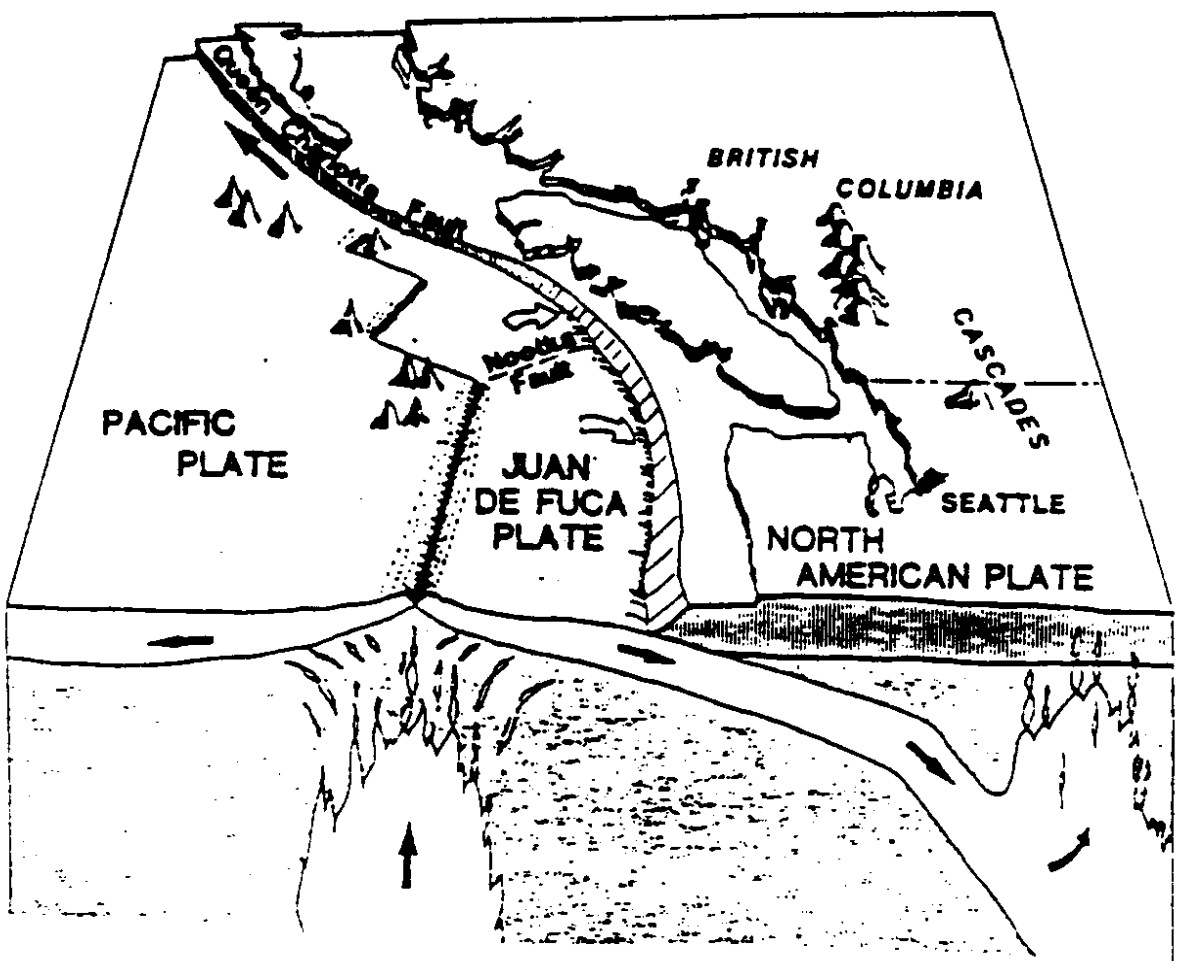

FIGURE 13. The subduction process that affect the seismicity of the region [21].

SUMMARY

In summary, earthquake induced ground motion is a function of the source mechanics and the dynamic properties of the propagating media. The local geological and topographical conditions strongly affect the temporal and spatial behavior of the ground motion. Attenuation relationships for ground motion developed by many researchers are based on specific earthquakes recorded at specific locations, such as, California earthquakes.

Washington State has a unique geology that is characterized by the thick deposits which resulted from the glaciation activity during the ice ages. Also, the seismicity of Washington State is unique; being affected by the subduction of Juan de Fuca plate beneath the American plate. Thus, a need for developing seismic response spectra that would reflect the unique geology and seismicity of Washington State is eminent.

In the next section the modeling and analysis procedures that were followed to come out with a family of seismic response spectra for Washington State are discussed in detail.

MODEL AND ANALYSIS

SHAKE

Several methods for evaluating the effects of local soil conditions on ground response during earthquakes are presently available. Most of these methods are based on the assumption that the main responses in a soil deposit are caused by the upward propagation of shear waves from the underlying bed formation [7]. The analytical procedure generally involves determination of the characteristics of the motion likely to develop in the rock formation underlying the site, determination of the dynamic properties of the soil deposit, and computing the response of the soil deposit to the base rock motion. Computer programs developed for this analysis are generally based on either the solution of the wave equation or on a lumped mass simulation. Some of these programs are based on constitutive modeling for the soil and use finite element analysis.

The program SHAKE computes the responses in a system of homogeneous, visco-elastic layers of infinite horizontal extent subjected to vertically travelling shear waves. The program is based on the continuous solution of the wave equation adapted for use with transient motions through the Fast Fourier Transform Algorithm. It involves the iterative use of strain-compatible soil properties in a frequency-domain-based analysis to account for the nonlinearity of the shear modulus and damping rations [7,17].

Several assumptions are required for the analysis. Among those are the following: the soil system is assumed to extend infinitely; each layer in the system is completely defined by its value of shear modulus, critical damping ratio, density and thickness. The

strain dependence of modulus is accounted for by an equivalent linear procedure based on the average effective strain level computed for each layer.

DYNA1D

DYNA1D [8] is a finite element computer program for nonlinear seismic site response analysis for dry, saturated, and partially saturated deposits. DYNA1D allows site response analysis to be performed taking into account the nonlinear, anisotropic and hysteretic stress-strain behavior of the soil materials, and the effect of transient flow of the pore water through the soil strata. This program uses procedures based on field and constitutive equations which are general and applicable to multidimensional situations. The required material constitutive parameters are identified in terms of "classical" soil mechanics parameters (elastic modulus, friction angles, permeabilities, etc).

In DYNA1D, the semi-infinite domain is represented by finite element model. The site response calculations are performed for a given seismic input motion prescribed in the form of an acceleration, velocity, or displacement time histories applied at the base of the soil column. Special boundary conditions can be prescribed which allow the seismic input motion to be prescribed as an incident propagating motion, or as the sum of an incident and reflected motion.

The finite soil column is modeled by using finite elements. For that purpose the horizontally-layered ground is divided into several finite elements. Each finite element is defined by two nodes. The nodes need not be equally spaced. Soil skeleton motions occur in both the horizontal and vertical directions. Therefore two solid kinematic

degrees of freedom are assigned to each node. Fluid motions can only occur in the vertical directions; therefore, for saturated deposits in which fluid motions can take place a third kinematic degree of freedom is assigned to the fluid motion in the vertical direction. Figure 14 shows modeling of the soil layers and input motion in DYNA1D.

A set of material properties is associated to each element. The material may be assumed linear or nonlinear. Nonlinear soil model is based on multi-yield levels plasticity constitutive theory. For detailed discussion of the theoretical background of the program DYNA1D, the reader is referred to the program's technical documentation [8].

Output for DYNA1D consists of nodal, element stresses, strains, pore water pressures, time histories, etc. The results are post-processed using the graphics past-processor which allow selective plots of field components time histories, Fourier spectra, velocity spectra, etc., and spatial plots at selected time of field components variations.

MODEL

The SHAKE program requires as input, shear modulus vs. strain and damping ratio vs. strain curves, a description of the soil profile, and time history input at the base of the profile. The following discussion illustrates how the input requirements for SHAKE were selected.

The shear modulus and damping in soil are important to the analysis of all soil vibration problems. In particular, the modulus and damping for small strain amplitudes are necessary for the analysis of foundation vibrations. The modulus and damping for a range of strain amplitudes are needed for the analysis of earthquakes effects. Strain

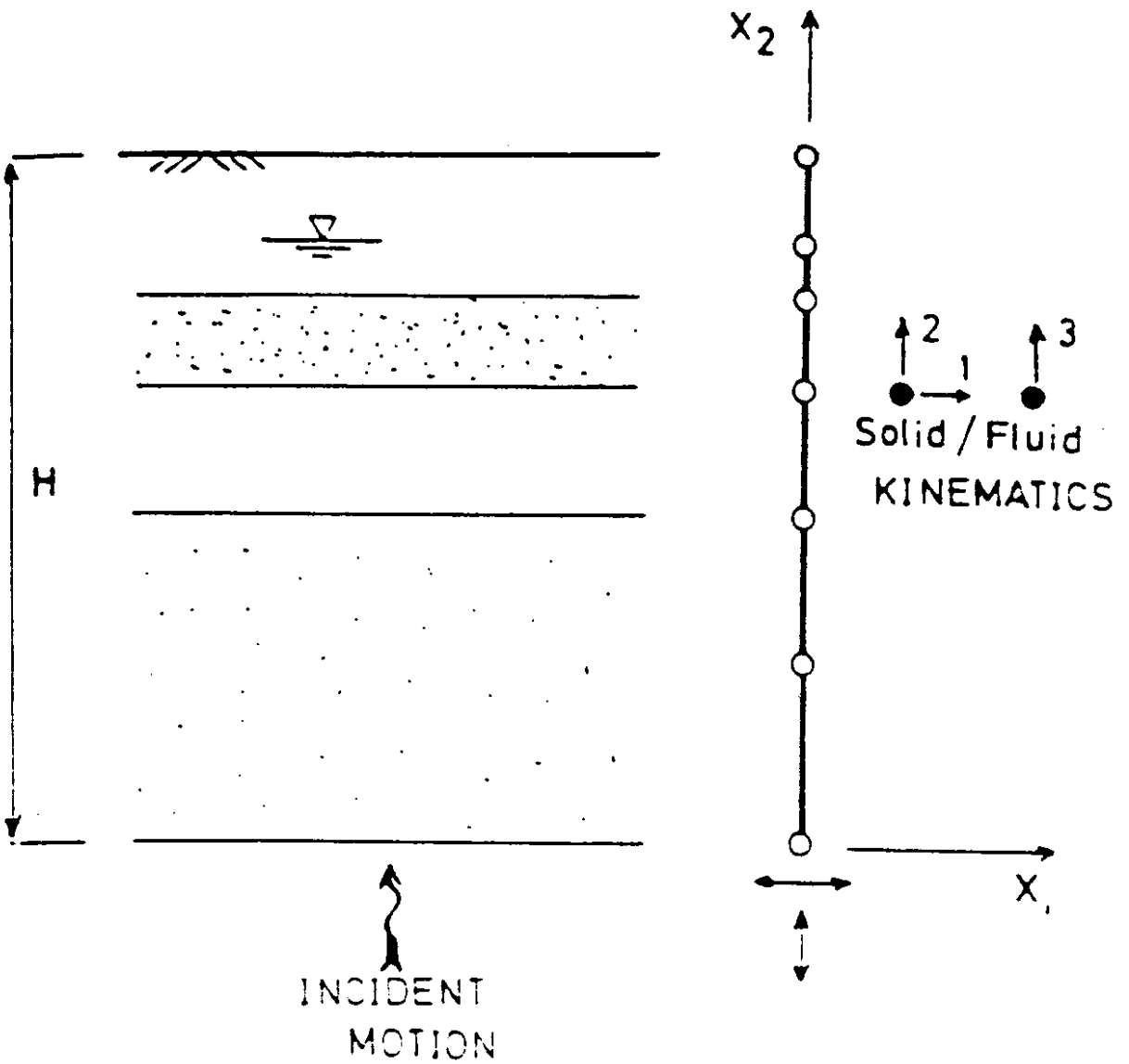

FIGURE 14. Semi-infinite layered soil profile and Finite Element mesh [8].

amplitude, effective mean principal stress and void ratio are the most important factors that affect shear modulus and damping of cohesionless soils. The above factors along with the degree of saturation are the most important factors that affect shear modulus and damping for cohesive soils [25].

In 1970, Seed and Idriss [26] developed curves giving shear moduli and damping values as function of shear strain for both cohesive and cohesionless soil. These curves were used in the previous study [6]. The shear modulus vs. strain curve for cohesionless soils was represented by Seed and Idriss by the following equation:

$$G = 1000\ K_2\ (\sigma_m')^{\frac{1}{2}} \qquad (2)$$

where k_2 is a function of the void ratio and strain amplitude and σ_m' is the effective mean principal stress.

For practical purposes, values for k_2 may be determined from a correlation with the void ratio or the relative density and the strain amplitude of the motion. Values of k_2 usually lie in the range 30 to 75 for loose to dense sands.

The damping ratio vs strain curves for sands were developed by Seed and Idriss [26] based on the work done by Hardin and Drnevich [25]. They concluded that the shear strain, effective mean principal stress, void ratio, and number of cycles were very important factors influencing the damping ratios of sands. Figure 15 shows the shear modulus and average damping ratio of sand as function of shear strain as presented by Seed and Idriss.

Accurate determination of the shear modulus of saturated clays is complicated by

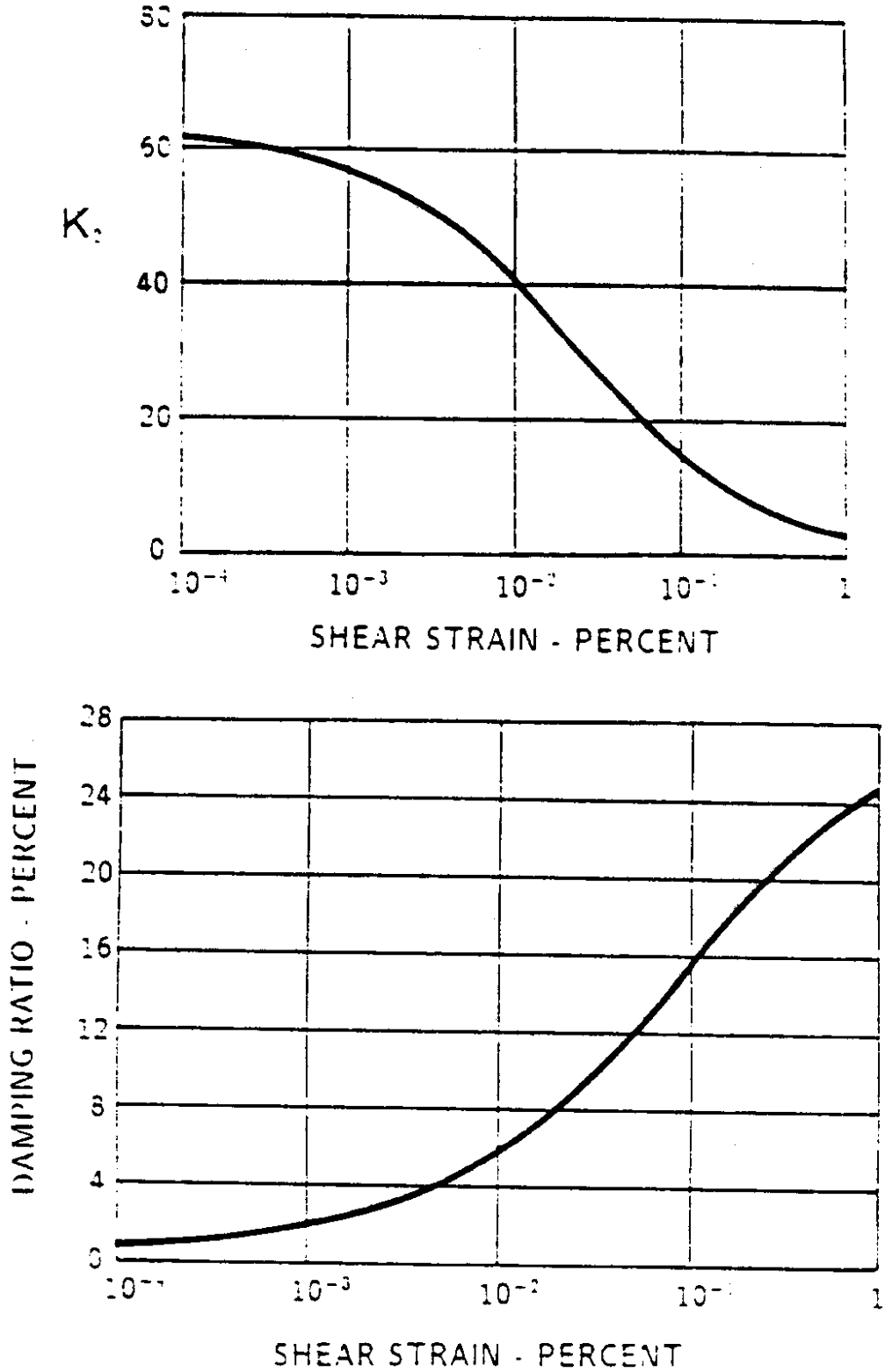

FIGURE 15. Shear moduli and damping ratio for sands from Seed and Idriss [27].

the large effects of strain amplitude and sample disturbance on modulus values [26]. Besides the effects of strain amplitude and disturbance, the moduli for different clays clearly depend on their relative strengths and stiffnesses. Hardin and Drnevich [25] expressed these effects in terms of the effective mean principal stress, void ratio, overconsolidation ratio, and effective stress strength parameters. Seed and Idriss [26] concluded that the effects of variations in clay characteristics on the shear moduli can be taken into account with reasonable degree of accuracy by normalizing the shear modulus, G, with respect to the undrained shear strength, S_u. G/S_u can be expressed as a function of shear strain. Damping ratio curves were also developed by Seed and Idriss using data from previous investigations. Approximate upper and lower bound relationship between damping ratio and shear strain were developed and a representative average relationship for all of the test data were obtained. Figure 16 shows the shear moduli and damping curves for saturated clays as presented by Seed and Idriss in 1970. These curves were used in the previous study [6].

As mentioned in earlier sections, new curves for shear modulus of saturated clays were recently reported by Sun et al. [1]. They concluded that unlike the modulus reduction curves reported for a variety of sands which show a relatively small variation from one sand to another, the modulus reduction curves for clays are highly variable. The rate of modulus reduction with shear strain (which is normally shown on a plot of G/G_{max} vs. strain, where G_{max} is the low strain modulus for a shear strain of the order of 0.0001 percent) is related to the characteristics of each individual clay. After examining many factors that might influence the form of the normalized modulus reduction relationships

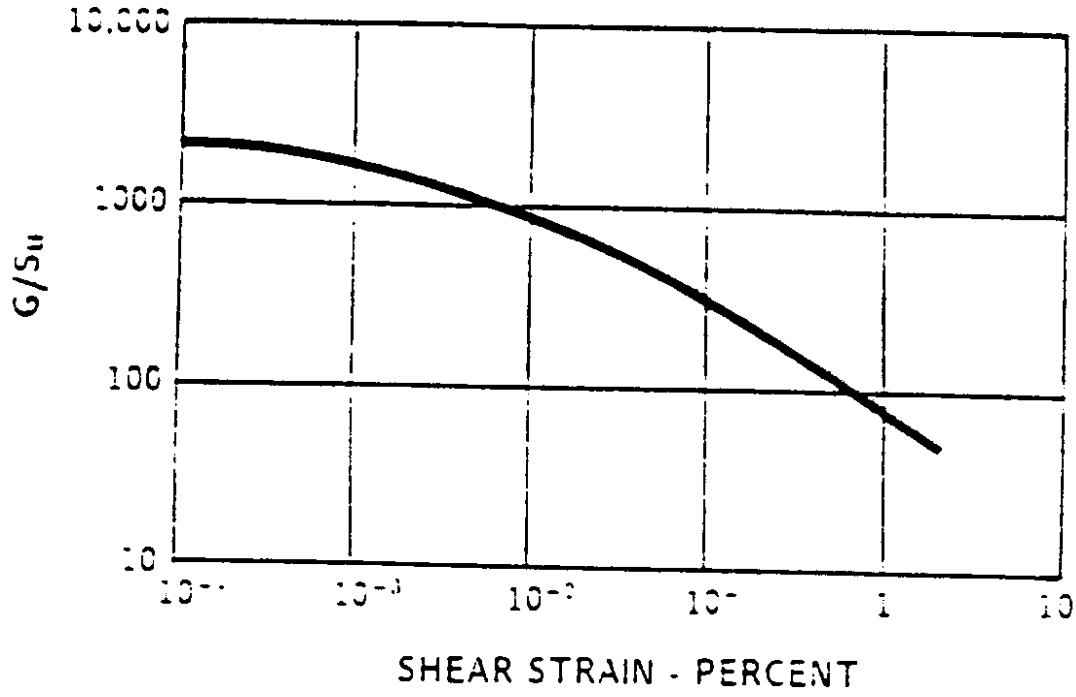

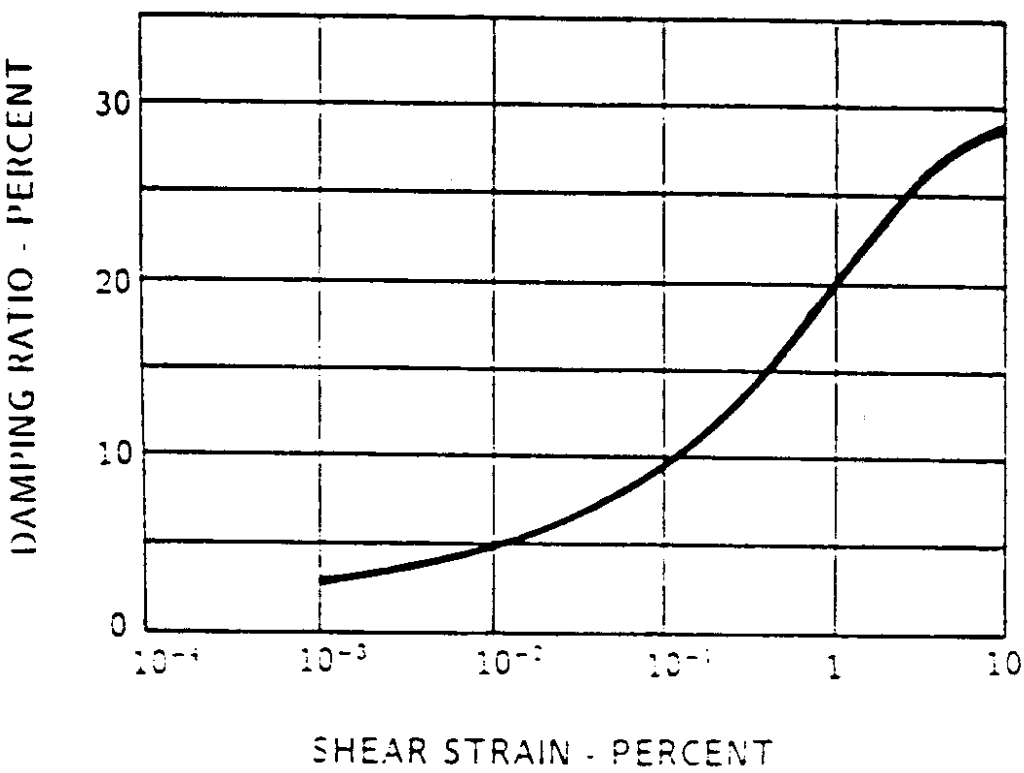

FIGURE 16. Shear moduli and damping ratio for saturated clays from Seed and Idriss [27].

for cohesive soils, Sun et al. [1] concluded that the plasticity index is the most dominant and consistent factor. Accordingly, curves for the normalized modulus reduction relationships for clays with different plasticity indices were provided. These curves are shown in Figure 17. These curves are multiplied by the value of the low strain modulus of saturated clays which is of the order of 2300 psf to get the proper values which were used in SHAKE.

Reported values for the damping characteristics of cohesive soils have not changed significantly over the years from the range given by Seed and Idriss in 1970. These curves were used in this study.

SOIL PROFILES

The soil profiles used in the previous study [6] where developed for 123 boring logs from actual bridge sites in Washington State. The main purpose of this study is to update the seismic design guidelines for Washington State bridges using the new information about the dynamic behavior of cohesive soils and the new information about the subduction zone events. Since the soil profiles used in the previous study covered many locations all over Washington State, it was decided to use the same 123 soil profiles in the analysis in this study. The soil profile input for SHAKE includes depths of layers, type of each layer, shear modulus of each layer, unit weight of layers in the profile, depth of water table, and scaling factors for the shear modulus and damping curves.

Kornher [6] developed the soil profile inputs for SHAKE from data collected from actual boring logs in Washington State. The data provided on the boring logs was limited

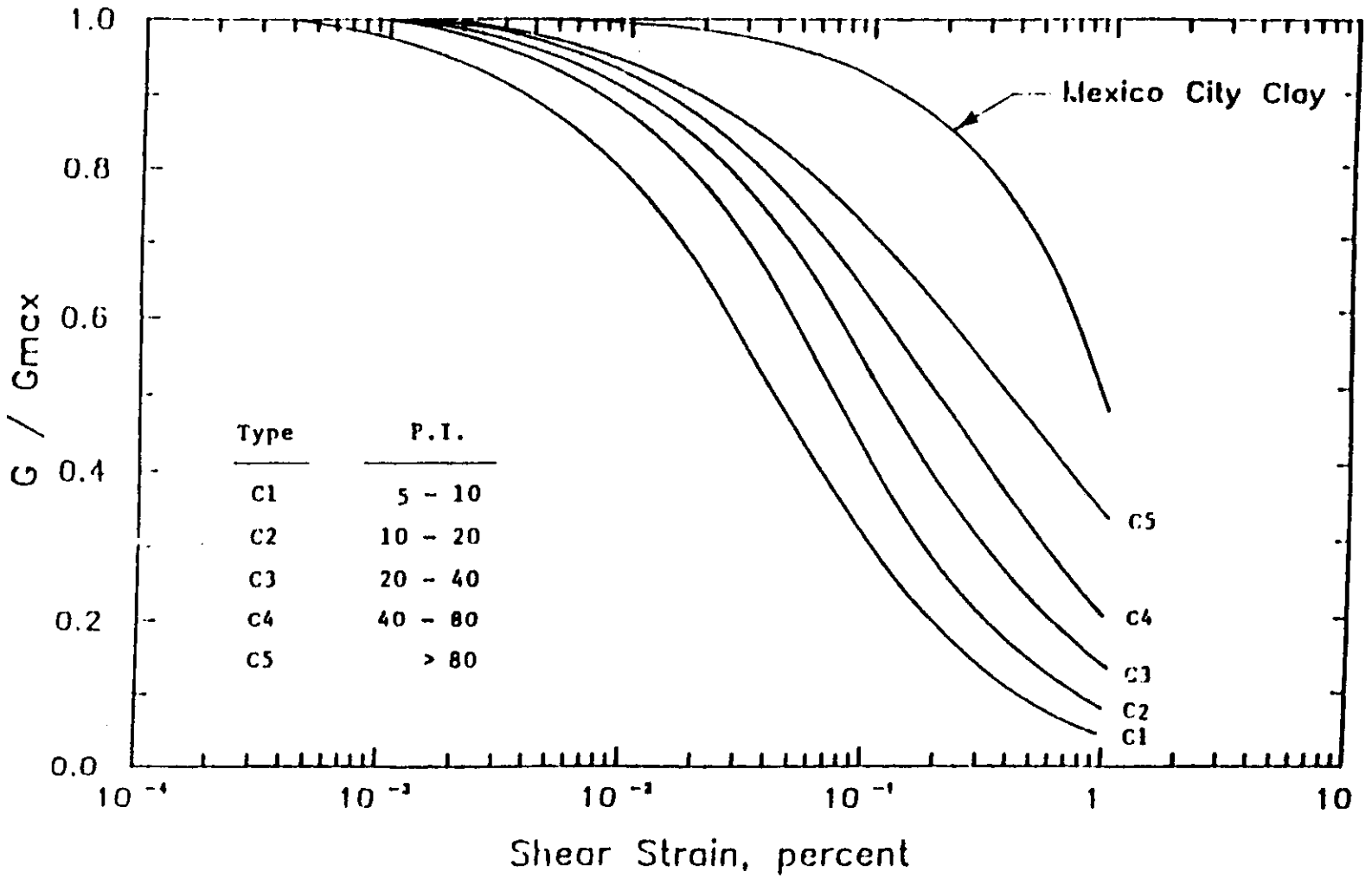

FIGURE 17. Normalized modulus reduction relationship for clays with different plasticity indices [1].

to geophysical description of the soils, approximate layering, depths of water table, Standard Penetration Test blow counts (SPT), and undrained shear strength where clays or organics were present in the deposits. The soil profiles were up to 150 feet in depth and the SPT values were up to 100 blows per foot.

Converting these data to the form required by SHAKE program required identifying the soil as sand or clay and then correlating the field and laboratory data to dynamic input parameters. Kornher investigated several relationships that correlate low-strain shear modulus to the Standard Penetration Test values (SPT). Ohsaki and Iwasaki's [27] relationship for uncorrected blow counts were chosen. This equation is expressed as follows:

$$G_{max} = 1.47\ N^{0.68} \tag{3}$$

where G_{max} is the shear modulus at low strain levels in tsf and N is the SPT number in blows per foot. This relationship was chosen since the correlation coefficient with down-hole velocity studies is high and the results are consistent with the results obtained by other researchers [28]. The low strain shear modulus G_{max} can then be converted to the k_2 coefficient using the equation:

$$K_2 = \frac{G_{max}}{(\sigma_m')^{\frac{1}{2}}} \tag{4}$$

dividing k_2 by 61 will give the proper multiplying factor for SHAKE [6].

Kornher also used the undrained shear strength, where available, for correlation with shear modulus for cohesive soils. The ratio G_{max}/S_u was found based on average

values from the variational relationships provided [29] (see Figure 18). The G_{max}/S_u value was multiplied by S_u to get better estimates for G_{max}. The SHAKE factor was obtained by dividing G_{max} by 2300 since SHAKE was formulated under the assumption that G_{max}/S_u is equal to 2300 under low strain levels.

As mentioned earlier, an earthquake record at rock site for a subduction zone earthquake was identified. Strong motion accelerations resulting from the magnitude 5.5 Pender Island, British Columbia earthquake of May 1976 were recorded at lake Cowichan telecommunication stations along with other soil sites in the region [9]. This record and the soil profiles where the strong motion was recorded were used in the non-linear analysis (DYNA1D) and compared with the results of the linear analysis (SHAKE).

These time histories were used as the bedrock motion in the program DYNA1D to calculate surface response of several soil profiles in the area. The modeling parameters for DYNA1D were correlated to the soil properties available for the profiles used in the analysis. The calculated surface motions were compared with the actual motions recorded for the 1976 Pender Island earthquake to estimate the accuracy of the modeling procedure and input parameters. With this knowledge, the second stage of the analysis could be undertaken. This involved subjecting the profiles developed in the first stage to the design earthquakes of the Puget Sound and then comparing the response of these profiles with the response of the nine soil groups of Washington State.

Because of the necessity of comparison between the recorded and measured responses of the Pender Island earthquakes, the soil profiles used in the analysis were limited to those where surface records had been obtained. Three sites satisfied this

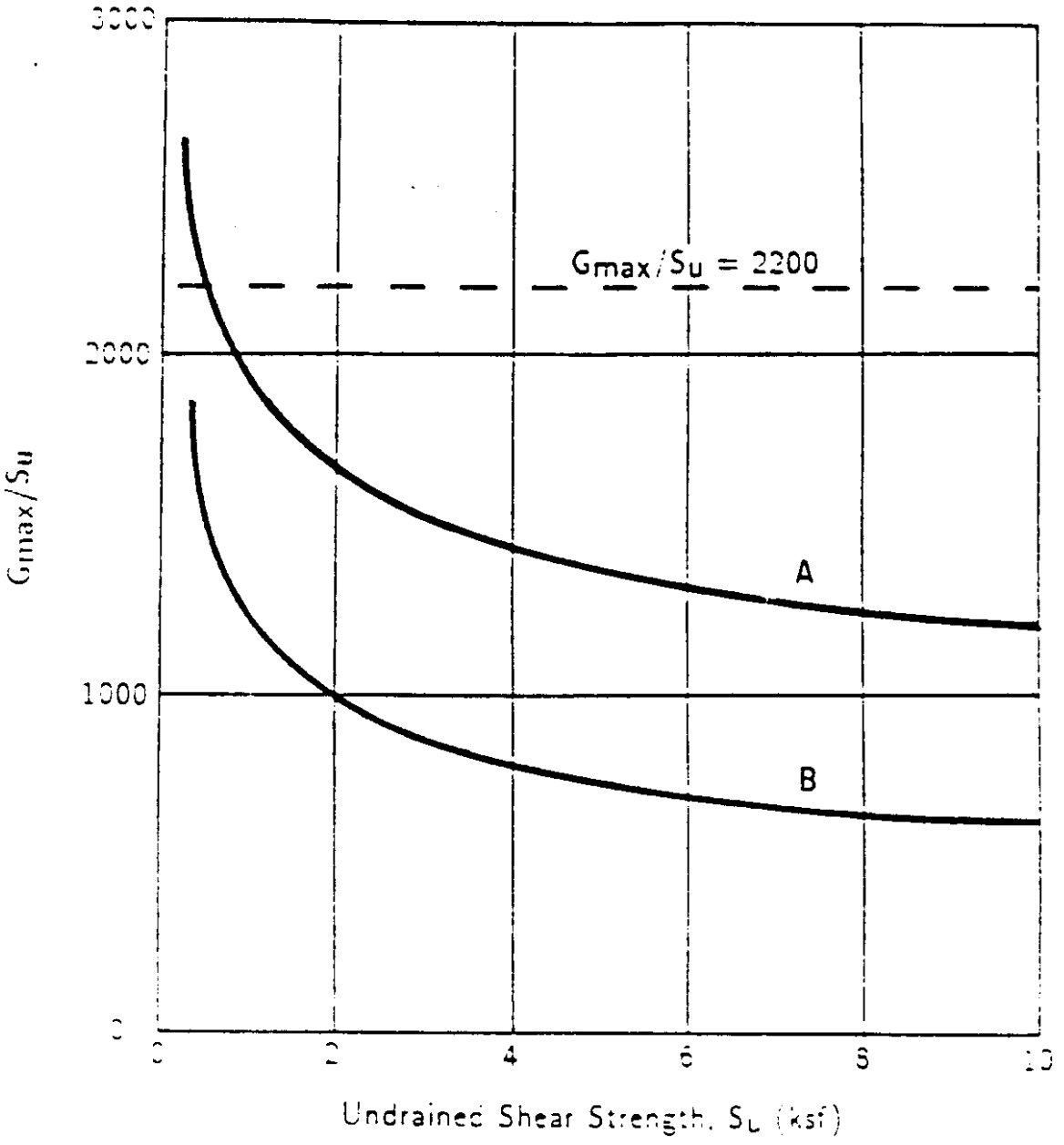

FIGURE 18. Variation of G_{max}/S_u as a function of undrained shear strength [6.29].

criterion [9]: Roberts Bank, Annacis Island, and Brighouse Library of Richmond, British Columbia. These three sites are widely spaced across the area; their profiles are representative of the soils usually found throughout Vancouver and the Puget Sound regions. The difference between these three soil profiles and the Washington State profiles is in the depth. The Vancouver profiles range from approximately 315 to 670 feet in depth while the Washington State profiles were much shallower. This difference would result in more amplification of the propagating waves in the Vancouver profiles compared to the Washington State profiles. The three profiles and the soil models which were used in the non-linear analysis are shown in Figures 19 through 21.

INPUT TIME HISTORY

In an attempt to select proper time histories that would represent the anticipated ground motion due to Washington State earthquakes, Kornher investigated two possible methods; deconvolution of the available strong ground-motions time histories recorded in Washington State using SHAKE, and using predictive equations to get appropriate target response spectra which would be used to attain simulated time histories. Earthquakes induced ground motions that affect Washington State could be represented by a single spectrum scaled by the appropriate severity coefficient, since the soil amplification factors are dependent on the strength of the record and since the strength of the record is defined by the severity coefficient.

As stated earlier, Washington State earthquakes are unique in nature. Therefore, some important factors must be considered when selecting appropriate time histories for

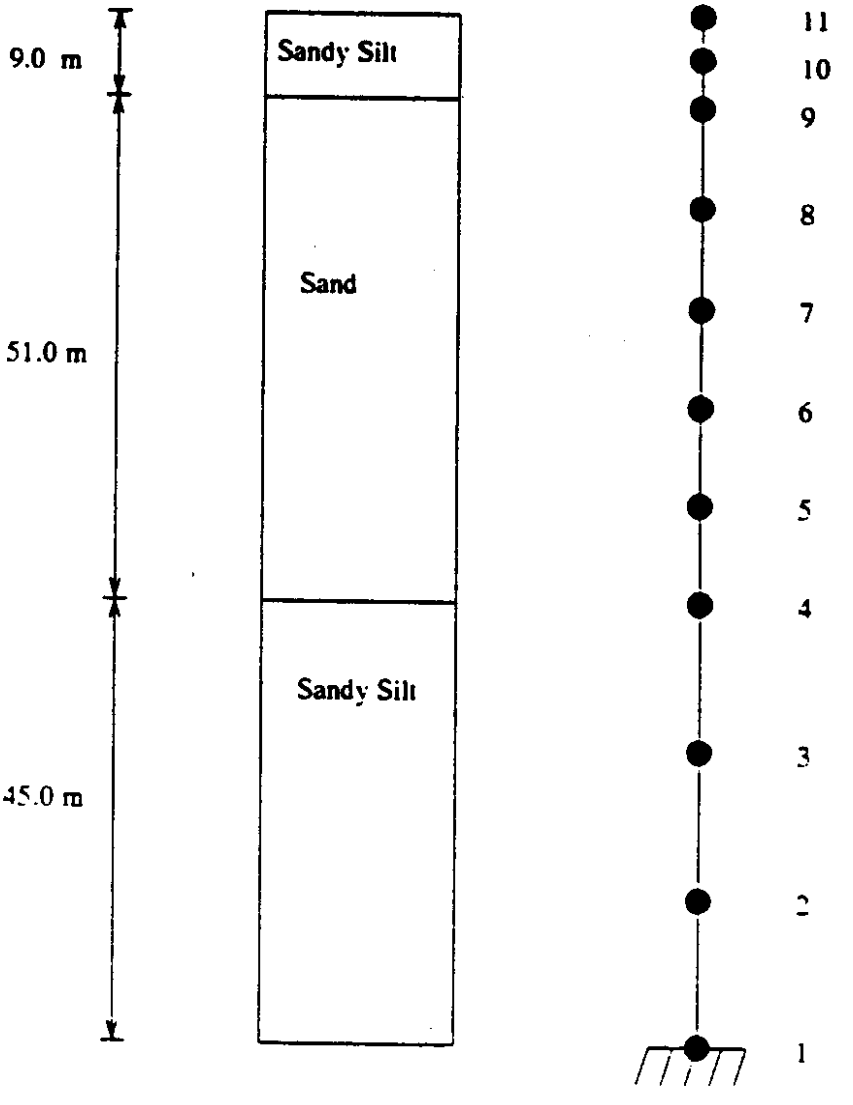

FIGURE 19. Roberts Bank soil profile and Finite Element model.

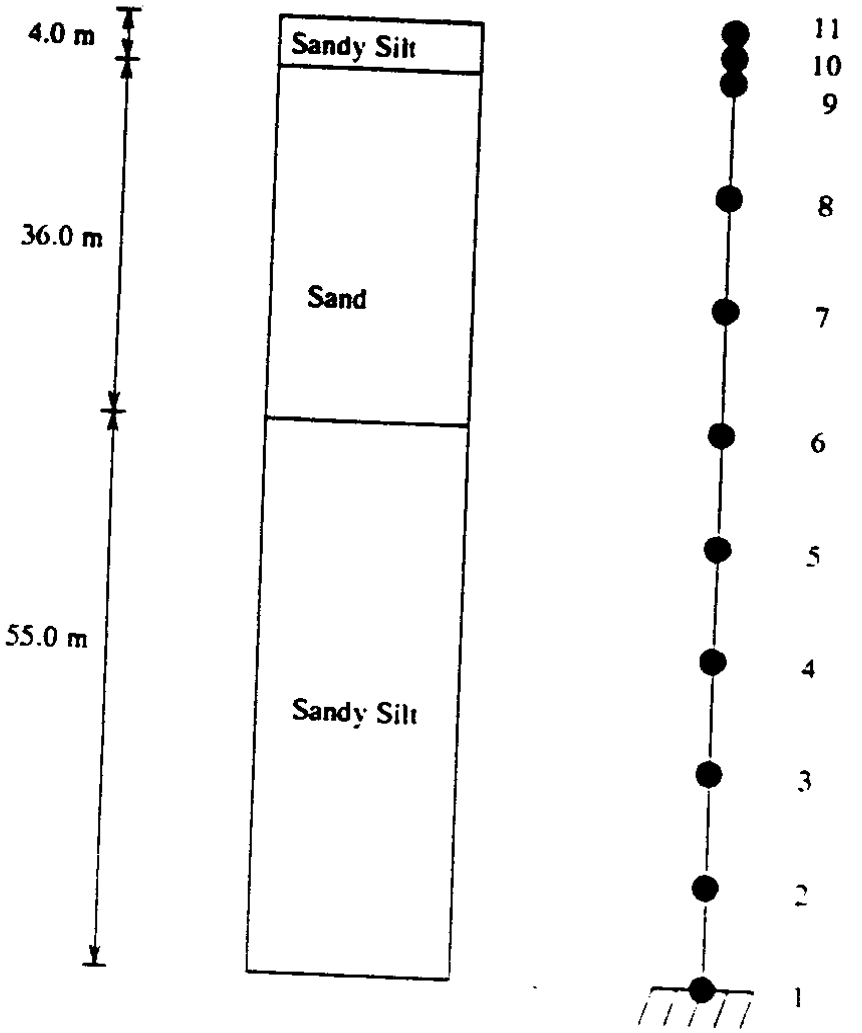

FIGURE 20. Annacis Island soil profile and Finite Element model.

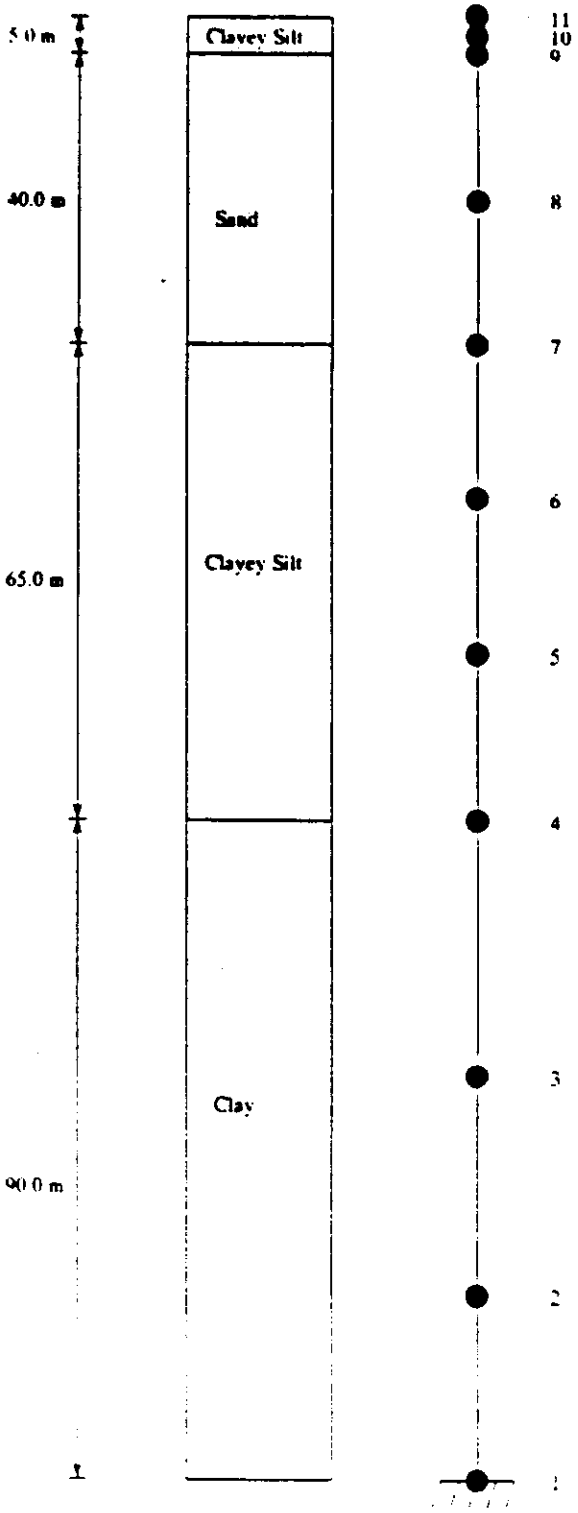

FIGURE 21. Brighouse soil profile and Finite Element model.

Washington State Earthquakes: the range of magnitudes and focal depths which can be expected to occur in this area; and the differences in spectral shapes associated with different epicentral distances.

Studies on the seismicity of Washington State [2,3] suggested that a magnitude 8 earthquake at a depth of approximately 31 miles (50 km) would be a reasonable estimate of the largest design earthquake in this area in light of the reasonable recurrence interval for such earthquakes. This choice of seismic source parameters is based on geologic and geomorphic evidence of subduction zone events in the Puget Sound region.

Deconvolution of the strong-motion records from actual Washington State events was considered in choosing input time histories for SHAKE and DYNA1D. The problems associated with this approach are mainly the tendency of SHAKE to produce unrealistically large high frequency components at the base spectrum, and the lack of sufficient strong motion records from the region. The use of a limited number of records may lead to serious misrepresentation of the motions that could be expected in future earthquakes. Another problem with using actual records is that the response is earthquake site specific. This means that for each site different earthquake motions would have to be used to obtain a realistic range of responses [6].

Joyner and Boore [30] developed empirical equations for predicting earthquake response spectra in terms of magnitude, distance, and site conditions by analyzing horizontal pseudo-velocity response at 5 percent damping for 64 earthquake records in Western North America. These equations do not consider the difference in spectral shape between deep and shallow focus earthquakes resulting from reduced inelastic attenuation,

greater stress drop and general suppression of surface waves for earthquakes with the increase in focal depths [19]. This results in an increase in the high frequency components and a decrease in the longer period components of ground motion from subduction zone earthquakes compared to shallow-focus earthquakes [6]. This trend is illustrated in Figure 22 by comparing the response of deep and shallow earthquakes from predictive equations [30,31,6]. Other researchers provided similar predictive equations for rock and soil sites [32,33,34]. Normalized curves from predictive equations provided by Crouse, Vyas and Kawashima for a magnitude 8 earthquake at a depth of 50 km (31 miles) were compared to the spectra provided by Seed and Idriss [12] in Figure 23.

Upon comparison, the Seed stiff curve, scaled by 0.2 was selected to be a target spectrum in the program SIMQUAKE to simulate acceleration time histories to be used in the SHAKE and DYNA1D analysis [35]. This scaling factor represents the average range of strengths of ground motion expected from the predictive equations. Actual rock records from the 1976 Pender Island earthquake were used in the analysis that involved the Vancouver soil profiles.

BASE SPECTRUM

The base spectrum selected to represent Puget Sound earthquakes is a modified Seed et al. 50 percent stiff curve. This curve was modified with the assumptions made in the AASHTO guidelines [4]. The modification addresses the increase in the response spectrum ordinates at longer periods because of concerns with inelastic response of longer period bridges [6]. The AASHTO guidelines state the spectra should be about 50 percent

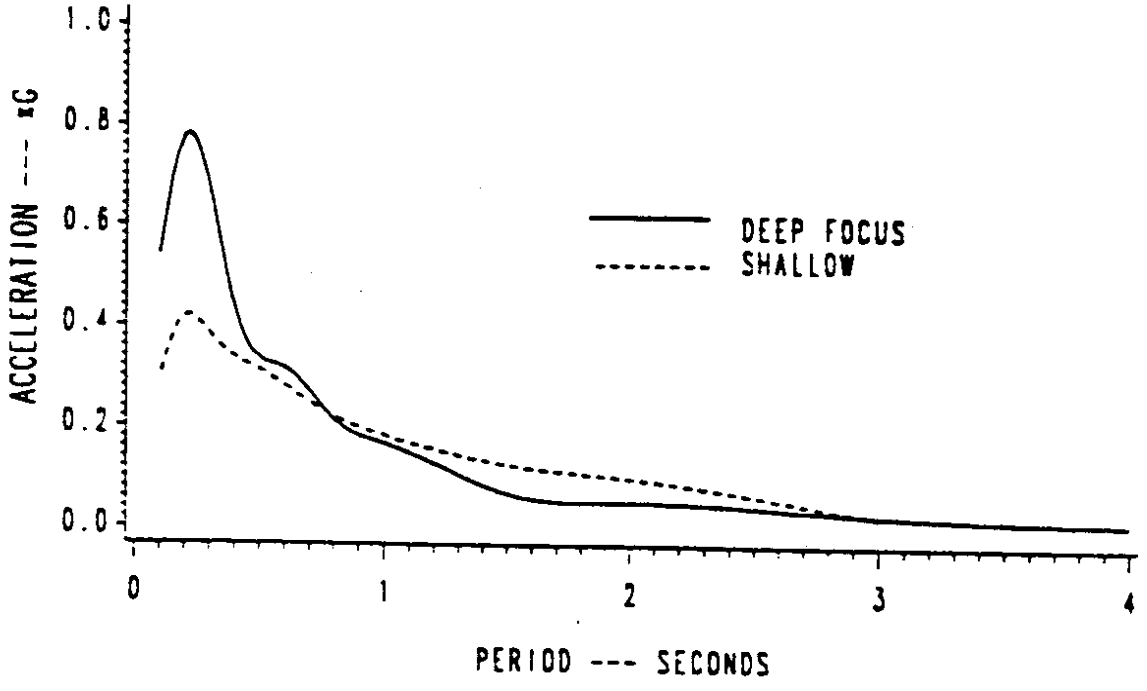

FIGURE 22. Response for deep and shallow earthquakes from predictive equations for magnitude 6.5 earthquake and a hypocentral distance of 12 miles (20 km) [6].

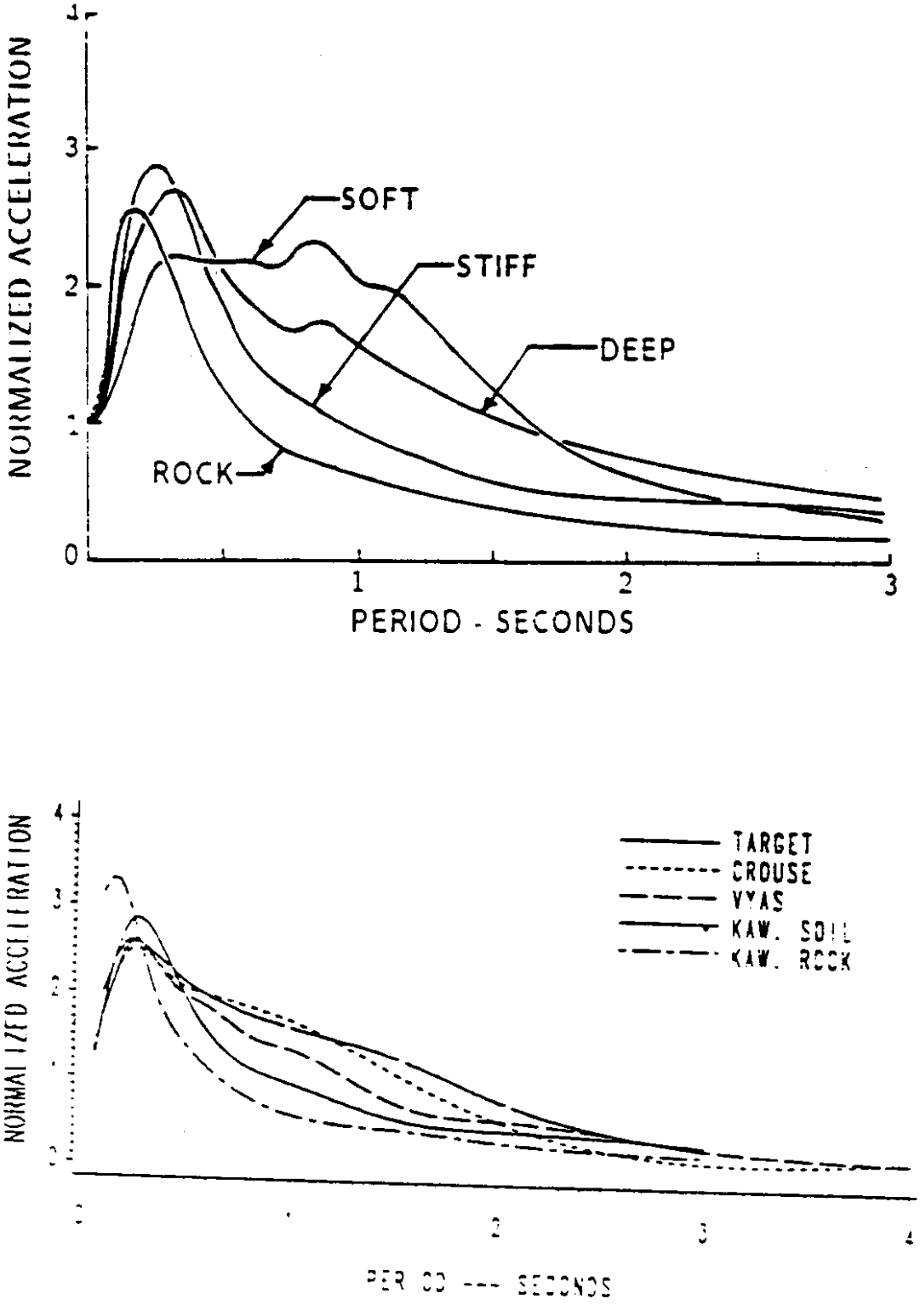

FIGURE 23. Spectra from Seed et al. and predictive equations for magnitude 8 earthquake and a depth of 31 miles (50 km) [6].

greater at a period 2 seconds. Because of SHAKE's tendency to attenuate very high frequency motions, it is appropriate to increase the spectral values at those periods to compensate for that reduction [6]. The base spectrum used in this study is shown in Figure 24.

SUMMARY

The modeling procedures for the linear SHAKE analysis and the non-linear DYNA1D analysis were discussed in detail. SHAKE computes the responses in a system of homogeneous visco-elastic layers of infinite horizontal extent subjected to vertically traveling shear waves based on the continuous solution of the wave equation. DYNA1D is a finite element computer program which allows site response analysis to be performed taking into account the non-linear, anisotropic, hysteretic stress-strain behavior of the soil materials.

The input requirements for SHAKE include shear modulus and damping ratio curves for sand and clay, description of the soil profile, and the time history input at the base of the profile. The required material constitutive parameters for DYNA1D are identified in terms of "classical" soil mechanics parameters.

The input time history for the linear analysis was selected based on the Seed stiff curve scaled by 0.2. Actual rock records from the 1976 Pender Island earthquake were used in the linear and non-linear analysis.

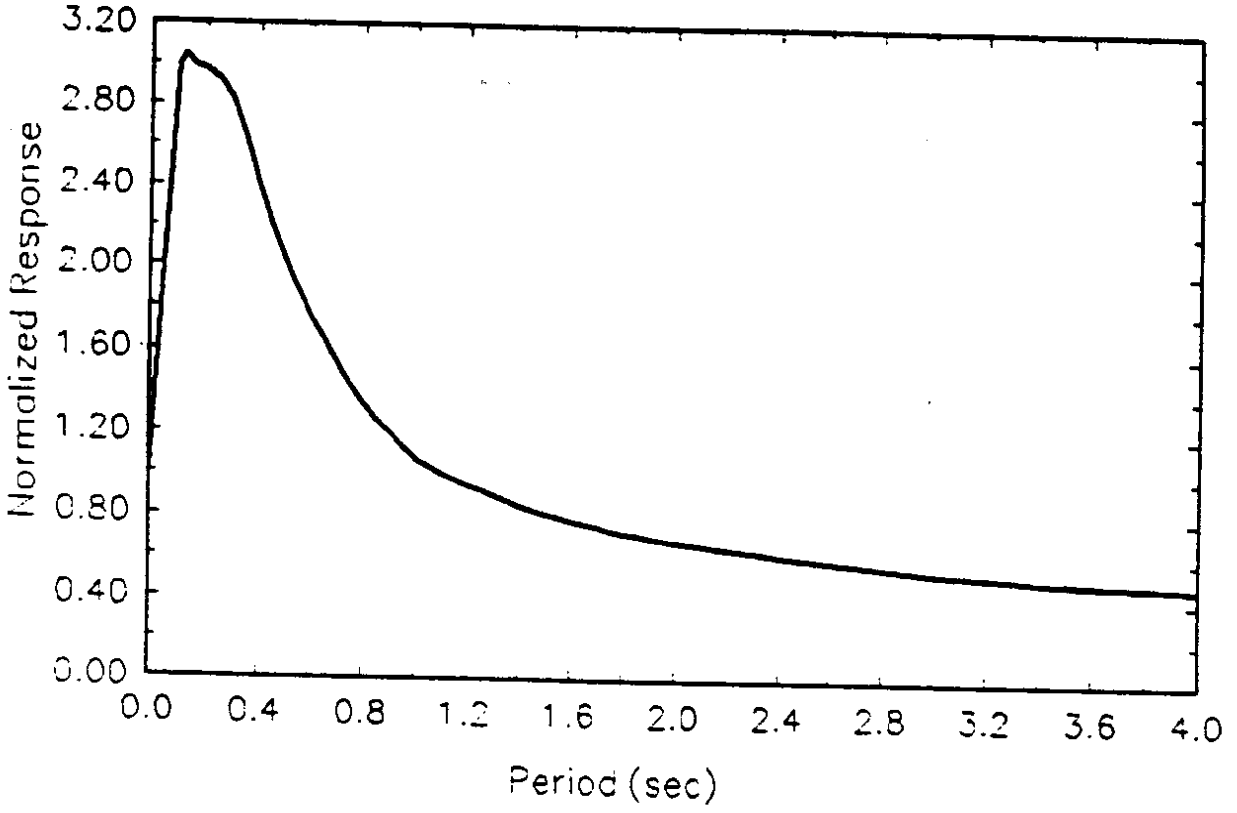

FIGURE 24. Base spectrum used in this study [6].

FINDINGS AND IMPLEMENTATION OF THE RESULTS

Soil Amplification spectra were developed for 123 actual soil profiles using the computer code SHAKE and a simulated input motion based on the seed 50 percent spectra scaled by 0.2. The soil profiles were grouped into the same nine groups used in Kornher's study [6]. Spectral amplification is a function of the depth of the profile and type of soils in the profiles. Table 1 is a describes of the nine soil groups used in this study. Spectral amplification factors were calculated for each group by taking the average values of the spectral amplification factors for all soil profiles in the group. Figures 25 through 33 show spectral amplification factors for the nine soil groups plotted as a function of period.

Spectral amplification factors were multiplied by the ordinates of the base spectrum to obtain the normalized response. Figures 34 through 42 show the normalized response plotted as function of the period for the nine soil groups. Ordinates of all curves can be found in Appendix 2.

SENSITIVITY STUDIES

Sensitivity of the soil amplification factors to the modeling input parameters for SHAKE was examined. The shear modulus was changed by ±30 percent for several soil profiles in the nine groups. Increased shear modulus decreases response while decreased shear modulus increases the response. It was found that a change in shear modulus has greater effect on the response when the soil profiles are looser and/or softer. This

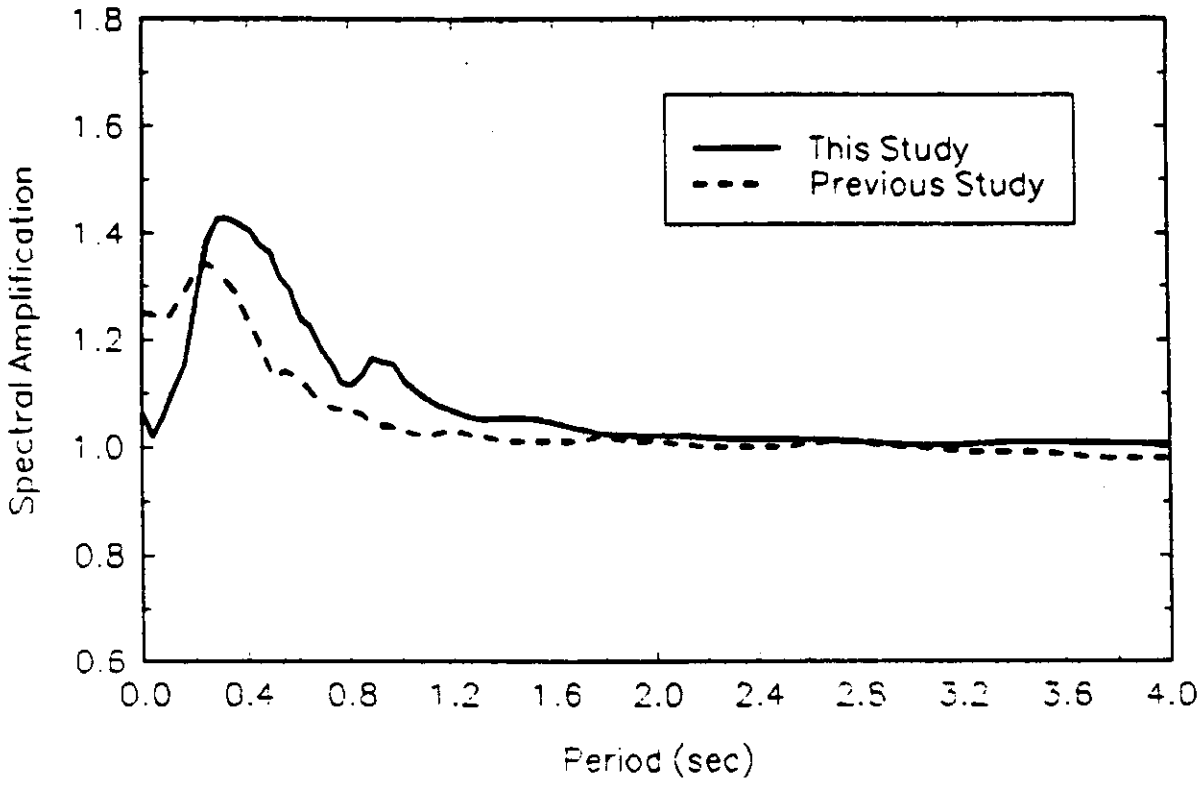

FIGURE 25. Amplification spectra scaled by 0.2 for Group 1 soils.

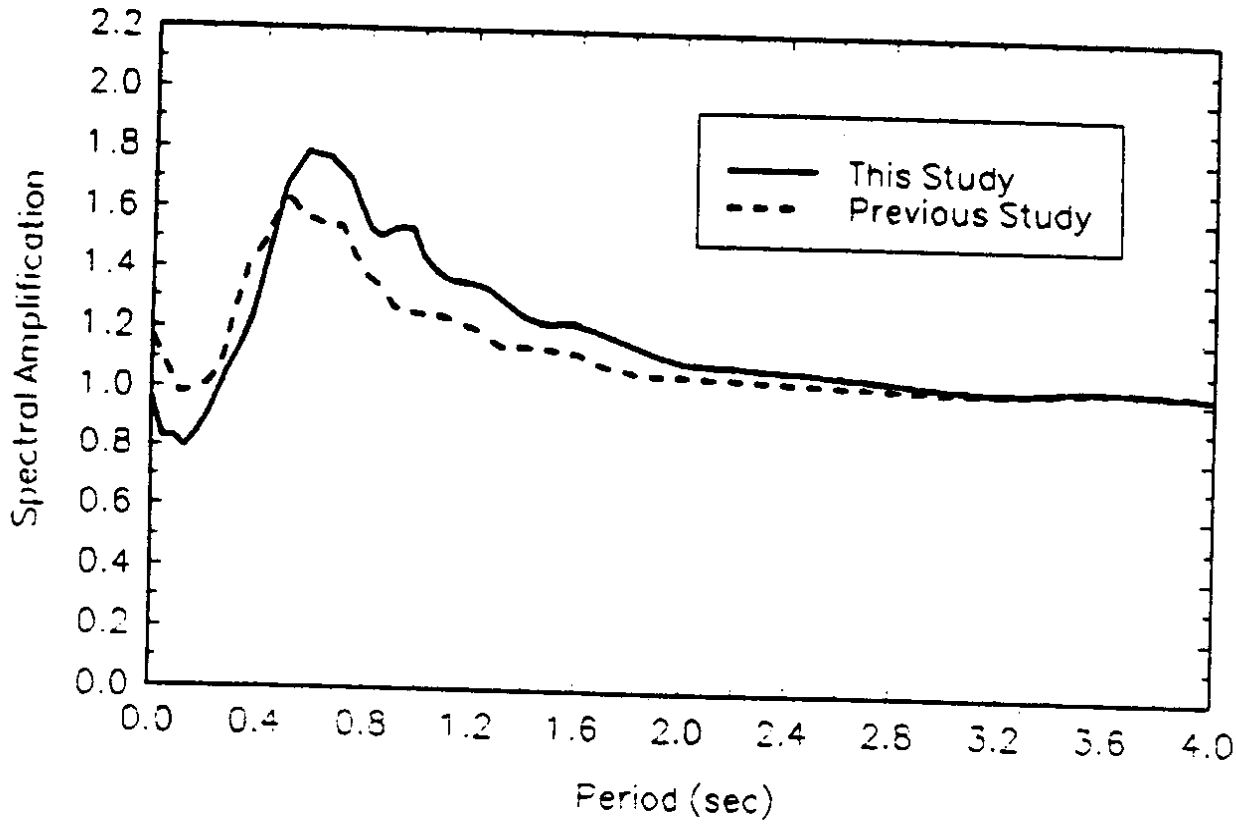

FIGURE 26. Amplification spectra scaled by 0.2 for Group 2 soils.

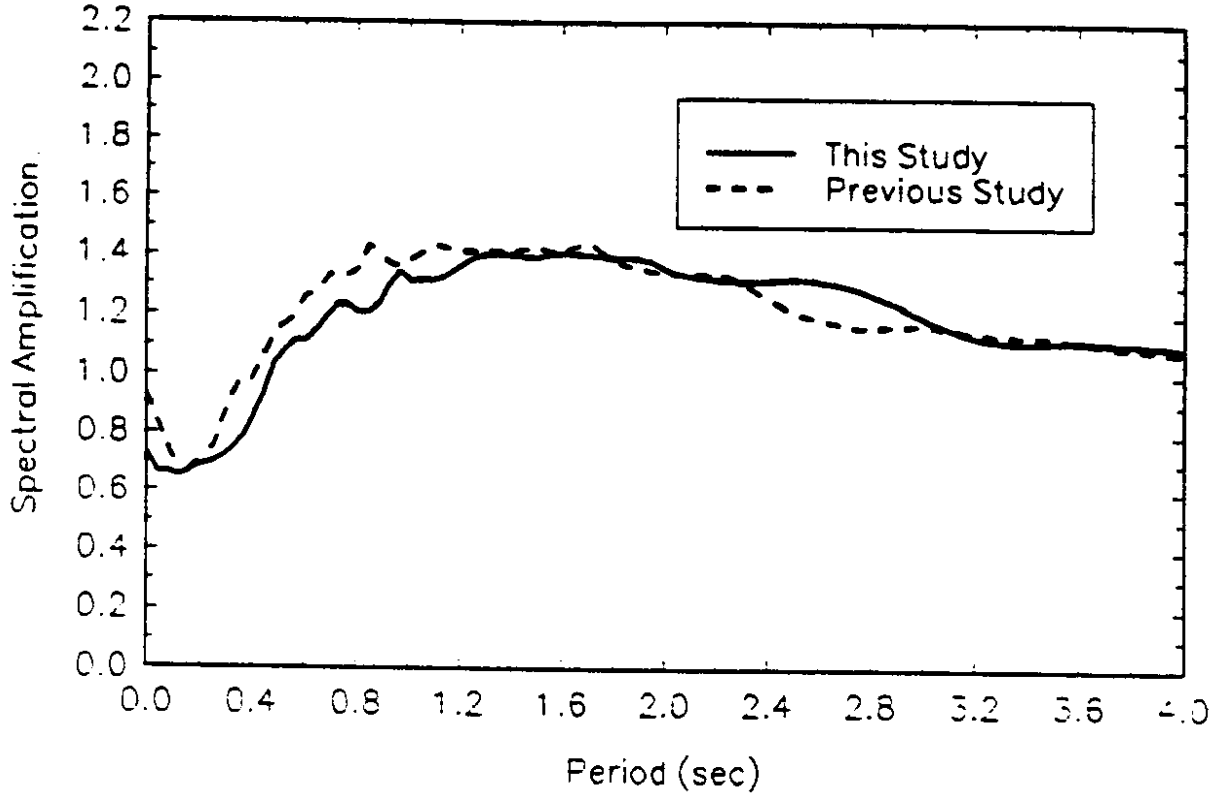

FIGURE 27. Amplification spectra scaled by 0.2 for Group 3 soils.

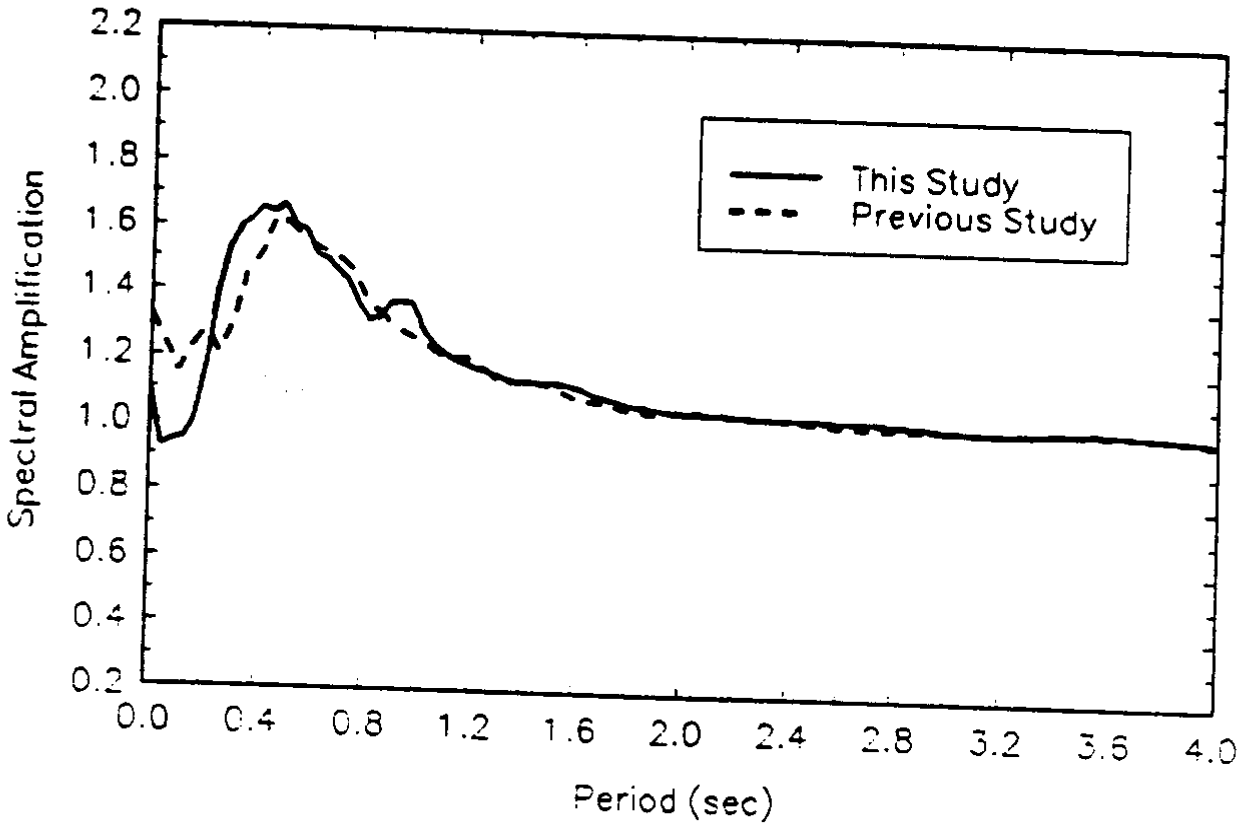

FIGURE 28. Amplification spectra scaled by 0.2 for Group 4 soils.

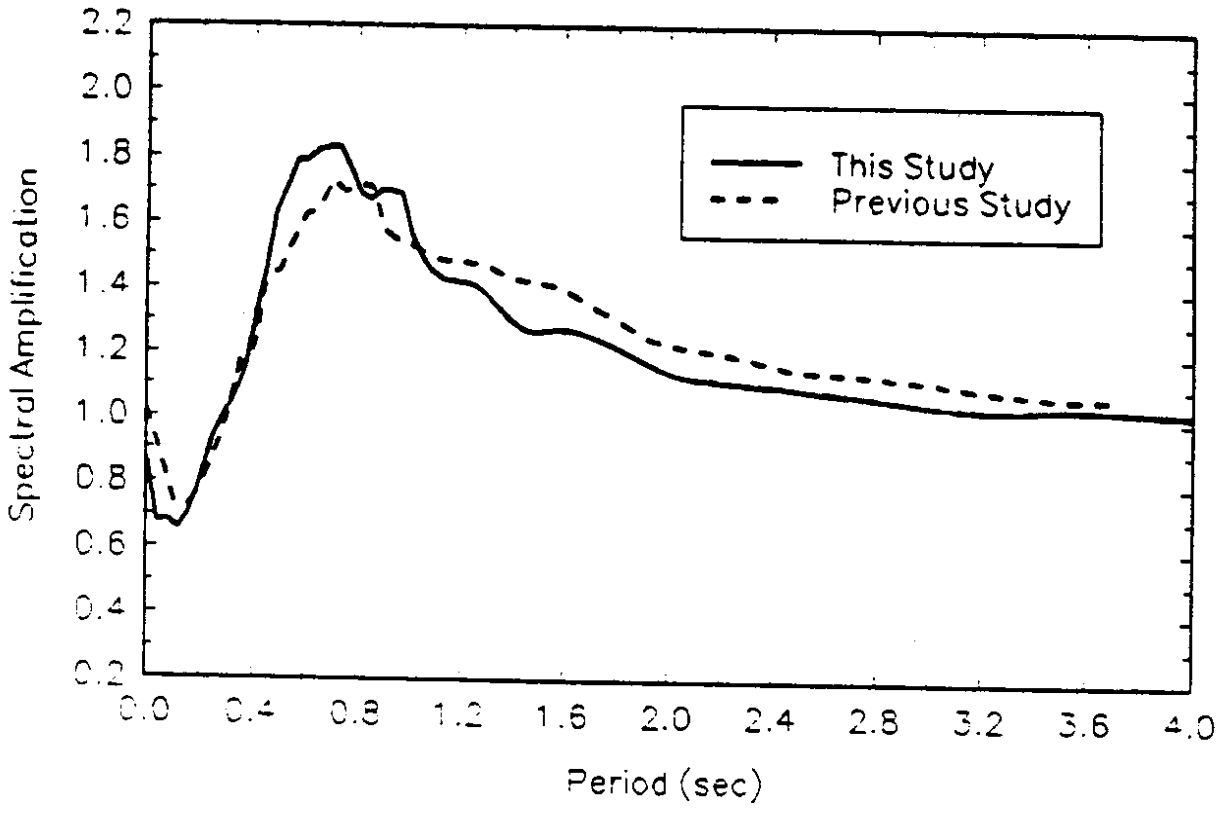

FIGURE 29. Amplification spectra scaled by 0.2 for Group 5 soils.

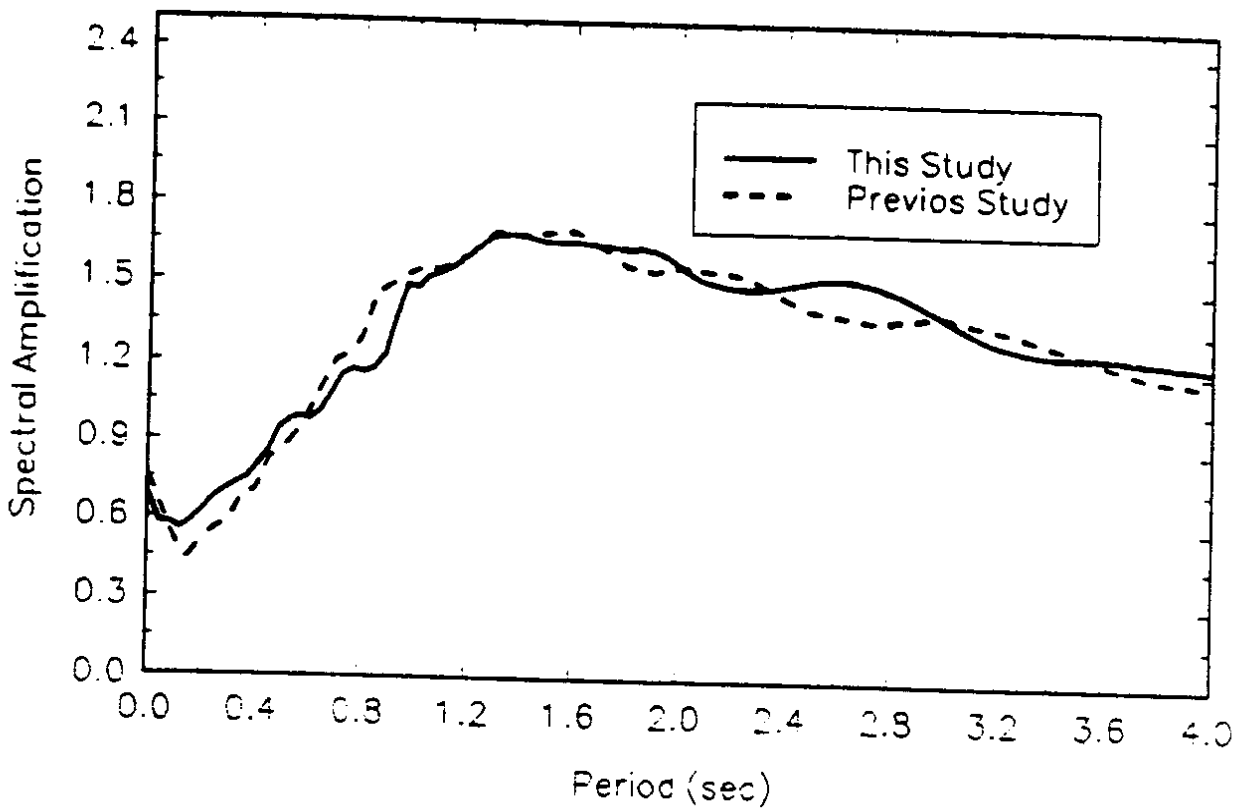

FIGURE 30. Amplification spectra scaled by 0.2 for Group 6 soils.

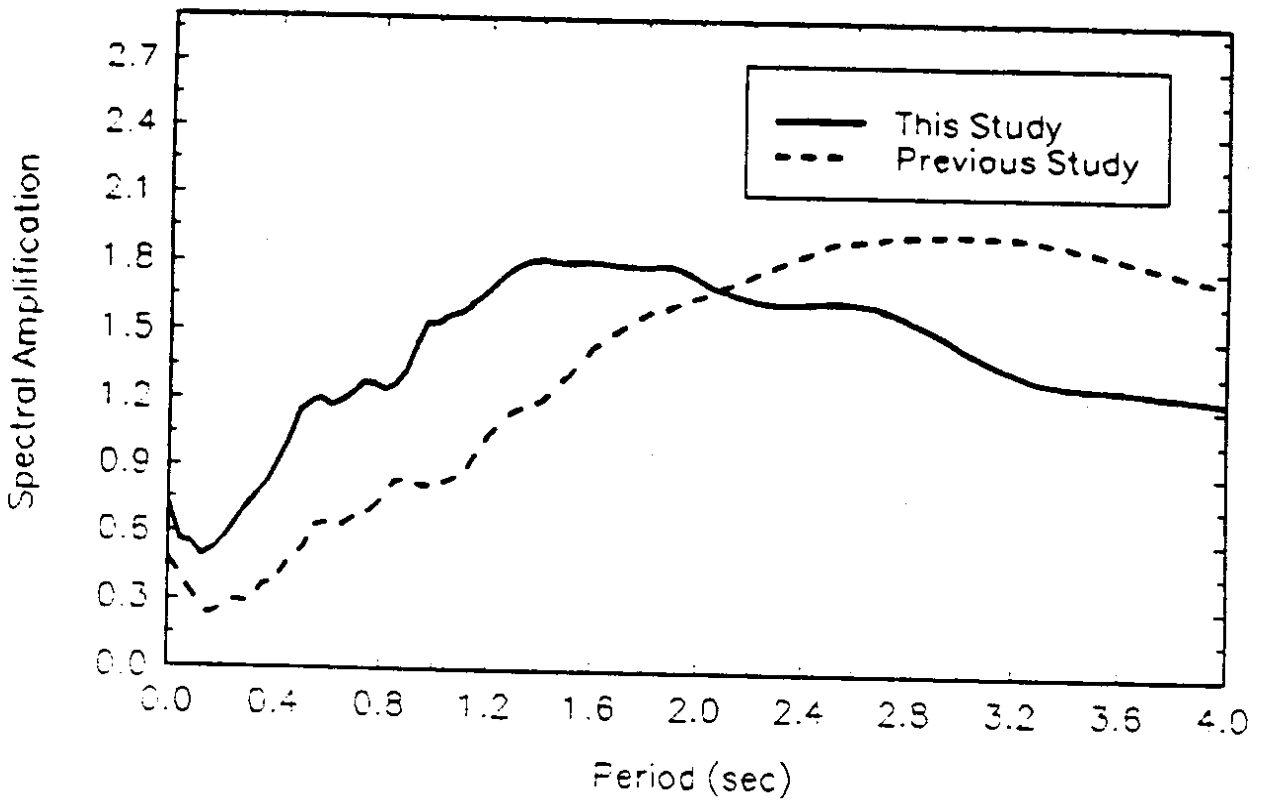

FIGURE 31. Amplification spectra scaled by 0.2 for Group 7 soils.

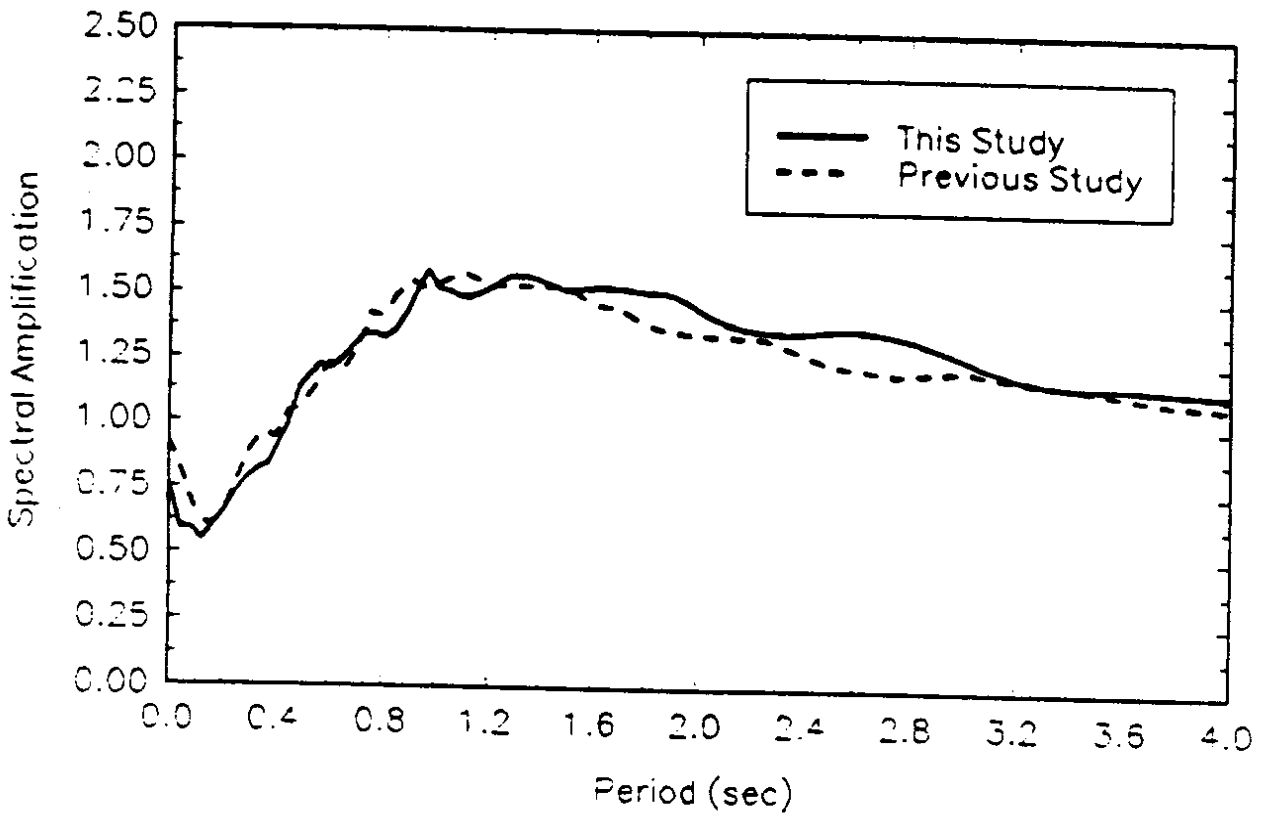

FIGURE 32. Amplification spectra scaled by 0.2 for Group 8 soils.

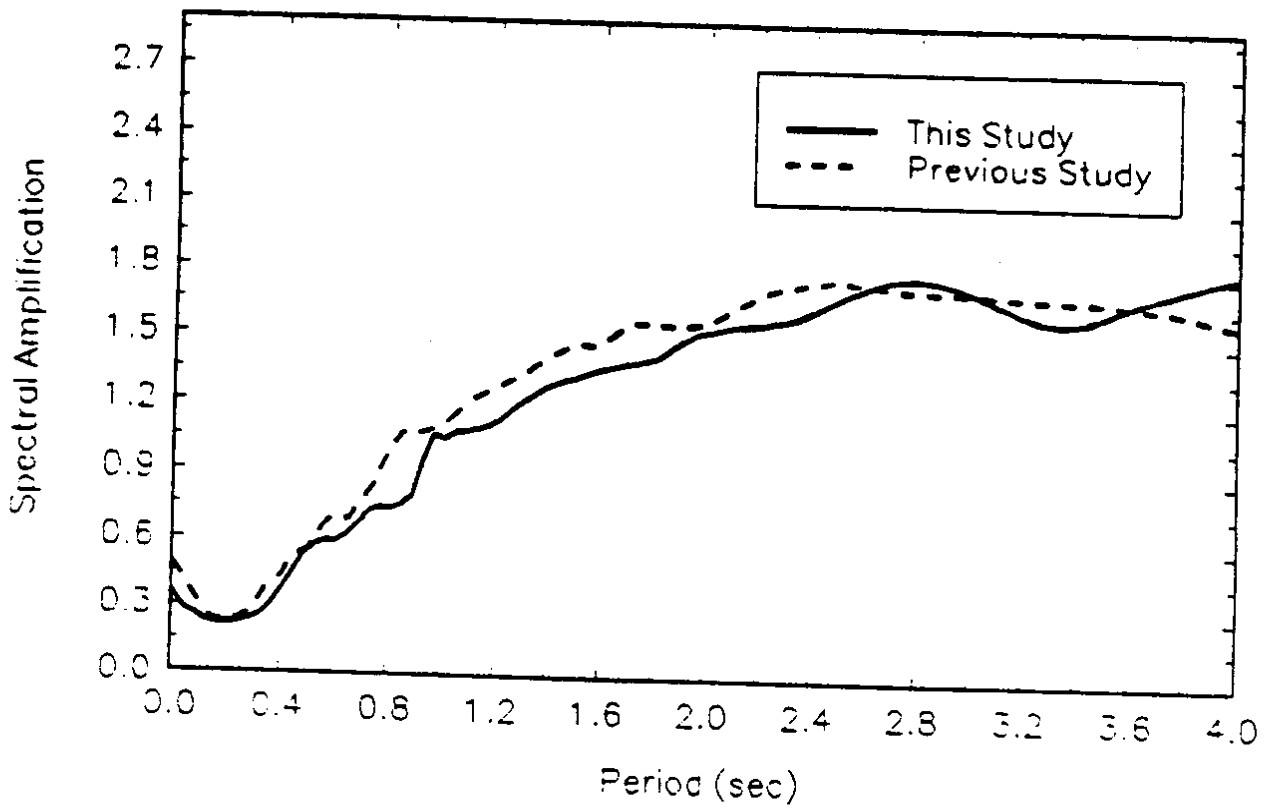

FIGURE 33. Amplification spectra scaled by 0.2 for Group 9 soils.

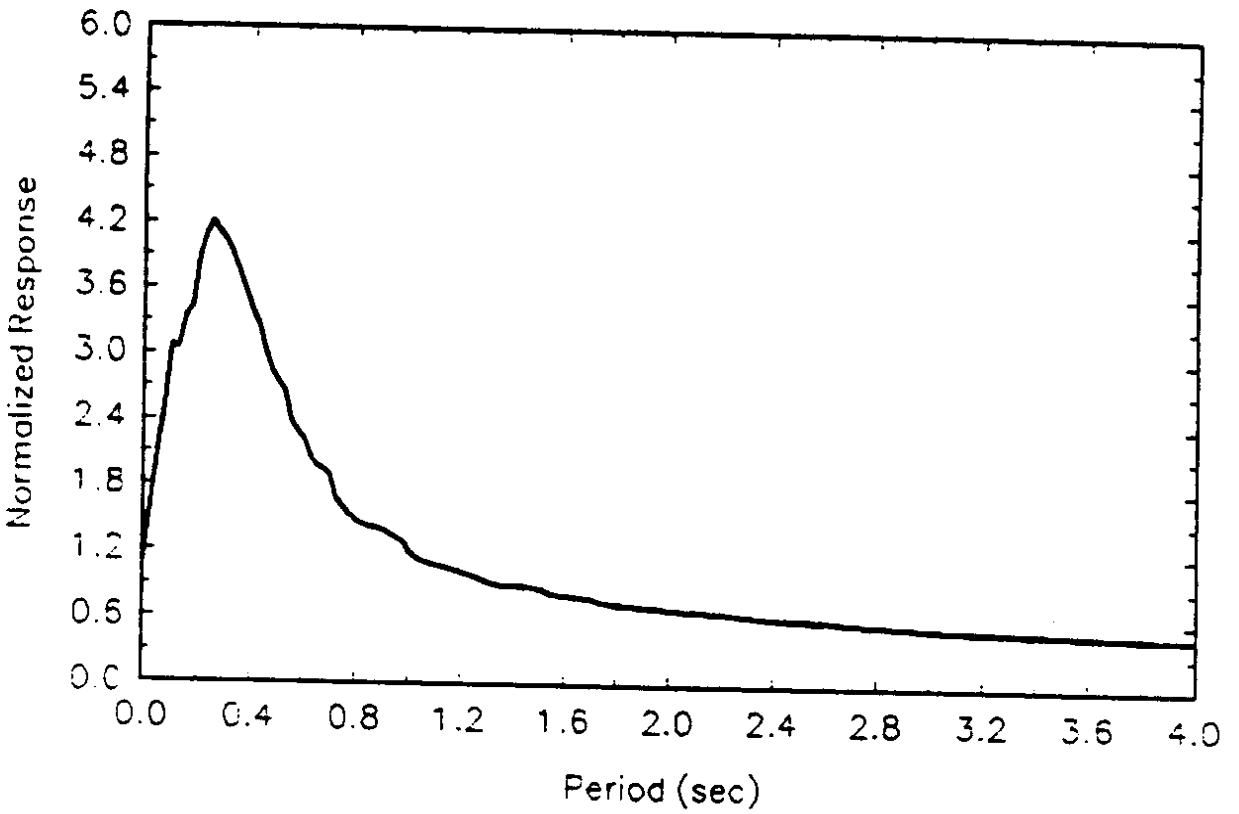

FIGURE 34. Normalized response scaled by 0.2 for Group 1 soils.

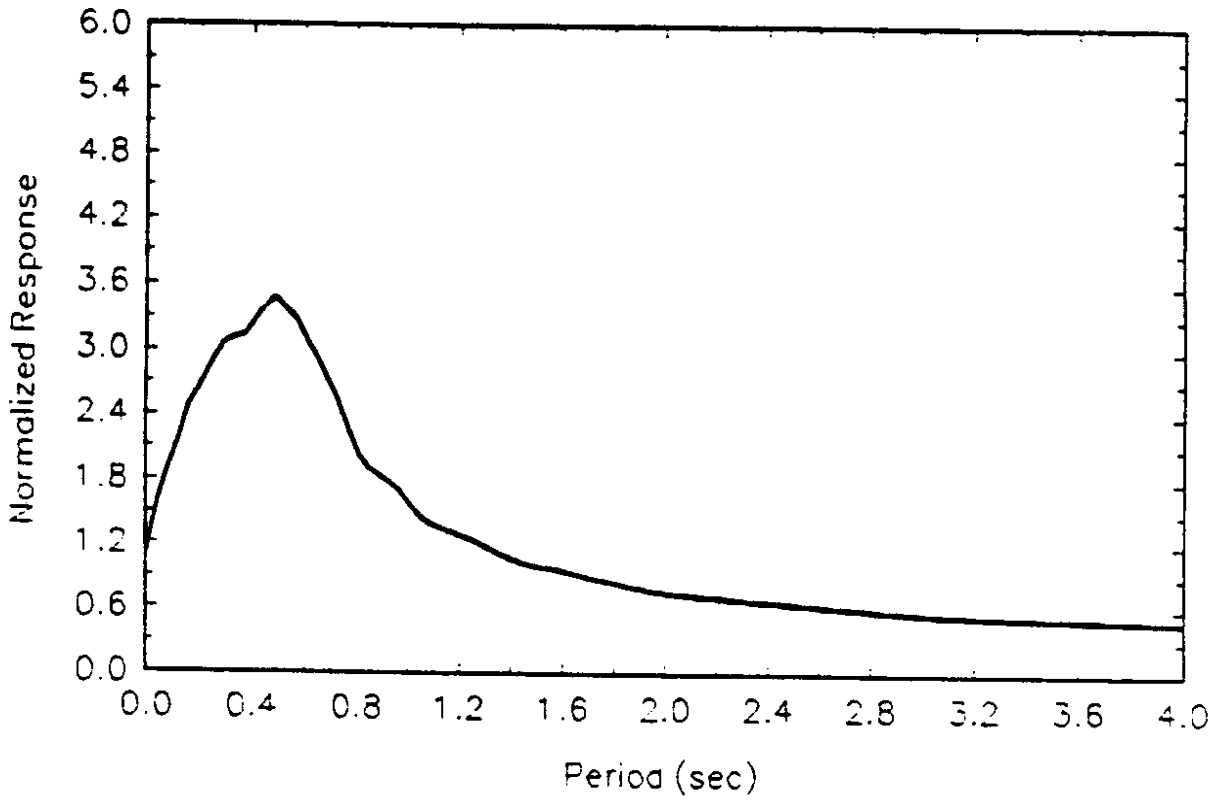

FIGURE 35. Normalized response scaled by 0.2 for Group 2 soils.

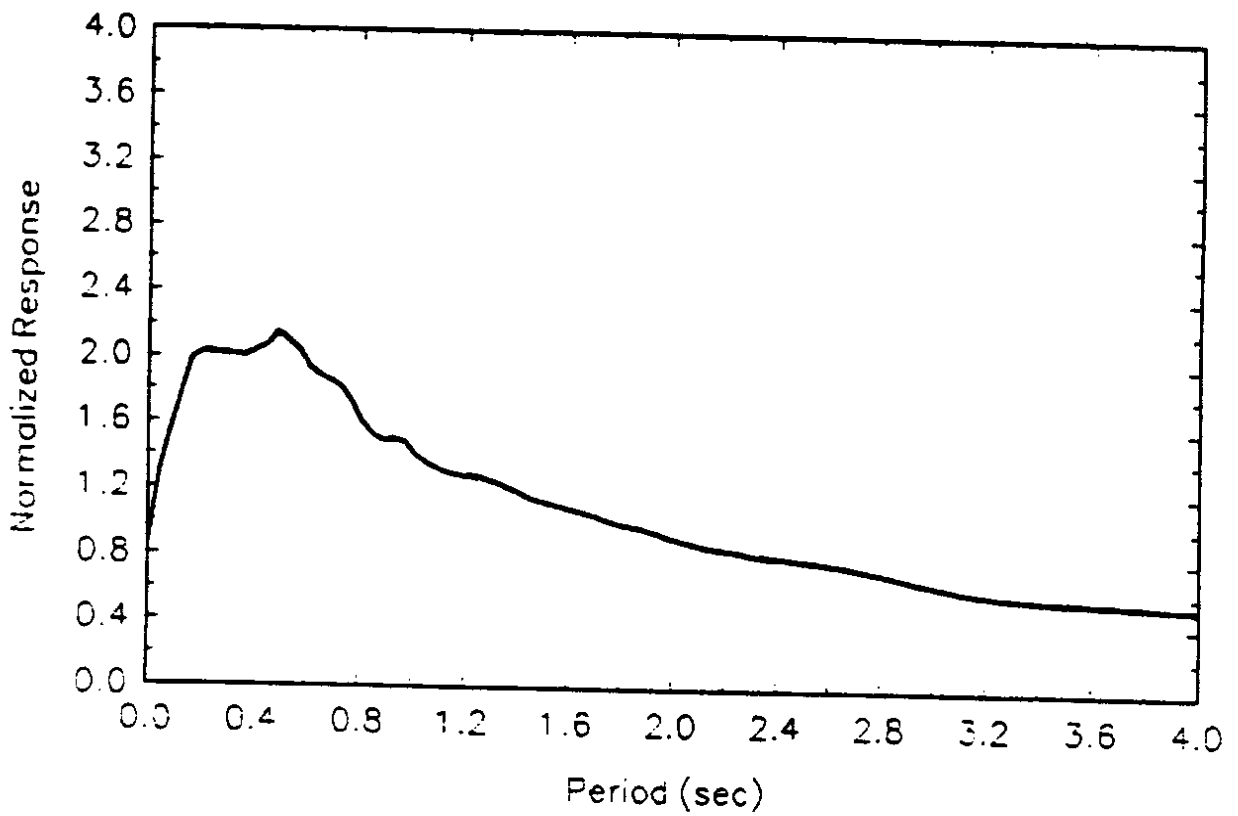

FIGURE 36. Normalized response scaled by 0.2 for Group 3 soils.

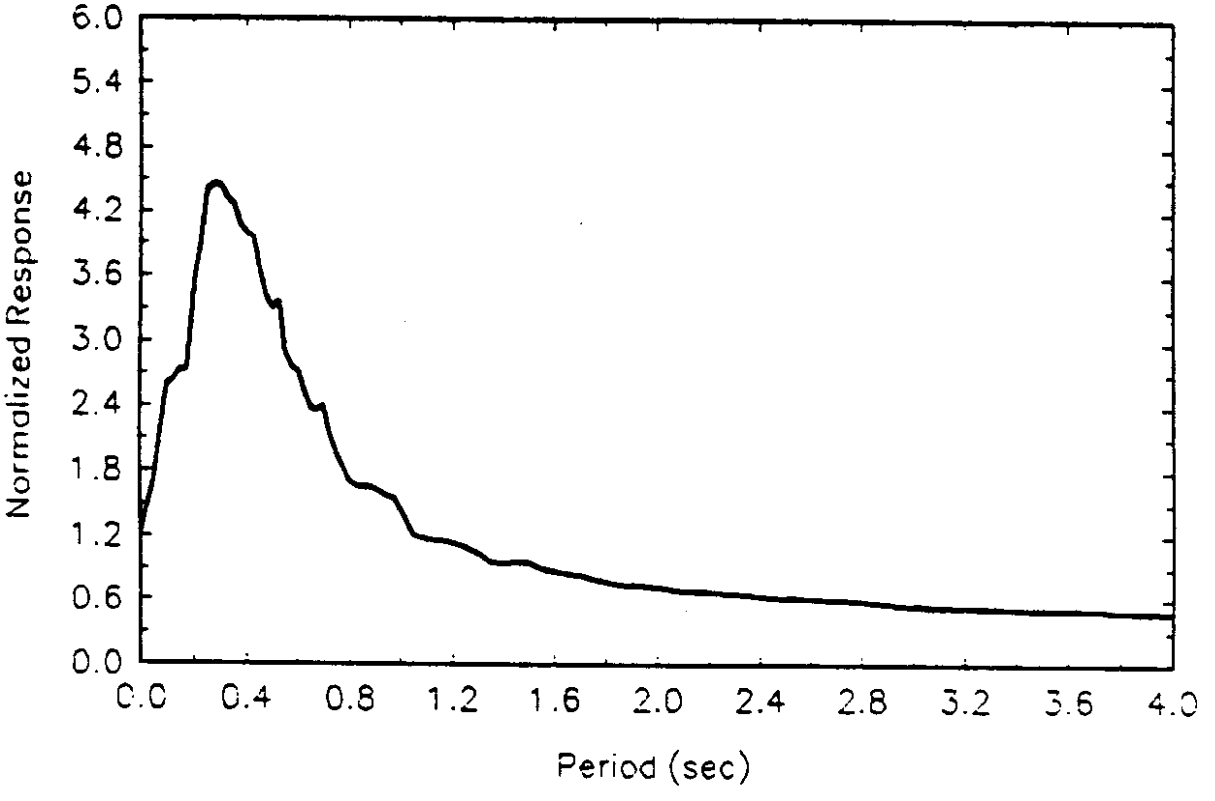

FIGURE 37. Normalized response scaled by 0.2 for Group 4 soils.

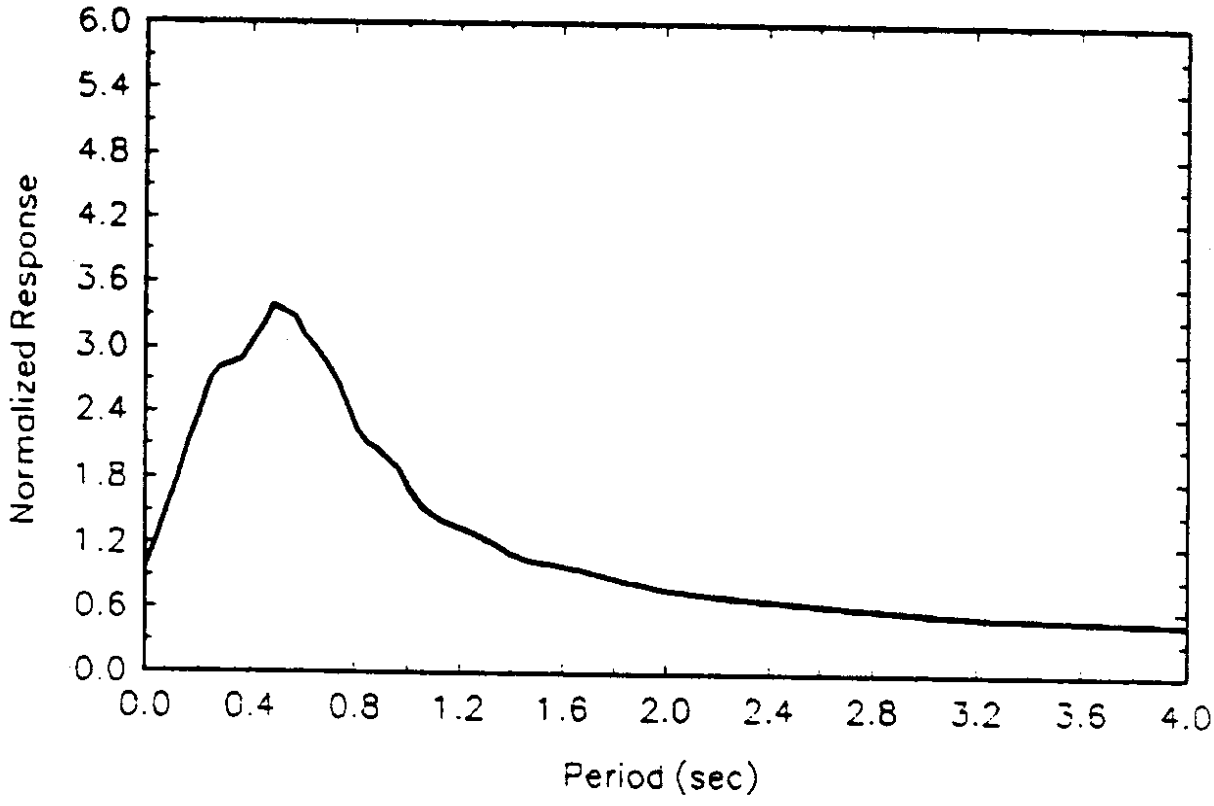

FIGURE 38. Normalized response scaled by 0.2 for Group 5 soils.

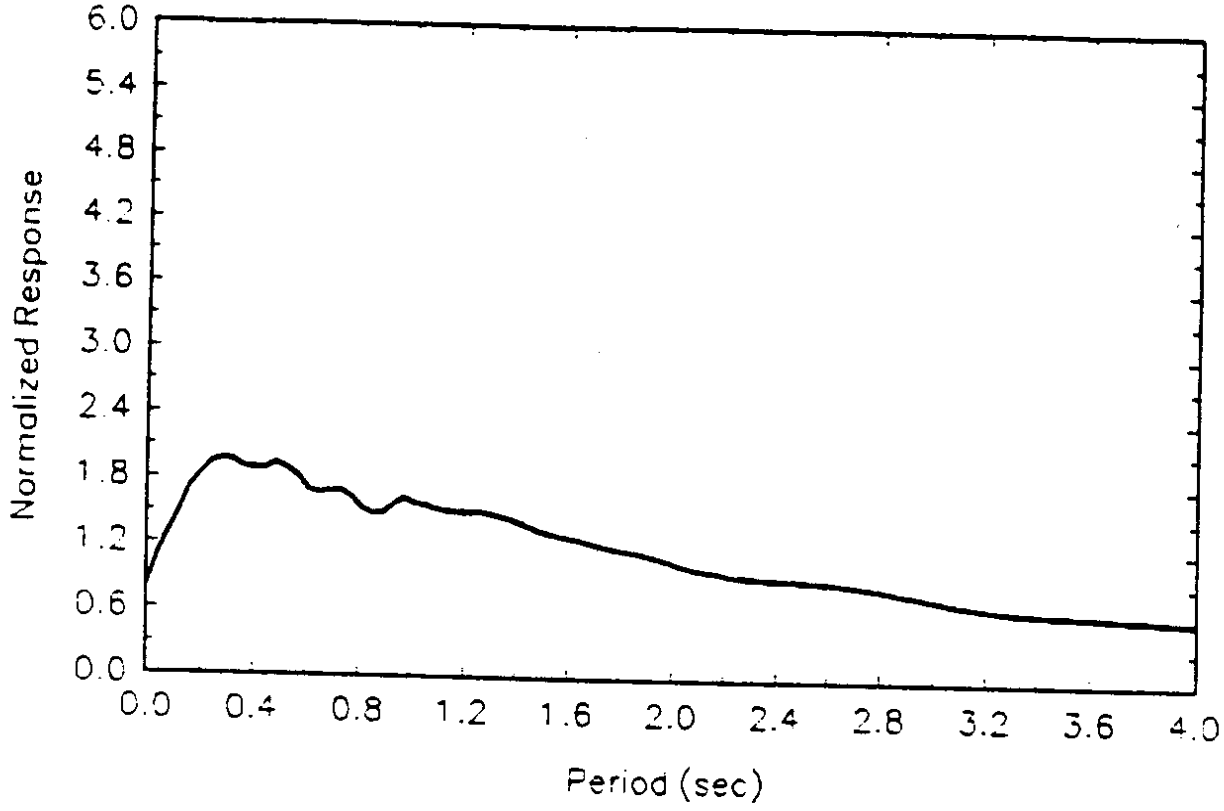

FIGURE 39. Normalized response scaled by 0.2 for Group 6 soils.

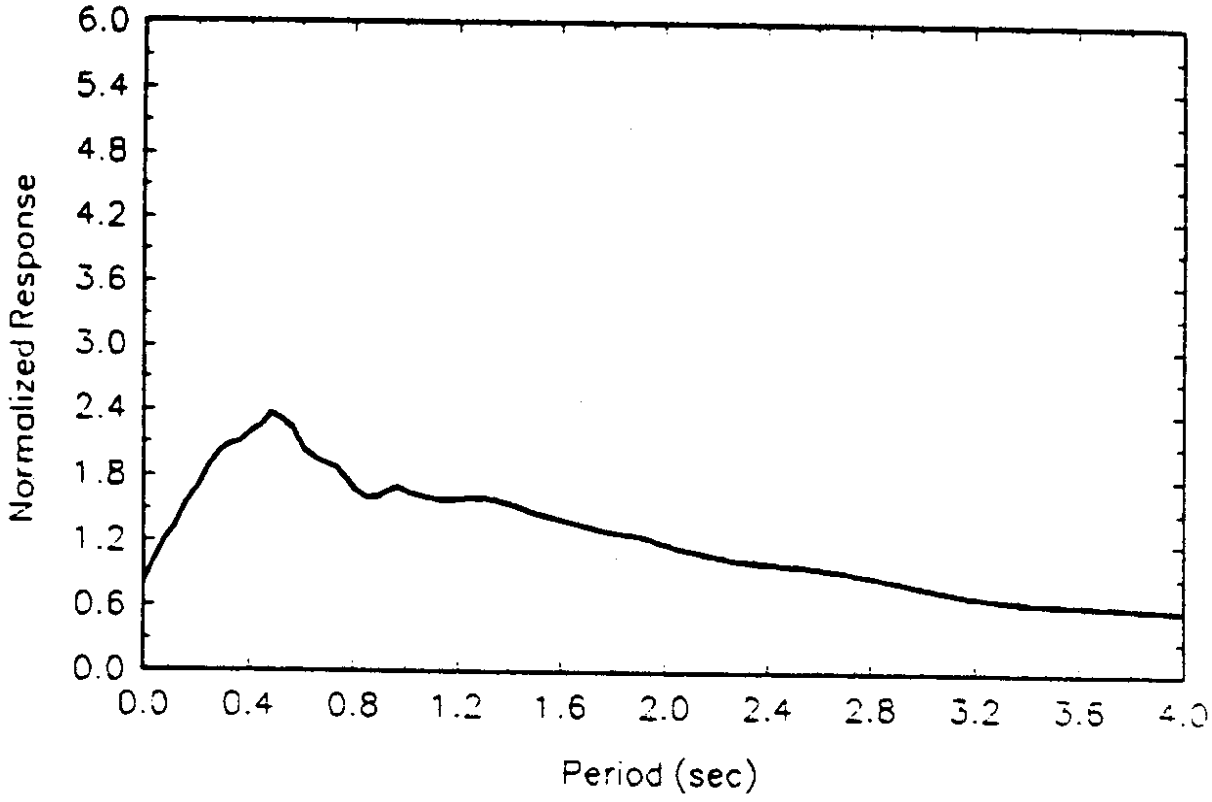

FIGURE 40. Normalized response scaled by 0.2 for Group 7 soils.

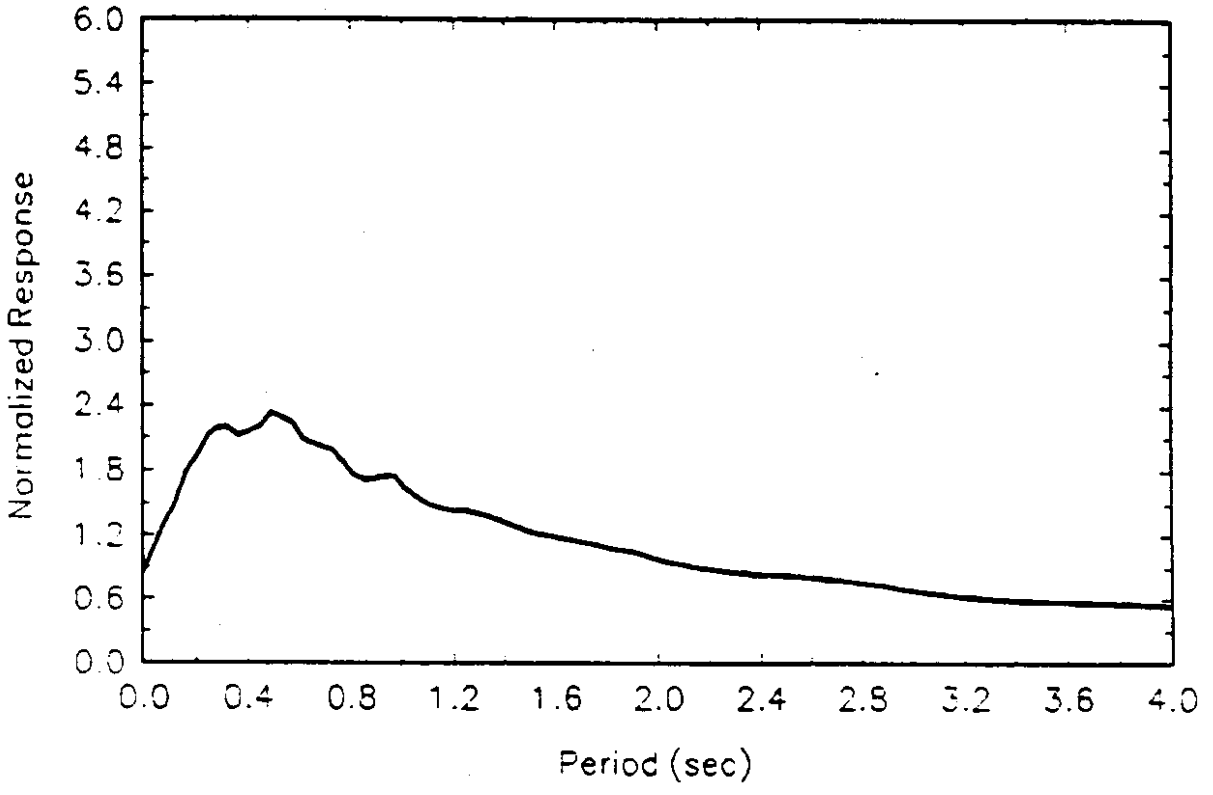

FIGURE 41. Normalized response scaled by 0.2 for Group 8 soils.

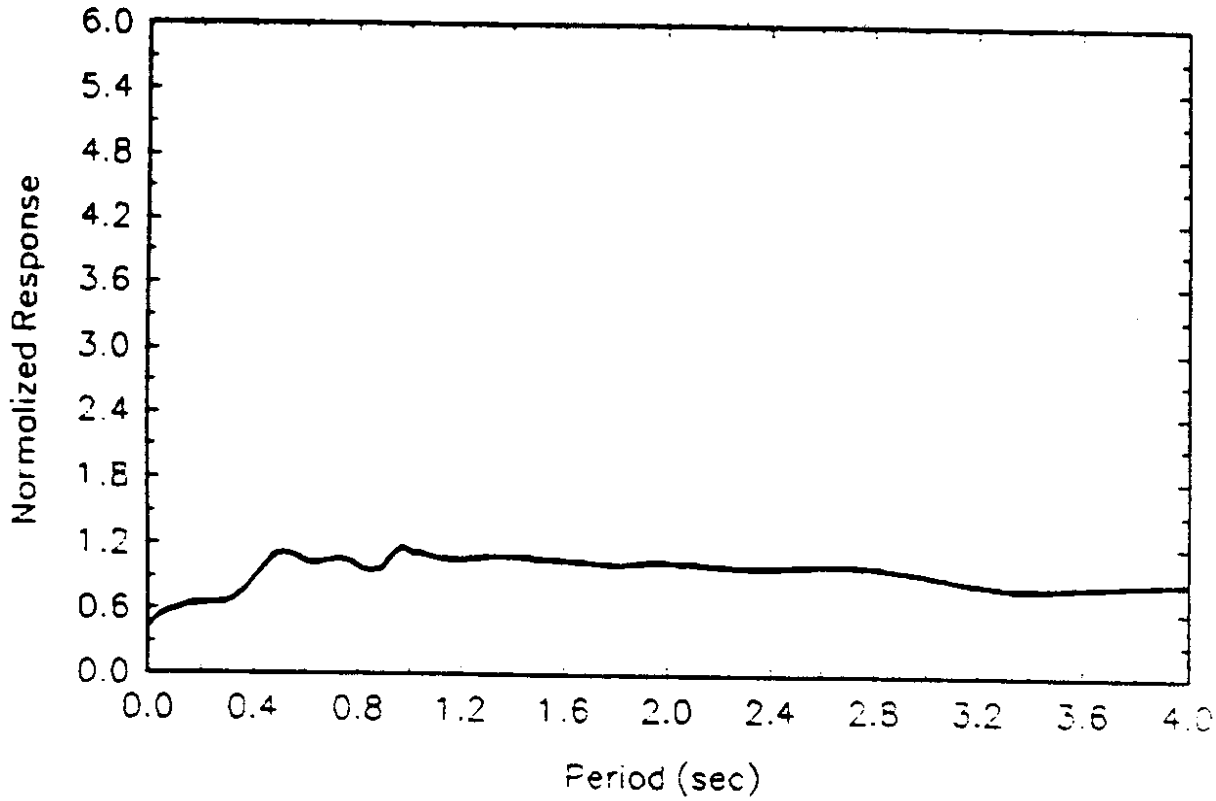

FIGURE 42. Normalized response scaled by 0.2 for Group 9 soils.

Table I SOIL GROUPS

Group 1:	20-50 ft to blow counts of 100 or greater of medium to dense cohesionless soils with up to 5 ft of loose soils (blow counts less than or equal to 10) at the surface. Variable layers of medium and dense soils, with no layers of loose soils beneath the top 5 ft.
Group 2:	51-100 ft to blow counts of 100 or greater of medium to dense cohesionless soils with up to 20 ft of loose soils at the surface. Variable layers of medium and dense soils, with no layers of loose soil beneath the top 20 ft.
Group 3:	100-300 ft to blow counts of 100 or greater of medium to dense cohesionless soils with up to 30 ft of loose soils at the surface. Variable layers of medium and dense soils, with no layers of loose soil beneath the top 30 ft.
Group 4:	10-50 ft to blow counts of 100 or greater of all other soils not in group 1
Group 5:	50-100 ft to blow counts of 100 or greater of all other soils not in group 2.
Group 6:	100-300 ft to blow counts of 100 or greater of all other soils not in groups 3, 7.
Group 7:	100+ ft to blow counts of 100 or greater of soils consisting primarily of clays or clays and loose sands.
Group 8:	COAST SITES, 10-50 ft of loose silt and sand (not necessarily to SPT=100).
Group 9:	COAST SITES, 50+ ft of loose silt and sand (not necessarily to SPT=100).

generally applies to profiles in groups 5 and 6. Figure 43 shows the effect of change in shear modules on the response of profile 043A from group 1.

The unit weights of soil layers were changed by ±10 percent for different profiles in different groups. In general, the results were not sensitive to the change in unit weight. Figure 44 shows the effect of change in unit weight on the response of profile 043A from group 1.

The effect of change in water table level on the response was also examined for several soil profiles. Figure 45 shows the response of soil profile 043A from group 1 with different water table levels. Lowering the water table level decreases the response. The effect of change in water table level on response is negligible.

The effect of change in the damping ratio on the response was tested. Lowering the damping ratio increases the response, while increasing the damping ratio decreases the response. Figure 46 shows the effect of change in damping ratio on the response of soil profile 094A from group 5.

COMPARISONS

By looking on the spectral amplification curves, one notices that spectra developed in this study tend to have smaller high frequency (short period) components and larger low frequency (long-period) components with increasing depth and softness of the soil profile. This agrees with the spectra developed by Seed et al. [12] and the spectra found in the AASHTO specifications [4]. Figure 47 shows a comparison between the spectra developed in this study and the spectra developed by Seed et al. [12] for four soil

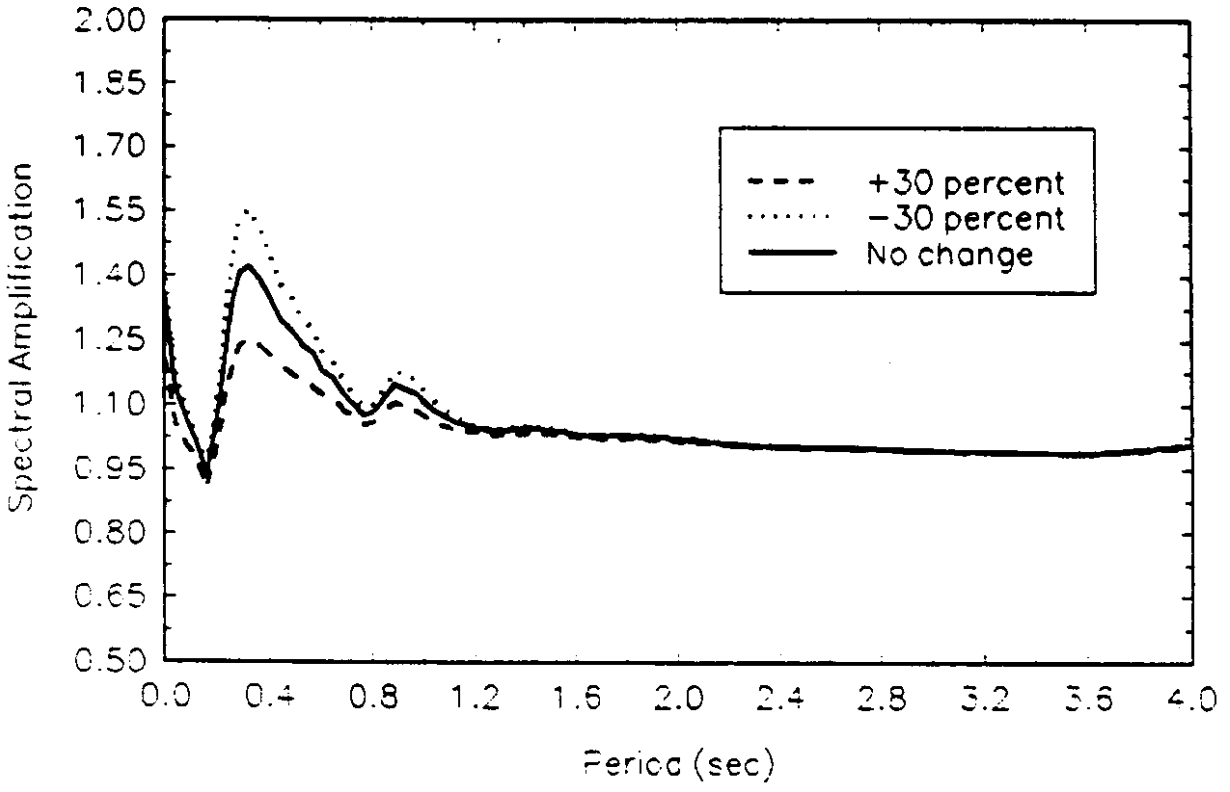

FIGURE 43. Effect of change in shear modulus on the response of profile 043A from group 1.

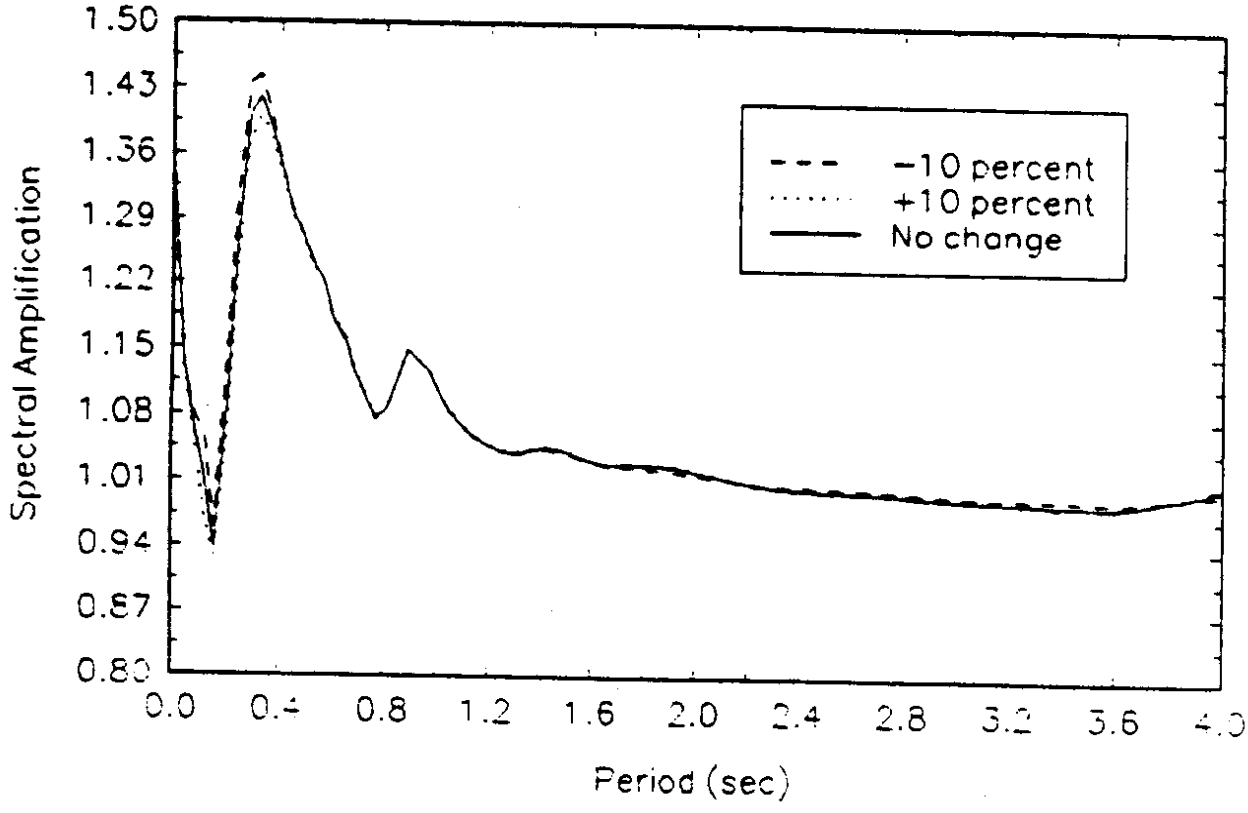

FIGURE 44. Effect of change in unit weight on the response of profile 043A from group 1.

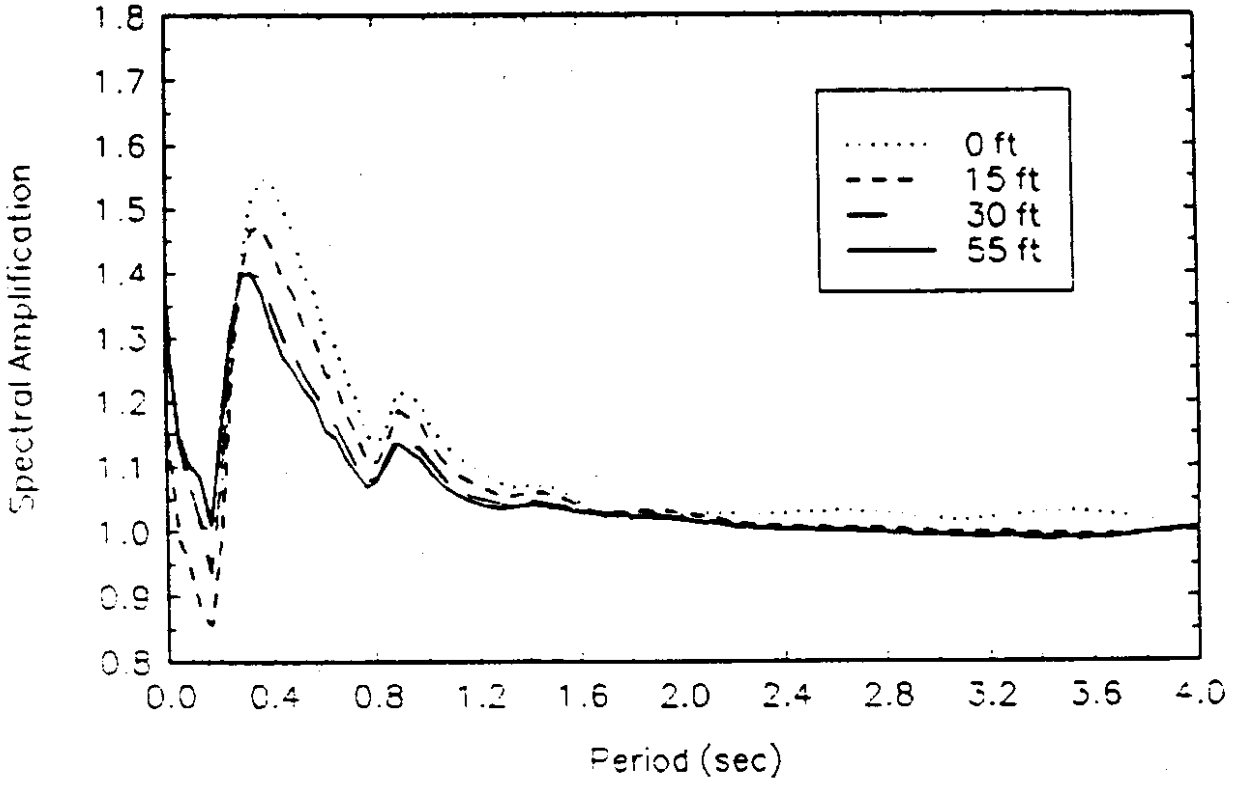

FIGURE 45. Effect of change in water table level on the response of profile 043A from group 1.

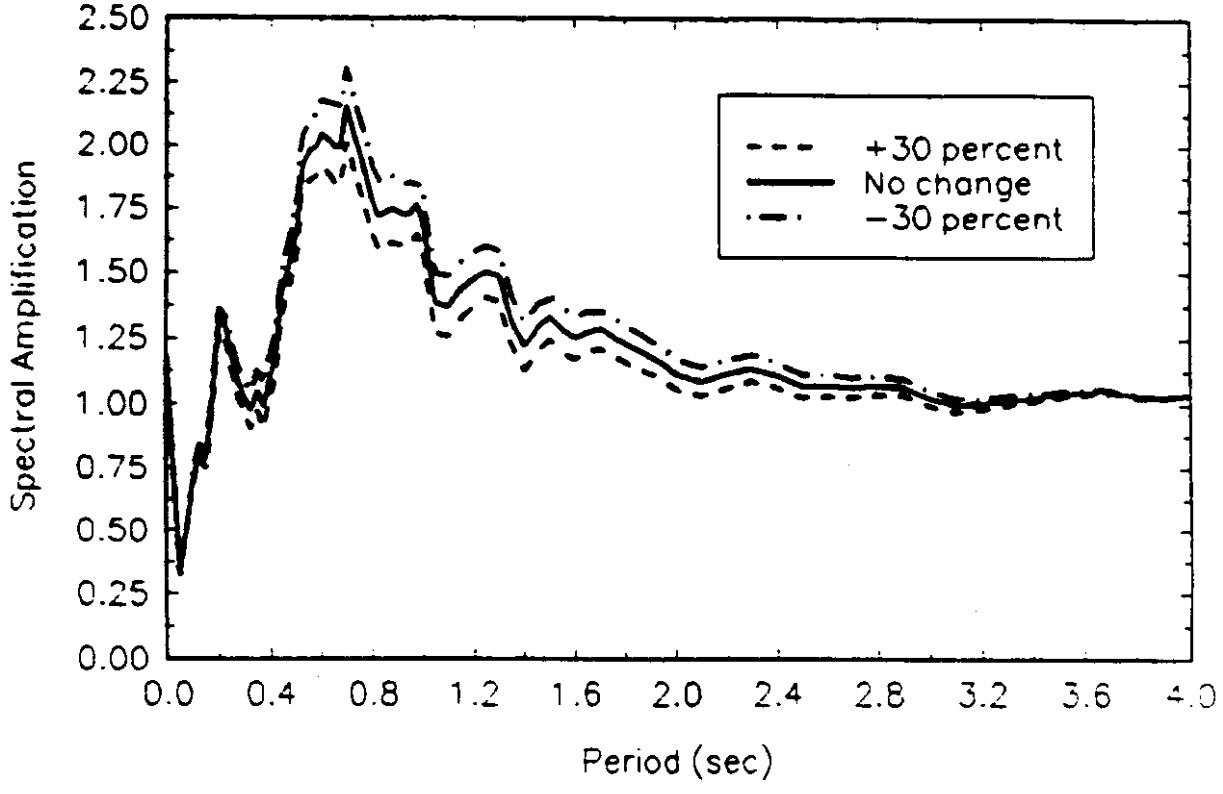

FIGURE 46. Effect of change in damping ratio on the response of profile 094A from group 5.

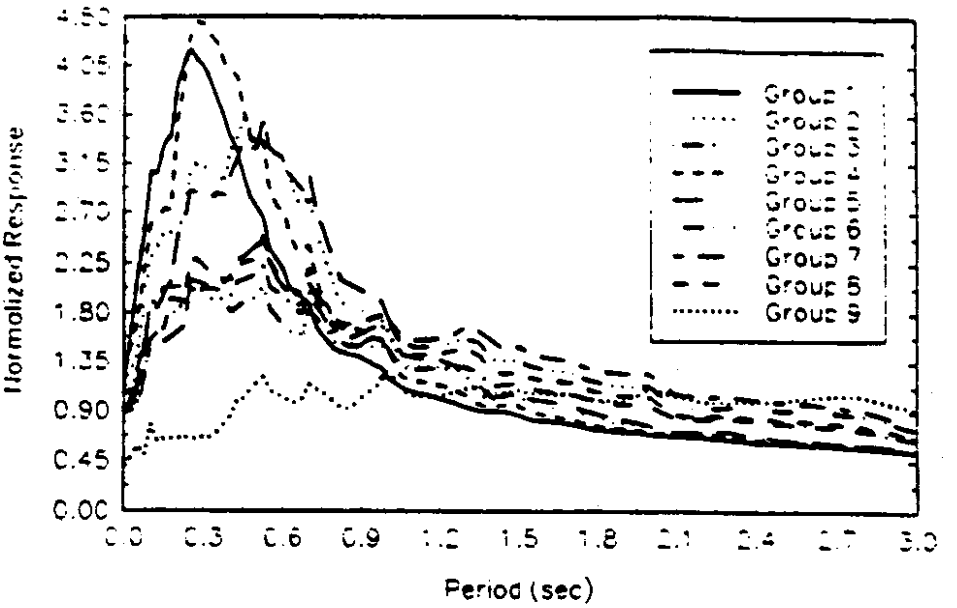

(a)

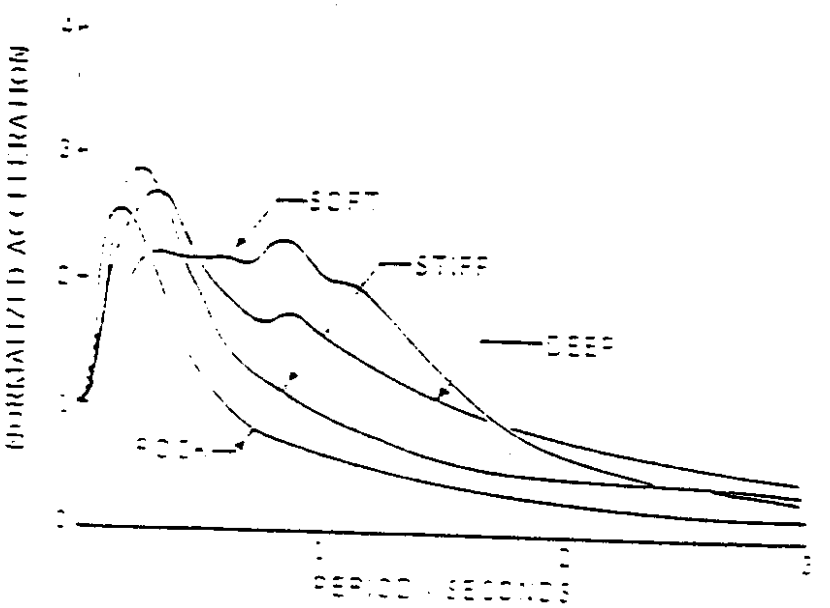

(b)

FIGURE 47. Comparison between (a): spectra developed in this study and (b): spectra developed by Seed et al. [12].

conditions. Figure 48 shows a comparison between the spectra developed in this study and the AASHTO spectra for three soil conditions; Type I soils, including rock and stiff soil conditions, Type II soils, including deep cohesionless or stiff clay soil conditions, Type III soils, including soft to medium clays and sands.

In making these comparisons, one should keep in mind that the AASHTO curves were developed based on research done on California earthquakes. Those earthquakes are different from the subduction zone earthquakes that usually occur in Washington State. California earthquakes have larger high frequency components. The differences in soils in the two states also contribute to the differences in response spectra.

These comparisons show that the results obtained in this study are generally consistent with the results of other researchers and the existing codes from a general point of view. In a more detailed sense, they represent the earthquakes and the soils in Washington State in a more realistic way.

The spectra can also be compared to the response of actual earthquakes that affected the region in the past. The responses of three soil profiles from Vancouver, British Colombia region resulting from the 1976 Pender Island earthquake were compared to the spectra developed in this study. Two of these soil profiles, Roberts Bank and Annacis Island can be classified as group 3 sites. The third soil profile, Brighouse Library, can be classified as a group 6 site. Scaled spectra from groups 3 and 6 are compared to the responses of these three soil profiles due to the Pender Island event and are shown in Figures 49 and 50. These figures show good correlation between predicted and measured spectra.

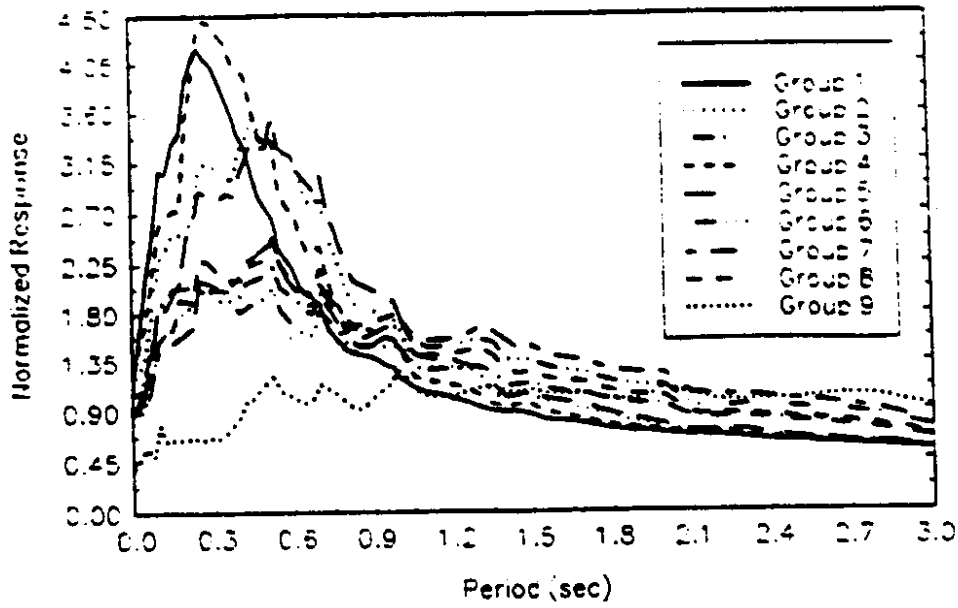

(a)

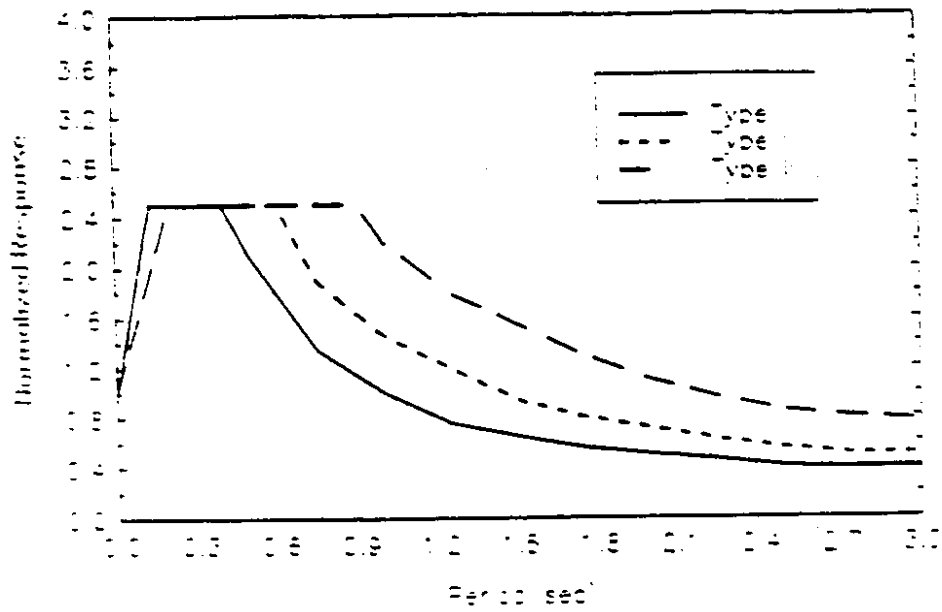

(b)

FIGURE 48. Comparison between (a): spectra developed in this study and (b): AASHTO's specifications.

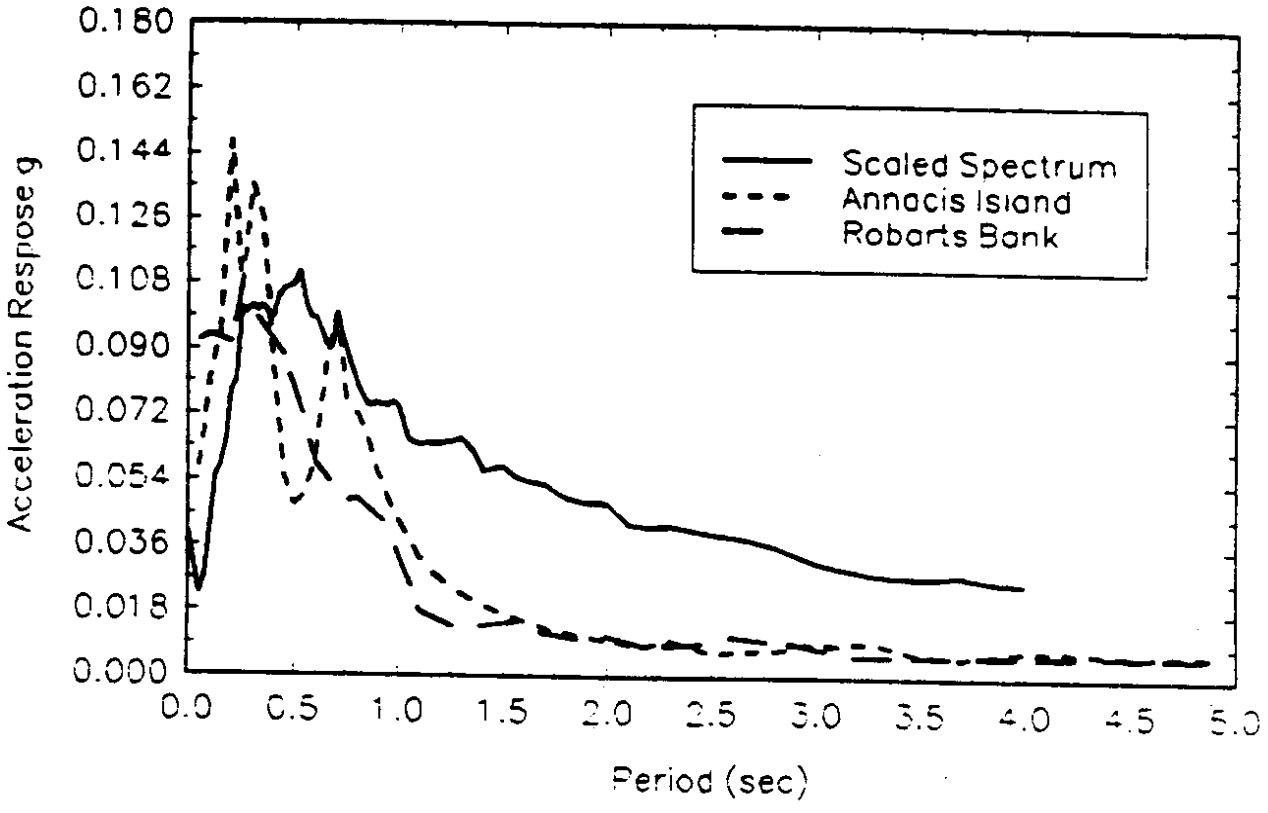

FIGURE 49. Comparison between spectra from group 3 scaled by .05 and the response of Roberts Bank and Annacis Island profiles due to the 1976 Pender Island earthquake.

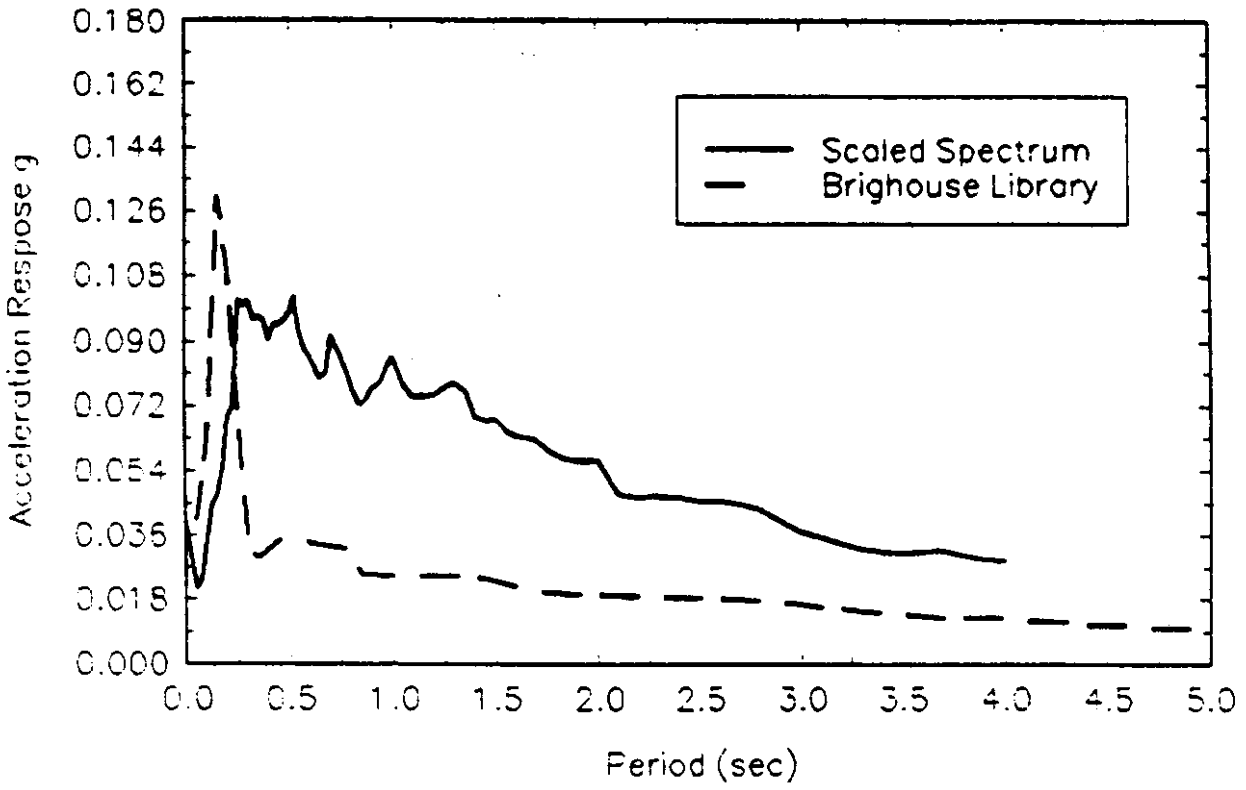

FIGURE 50. Comparison between spectra from group 6 scaled by .05 and the response of Brighouse Library profile due to the 1976 Pender Island earthquake.

The three soil profiles from British Colombia were also used the in non-linear analysis of the response of the Pender Island earthquake. DYNA1D [8] was used to calculate the surface motion of the above soil profiles. The computed motions were compared to the actual recorded motions at these sites. See Figures 51 through 52

Spectra developed in this study was compared to the response of three soil profiles due to the 1976 Pender Island earthquake. Scaled group 3 and 6 spectra are compared to the response of Roberts Bank, Annacis Island and Brighouse Library soil profiles due to the above event. The actual responses are compared well to the scaled spectra.

The measured surface motions of the same three soil profiles due to the Pender Island event were compared to the computed motions due to the same event using the non-linear model. The results did not compare well. This could be due in part to uncertainties in the data available for the soil profiles. Also, the input time history at the base of the three profiles was recorded on rock for the same earthquake at Lake Cowichan Satellite Station. The question whether scaling of the input earthquake motion would be necessary should be examined. This scaling could be necessary because of a difference in the earthquake source to the Lake Cowichan site and the other three sites, or a difference in the rock type through which the seismic waves passed. Scaling could also be necessary because the motions recorded at the surface rock outcrop would be different than those experienced by a buried rock surface, even if the two sites are close to each other. These problems along with the uncertainties in the data about the dynamic soil properties at the sites could have contributed to the results. Another factor to keep in mind is that the computer code DYNA1D increases high frequency response with shorter

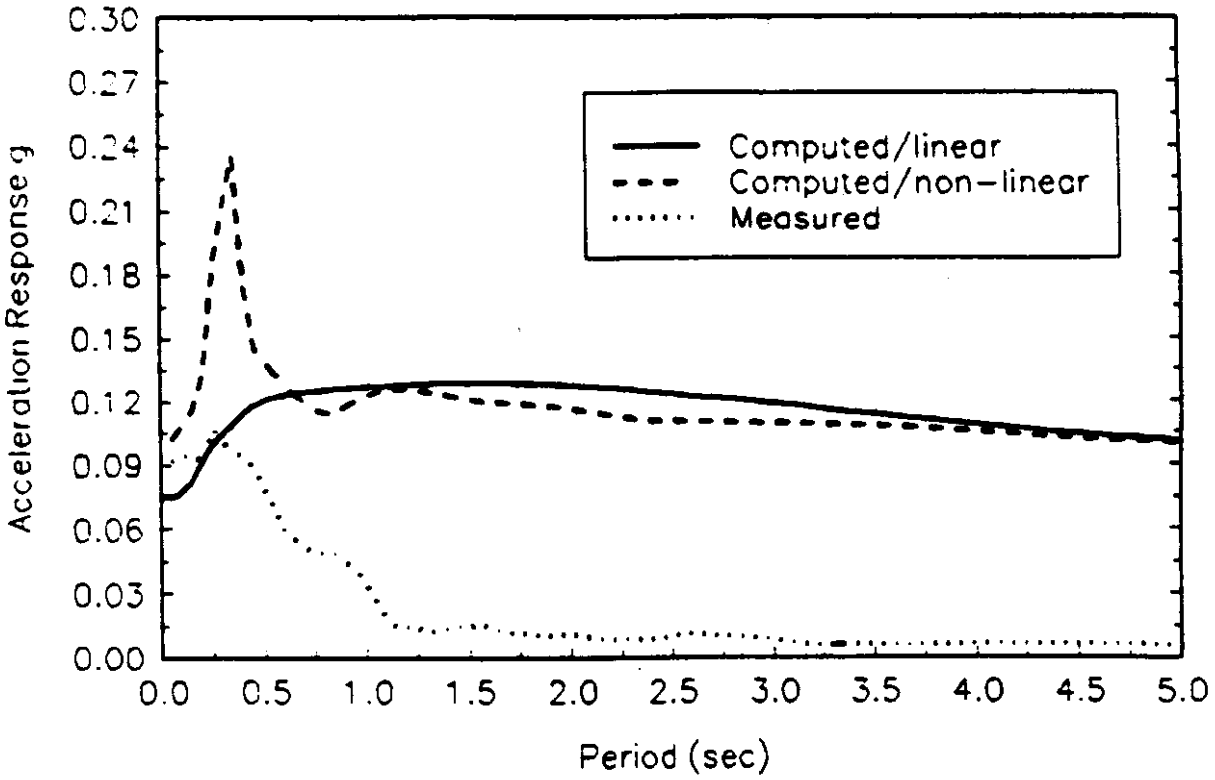

FIGURE 51. Comparison between measured and computed surface motions of Roberts Bank profile due to the 1976 Pender Island earthquake using non-linear modeling.

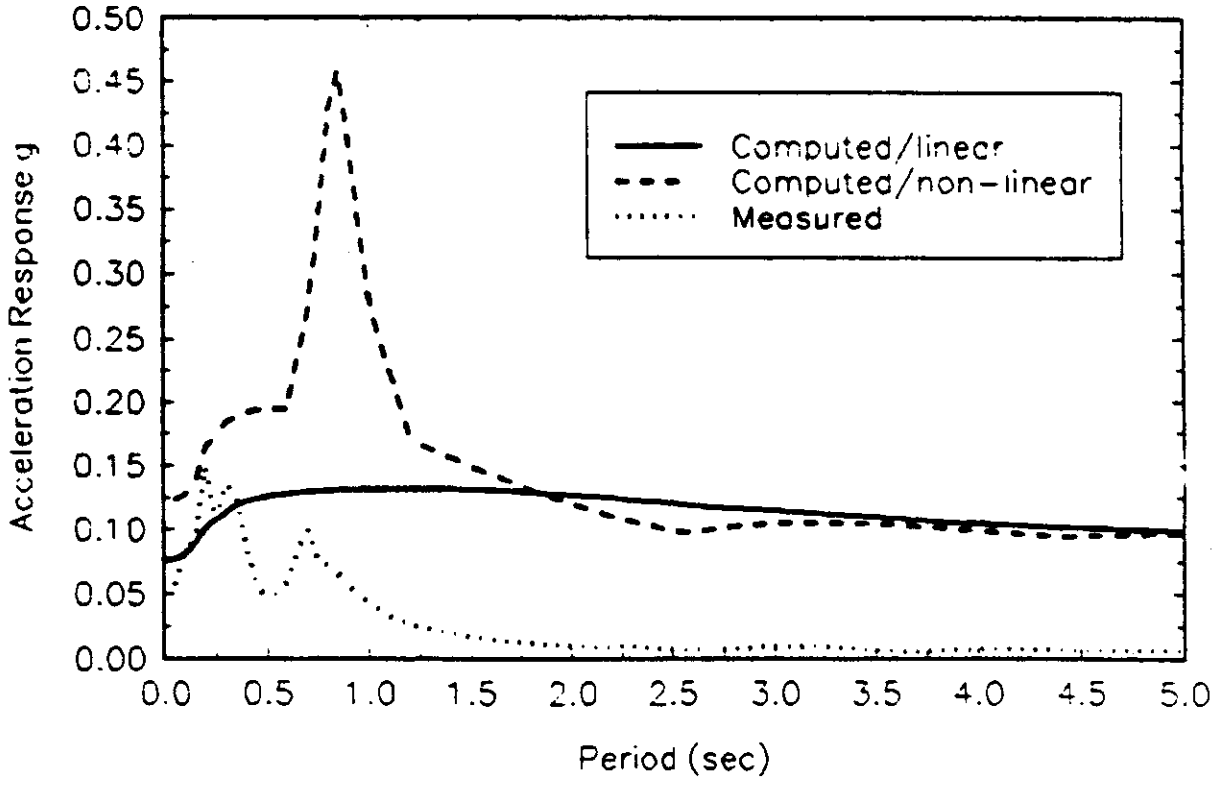

FIGURE 52. Comparison between measured and computed surface motions of Annacis Island profile due to the 1976 Pender Island earthquake using non-linear modeling.

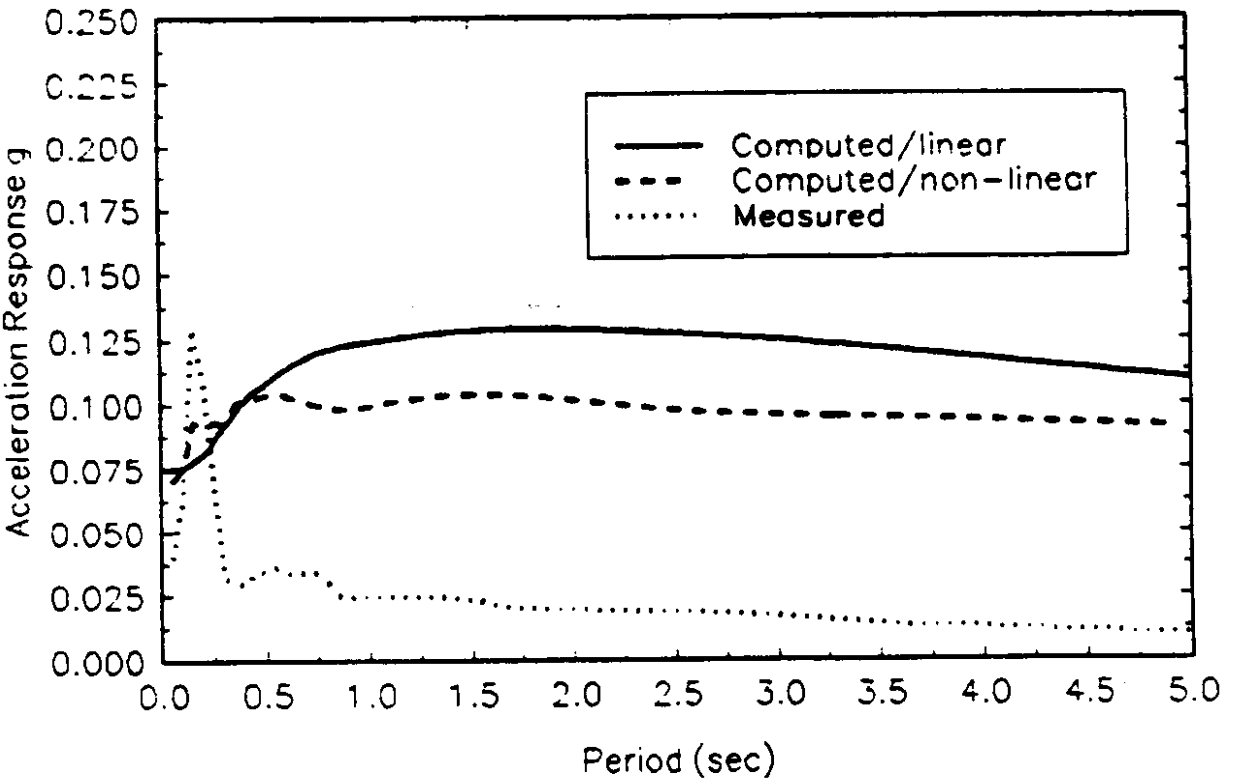

FIGURE 53. Comparison between measured and computed surface motions of Brighouse Library profile due to the 1976 Pender Island earthquake using non-linear modeling.

time steps. This last point is most likely responsible for the high frequency peaks in the Roberts Bank and Annacis Island spectra.

Finally, the computed surface motions for the same three sites due to the Pender Island events using linear and nonlinear analysis were also compared in Figures 51 through 53. The results show fair agreement between the two methods of analysis especially for the long period range. The only major discrepancy was in the high frequency response for the Roberts Bank and Annacis Island spectra. Otherwise, the two methods predict essentially the same response.

IMPLEMENTATION

The soil amplifications factors developed in this study can be used along the base spectrum and the severity coefficient map to calculate seismic design factors. These factors would be used to calculate the seismic forces experienced on highway bridges resulting from the anticipated ground shaking in Washington State due to earthquakes.

For any period of interest at a certain site, the soil amplification ordinate is multiplied by the ordinate of the base spectrum at that period. The appropriate severity coefficient for that site would give the value of seismic design coefficient (g). Choosing one of the nine soil amplification curves developed in this study would depend on the characteristics of the soil under that site and on the depth of the soil profile. For sites where the soil in extremely stiff and/or shallow, the base spectrum alone should be used. Figure 54 schematically shows that the seismic design coefficient Gs is obtained from the base spectrum and the soil amplification factors developed in this study.

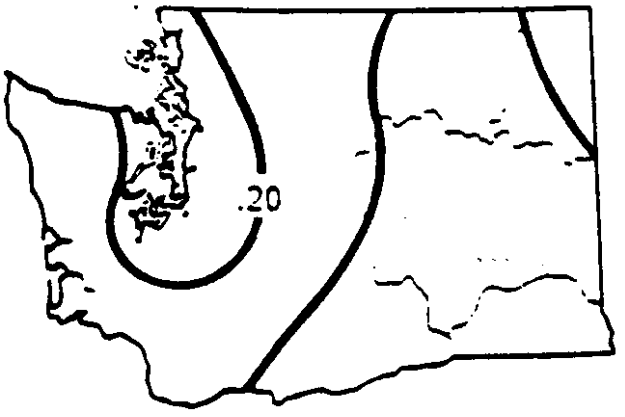

1.) FIND APPROPRIATE SEVERITY COEFFICIENT FOR SITE, EG: .20

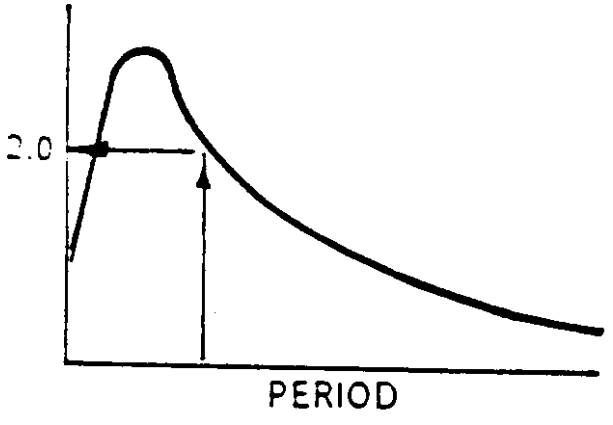

2.) FIND BASE SPECTRUM ORDINATE FOR PERIOD OF INTEREST, EG: 2.0

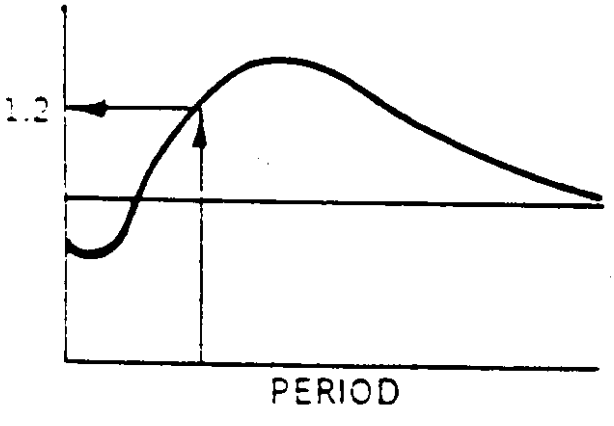

3.) FIND SOIL AMPLIFICATION ORDINATE FOR PERIOD OF INTEREST, EG: 1.2

THEN $C_s = 2.0 * 1.2 * .20$
$= .48$

FIGURE 54. Using the base spectrum and soil amplification spectra developed in this study [6].

SEISMIC ZONATION MAPPING

BACKGROUND

A seismic zonation map displays the spatial variation of some ground motion parameter, typically peak horizontal acceleration or intensity. The zonation process divides a region into areas or zones of similar ground shaking potential. It is usually assumed that peak ground motions are equally likely to occur at any location within a given source zone [21].

The earthquake hazards in the United States have been estimated in a variety of ways since the early fifties. The earlier maps provided an estimate of the severity of ground shaking or damage, but not the frequency of occurrence or damage. While some maps showed the distribution of expected damage in terms of no damage, minor, moderate and major damage, other maps estimated the ground motion in terms of maximum Modified Mercalli Intensity.

In 1976 Algermissen and Perkins [22] developed a probabilistic hazard map covering the contiguous United States. This map of maximum ground acceleration to be expected from earthquakes was based primarily upon the historic seismic record which was rated as incomplete before 1930 to partially complete after 1960. Geological data were not incorporated in the development of this map.

In 1982, Algermissen and others [36] developed a set of probabilistic maps for both acceleration and velocity using three different exposure times. The basic procedure for generating these maps was not greatly different from that for the 1976 map.

New ground motion maps of the contiguous United States were published in the 1988 edition of the NEHRP Recommended Provisions for the Development of Seismic Regulations for New Buildings [37]. These new maps represent the expected maximum horizontal acceleration and velocity in rock for periods of interest (exposure times) of 50 and 250 years. The mapped accelerations and velocities have a 90% probability of not being exceeded in the appropriate exposure times. The new maps are based on the work of Algermissen and co-workers [36]. The NEHRP map of horizontal acceleration in rock with 90% probability of not being exceeded in 50 years was adopted in the 1991 addition of AASHTO Standard Specifications for Seismic Design of Highway Bridges [4].

This section illustrates the model and procedures followed in producing the new map with concentration on the Pacific Northwest region.

THE 1991 AASHTO MAP-MODEL

The concept of hazard mapping used here is to assume that earthquakes are exponentially distributed with respect to magnitude and randomly distributed with respect to time. Seismicity is modeled by grouping it into discrete areas termed seismic zones. A seismic zone is defined as a geologic feature or group of features throughout which the style of deformation and tectonic setting are similar and a relationship between this deformation and historic earthquake activity can be inferred [36].

DEVELOPMENT OF PROBABILISTIC GROUND MOTION MAPS

Producing of probabilistic ground motion maps usually requires three steps:

determination of seismic source area; study the statistical characteristics of historical earthquakes in each seismic source area; calculation and mapping of the extreme cumulative probability of ground motion during certain periods of time. The procedure for developing probabilistic ground motion maps is illustrated in Figure 55 [21].

Earthquakes within a given seismic source can be modeled in three different ways: point sources where the fault rupture length is small compared with the used map scale, finite rupture lengths, or as mixed source. The boundaries of a source zone are defined based on historic seismicity and the interpretation of a variable geologic and tectonic evidence where possible.

Once the source zone has been defined, the magnitude-recurrence relationships are defined for each source zone as:

$$Log\ N = a - b\ M \tag{5}$$

where N is the number of earthquakes in a given magnitude range, M, per unit time and a and b are constants to be determined. If the seismicity of individual source zones in a region is low, the b-value in equation 5 is determined by considering the seismicity of a group of source zones. The a-value for each source zone is determined by fitting a time with slope b through the seismicity data for each zone.

The spatial occurrence of future activity is assumed to be uniform within a given source zone. Thus if the source zone is divided into n subzones and the number of occurrences for a given magnitude range is N, the number of earthquakes likely to occur in each subdivision, n, for the given magnitude range is N/n.

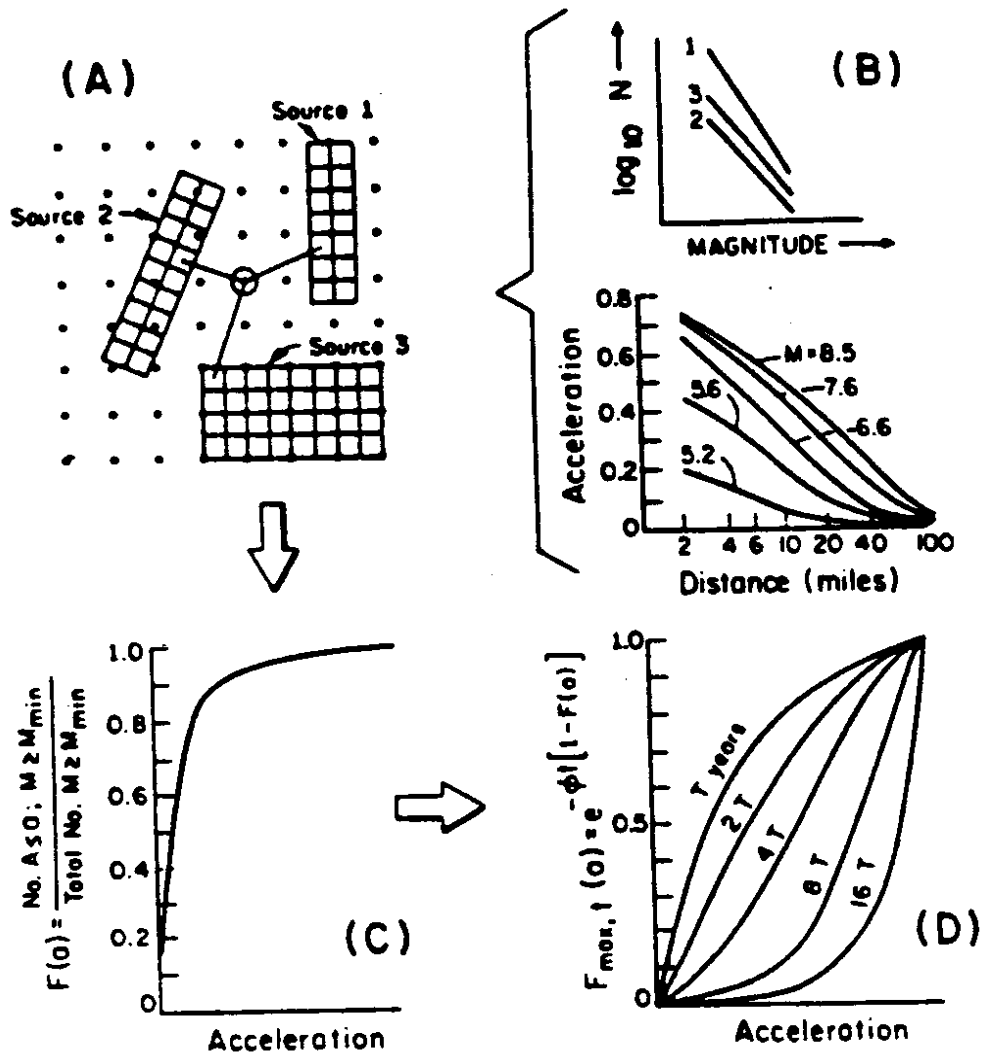

Elements of the hazard calculation:

(A) Typical source areas and grid of points at which the hazard is to be computed.

(B) Statistical analysis of seismicity data and typical attenuation curves.

(C) Cumulative conditional probability distribution of acceleration.

(D) The extreme probability $F_{max,\ t}(a)$ for various accelerations and exposure times (T).

FIGURE 55. Development of ground motion map [21].

If seismicity is distributed along a fault of length L, the distribution of earthquakes is somewhat more complicated. Mark [38] suggested the following relationship between fault length and magnitude:

$$Log\ L = 1.915 + 0.389\ M \qquad r=0.70 \qquad s=0.52 \tag{6}$$

where L is the average fault rupture length in meters, M is magnitude, and s is the variation in attenuation of Log L.

After determining the distribution of earthquakes likely to occur in each subdivision of the source or along a fault, the ground motion at many sites, usually on a regular grid spacing is calculated. From the distribution of ground motion at each site on the grid it is possible to calculate the expected number of times a particular amplitude of ground motion is likely to occur in a given period of years at a given site. Then, the maximum amplitude of ground motion in a given number of years corresponding to any level of probability. This procedure is summarized in the following paragraphs [36].

The cumulative conditional probability distribution, F(a) of the desired ground motion parameter, such as acceleration, is calculated, see Figure 55C.

$$F(a) = \frac{expected\ No.\ of\ occurrences\ with\ A \le a\ \wedge\ M \ge M_{min}}{total\ expected\ number\ of\ occurrences\ (M \ge M_{min})} \tag{7}$$

or

$$F(a) = P\ [\frac{A \le a}{M \ge M_{min}}]$$

where a is equal to the maximum value, and A is equal to the observed value. M_{min} is a predefined minimum magnitude. The peak ground motion corresponding to some

extreme probability, $F_{max,t}(a)$, is calculated for different exposure times (see Figure 55D). The extreme probability function $F_{max,t}(a)$ is defined as:

$$F_{max,t}(a) = e^{-\phi t [1-F(a)]} \quad (8)$$

where ϕ is the mean ratio of occurrence of earthquakes $M \geq M_{min}$ per year and t is the number of years in the period of interest (exposure time) and F(a) is the cumulative probability function. A table of accelerations (a) and F(a) is constructed. For a particular exposure time t=T, $F_{max,t}(a)$ is calculated, and the values of (a) for a given extreme probability, say $F_{max,t}(a) = 0.90$ is found by interpolation.

The term return period can also be defined as:

$$R(a) = \frac{1}{1-F(a)} \quad (9)$$

where R(a) is the average number of events that must occur to get an acceleration exceeding a. Therefore, the return period in years $R_y(a)$ is given approximately by

$$R_y(a) = \frac{R(a)}{\textit{expected No. of events per year } (M \geq M_{min})} \quad (10)$$

or

$$R_y(a) = \frac{-t}{\ln[F_{max,t}(a)]}$$

Thus for extreme probability of 0.90 and exposure time of 10 years the return period $R_y(a)$ = 94.9 years.

SEISMIC SOURCE ZONES IN THE PACIFIC NORTHWEST

The probabilistic ground motion calculations use, as input, a model of future seismicity. This model consists of source zones and their associated rates of activity for earthquakes of various magnitudes up to the maximum magnitude assumed for each zone. The seismicity is assumed to be uniformly distributed within each zone. The size of the source zone is determined by the amount of geological and seismological information available, seismic history, and the scale of mapping.

Unlike the coastal parts of California where individual seismogenic faults and general Cenozoic tectonic development are well known, the Pacific Northwest lacks a detailed regional tectonic model for Cenozoic tectonics. An important question related to the tectonic development of the Pacific Northwest is the origin of deep focus earthquakes in the Puget Sound area. As mentioned in previous sections, many researchers provided geophysical, stratigraphic, or tectonic arguments in favor of the subduction of Juan de Fuca plate beneath the west coast. The rate of subduction, the degree of coupling and the shape of subduction are all still a matter of debate[21].

Instead of developing regional tectonic model, observations on the geographical distribution of seismicity as it relates to geological features are useful. The youngest orogenic province in the region is the Cascade Range which has large volumes of Quaternary Volcanic rocks. Within the Puget Sound area, zones boundaries are based on seismicity alone as there are no dominant faults on known specific geologic structures that govern the spatial pattern of seismicity. The Puget Sound zones are within a broad region that encloses the Puget Sound-Willamette Depression [36].

In northeastern Oregon and southeastern Washington, seismic zones have a northwest trend that is sub-parallel to the Intermountain Seismic Belt in western Montana. Figure 56 shows a map of nineteen seismic source zones in the Pacific Northwest [39]. The estimates of uncertainty for fault rupture length relationships used for the maps were based on the following relationship which was provided by Mark [38].

ATTENUATION

The acceleration attenuation relationships for the western United States provided by Schnabel and Seed [40] were used in producing the new maps. In the Puget Sound area, the Schnabel and Seed curves were modified to reflect the greater focal depths of earthquakes originating at this region. Figure 57 shows acceleration attenuation relationships applicable for the western United States given by Schnabel and Seed. The velocity attenuation used in the preparation of the maps was developed by Perkins and Harding [41] using a data set and methods of analysis similar to that of Schnabel and Seed [40]. The current AASHTO map of acceleration coefficient is shown in Figure 19.

WSDOT MAP OF ACCELERATION COEFFICIENT

The map of acceleration coefficient currently used by WSDOT was developed by Higgins et al. 1988 [21]. This map is based on the maps of peak acceleration and velocity on rock for the Pacific Northwest developed by Perkins et al. in 1980 [11].

The Perkins et al. [11] maps display peak accelerations and velocities for return periods of 100, 500 and 2500 years based on 19 source zones. Discrimination of these

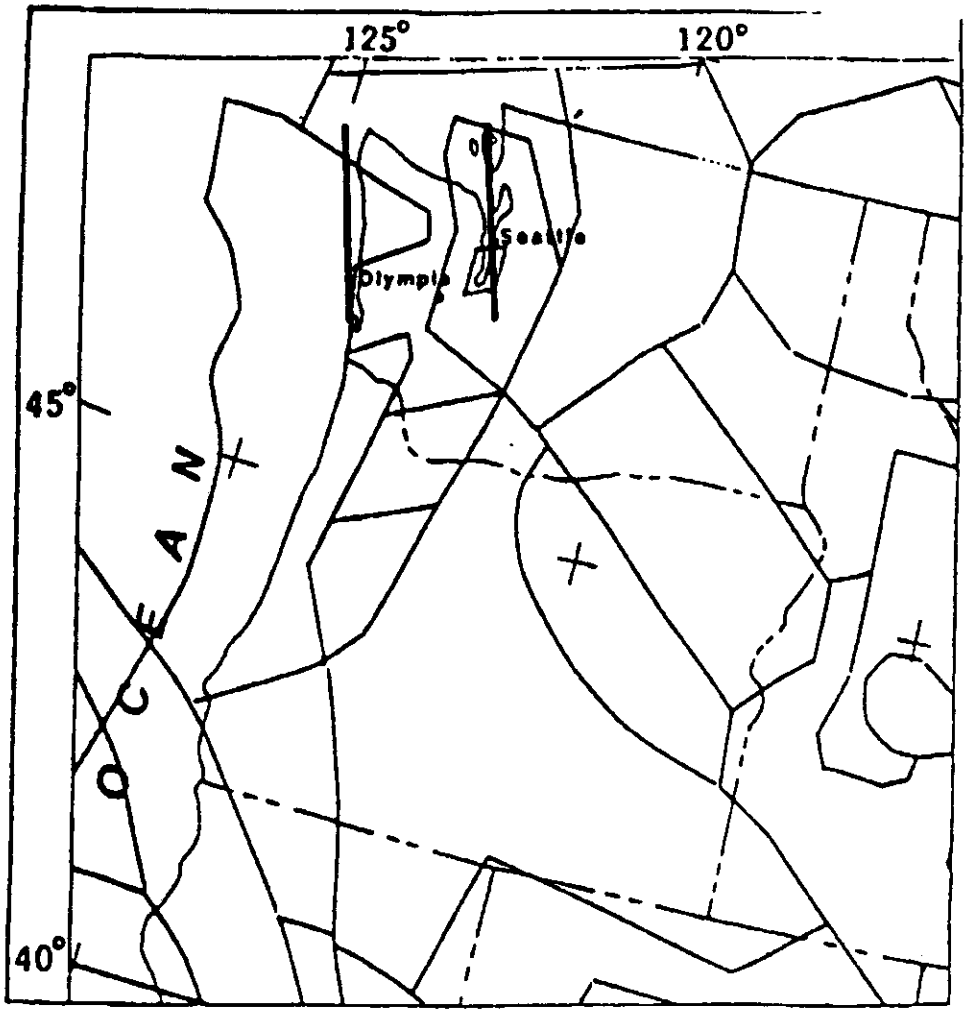

FIGURE 56. Seismic source zones in the Pacific Northwest [39].

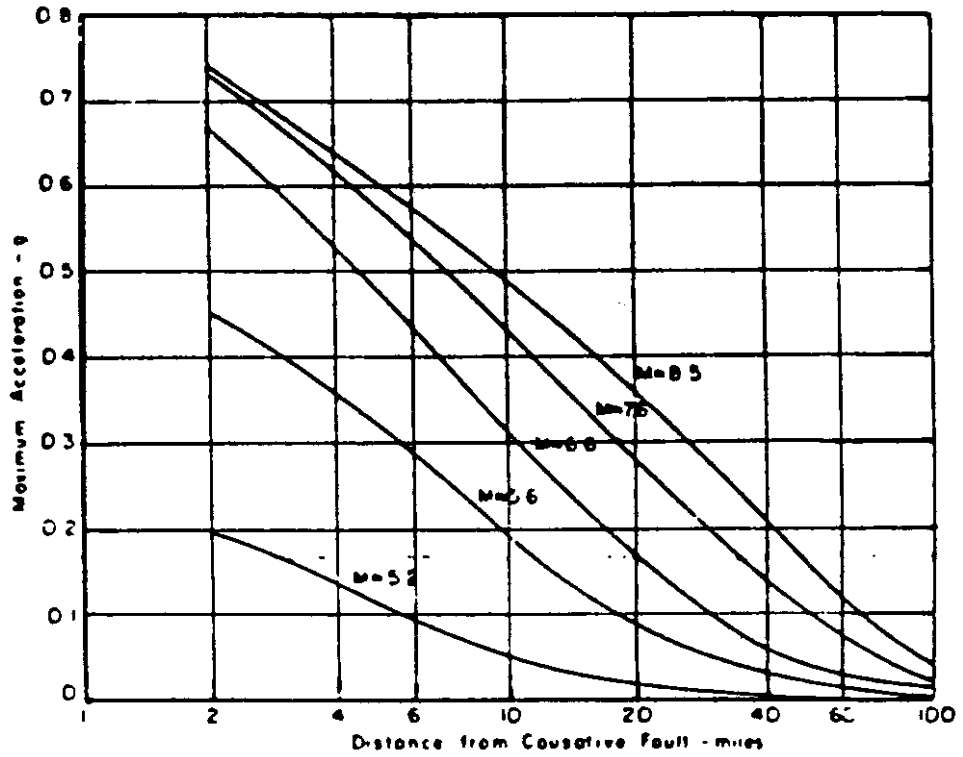

FIGURE 57. Acceleration attenuation curves for the Pacific Northwest [40].

zones followed a method based on integrating historic seismicity with available geologic information [11]. Because many seismogenic zones do not have enough earthquakes to make a reliable estimate of the underlying rates of seismic activity, Perkins et al. combined all of the seismogenic zones into one of five groups. The appropriate group was determined by contiguousness and general tectonic character. Recurrence rates were calculated for each group based on the relationship:

$$Log\ N = a + b\ M_s \tag{11}$$

where N is the annual occurrence rate, Ms is surface wave magnitude, and a and b are regression constants.

Acceleration attenuation relationships based on these developed by Schnabel and Seed [40] were used. The velocity attenuation curves were developed similarly to the acceleration attenuation curves of Schnabel and Seed.

After reviewing all the efforts of producing seismic zonation mapping applicable to the Pacific Northwest, Higgins et al. [21] chose the maps of peak acceleration and velocity on rock developed by Perkins et al. in 1980 [11] to be the basis of developing a new map for the specific use of WSDOT. The Perkins et al. maps were chosen in Higgins et al. study for two reasons: they are considered an improvement over the original 1976 maps, and they express velocity in the same probabilistic terms as acceleration, making it possible to develop a velocity-related acceleration.

The purpose of the velocity-related acceleration coefficient, A_v, is to account for the slower attenuation of velocity than acceleration with distance from the source, and to consider the influence of velocity on the damage of long period structures at a distance

from the source. Higgins et al. argued that a map of A_v could be developed based on the work of Perkins et al., and such a map would provide greater accuracy than the existing AASHTO codes.

Higgins et al. suggested that the A_v contours can be constructed based on the velocity contours by multiplying the a/v ratio at a source by the velocity contour value located at some distance from the source, generating an acceleration coefficient attenuated at the same rate as velocity; i.e., velocity-related acceleration coefficient. For multiple source zones both acceleration and velocity attenuation are dependent on magnitude, and the v/a ratio also varies with magnitude. Thus, the a/v ratio used to transform the velocity contours to A_v contours will vary with the statistical parameters of the seismic source zone influencing the contour at a particular location. If a velocity contour is influenced by more than one seismic source zone and the influencing zones have different statistical parameters, the v/a ratio applied to the contour will vary. Usually this will require a shift in the contour location [21]. Higgins et al. obtained values of a, v, and v/a at various distances from the source for magnitudes of 5.6, 6.6, and 7.6 from the velocity and acceleration attenuation curves used in Perkins et al. study [11]. Using the data and procedures explained above, Higgins et al. constructed the velocity-related acceleration coefficient map of Washington State. This map is shown in Figure 58.

DISCUSSION

It is useful to point out that the old editions of the AASHTO specifications incorporated maps that showed contours of velocity-related acceleration coefficient and

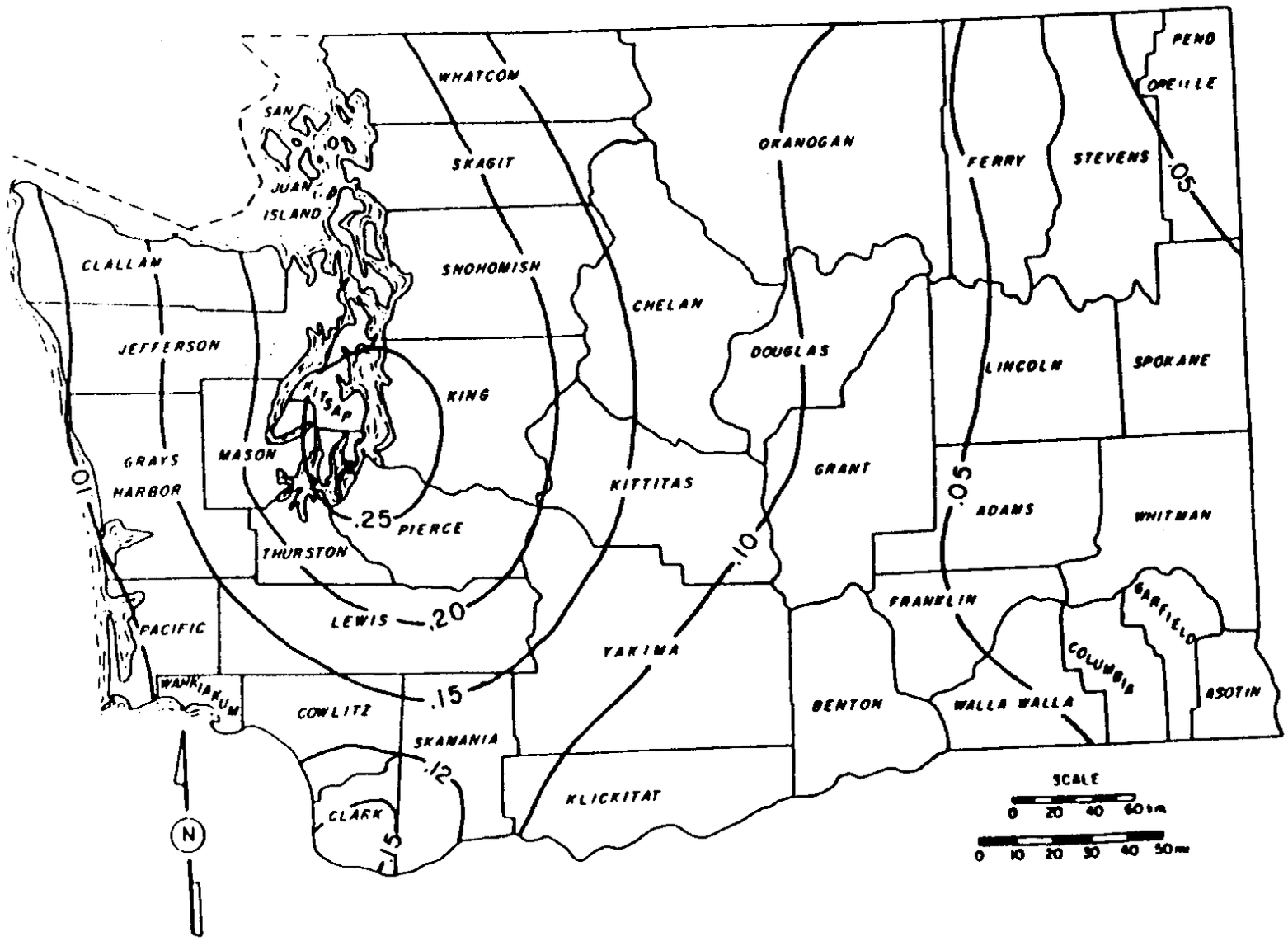

FIGURE 58. Velocity-related acceleration coefficient map of Washington State [21].

not expected peak ground acceleration. This acceleration coefficient was developed specifically as a response spectrum scaling factor for a combination of rock and stiff soil conditions (Applied Technology Council, [23]). The map of acceleration coefficient found in the old editions of the AASHTO specifications is shown in Figure 59. On the other hand, the maps found in the 1991 editions of the AASHTO specifications and based on the maps developed by Algermissen and others [37] show expected peak acceleration and velocity on rock.

The maps of peak ground acceleration developed by Perkins et al. [11] in 1980 are based in the same model and methodology that were followed by Algermissen and others[37] to produce the 1982 national maps. This means that the 1991 ASSHTO maps and the current WSDOT maps are based on the same basic model. The authors feel that the new AASHTO maps represent a step foreword because they were developed with a deeper understanding of the seismicity of the region. The remaining task is to develop a map of velocity-related acceleration coefficient using a method similar to the procedures followed by Higgens et al. to be used according to the methodology of the AASHTO guidelines.

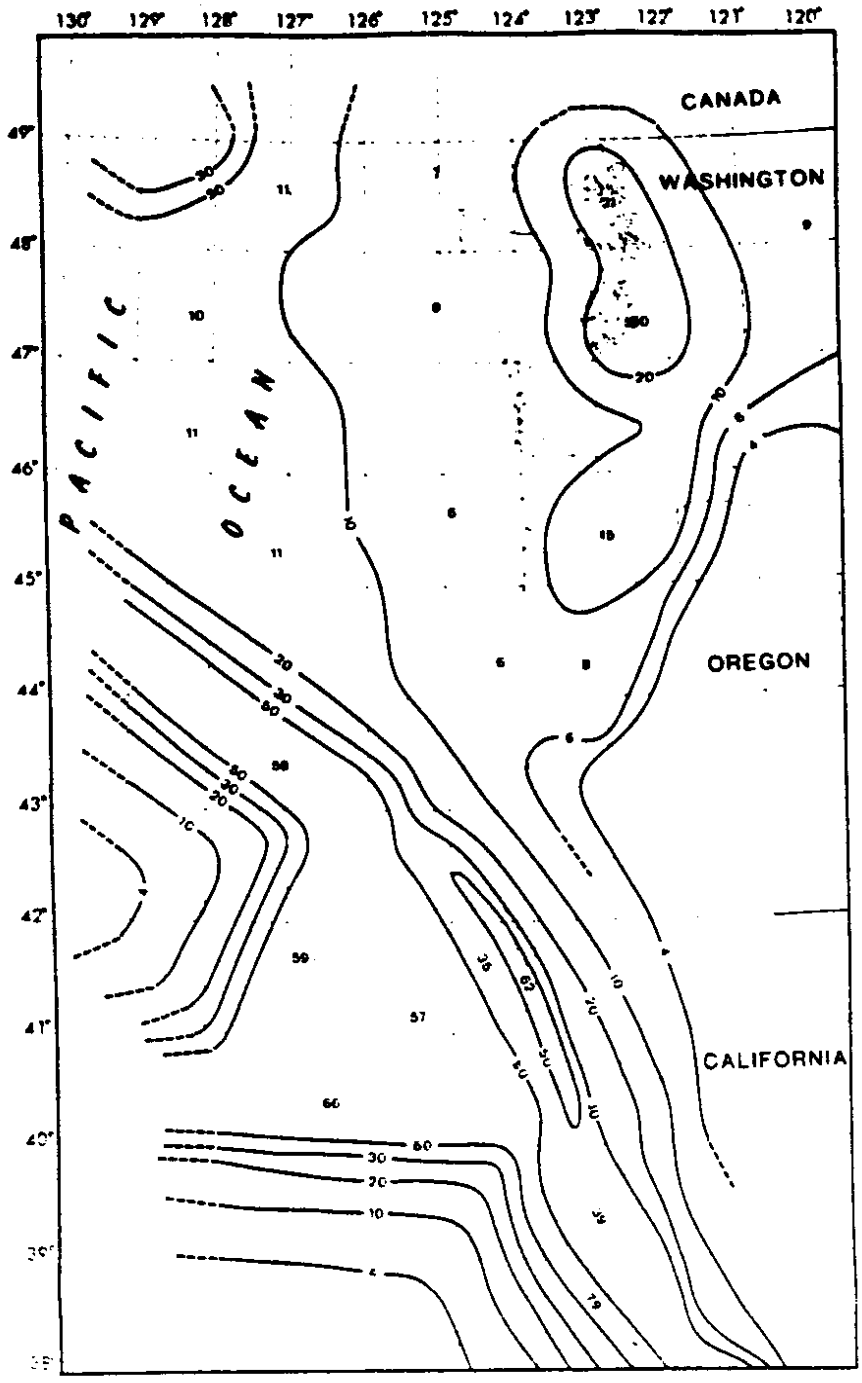

FIGURE 59. Acceleration on rock with 90% probability of not being exceeded in 50 years developed by Perkins et al. in 1980 [11].

ACKNOWLEDGMENT

The authors would like to thank the many people from various agencies who contributed to this study. Special thanks is made to Ms. Karen Kornher and Dr. C. B. Crouse. Also, a great amount of gratitude must be given to Mr. Myint Lwin and the Washington State Department of Transportation for their assistance and patience in completion of this project.

REFERENCES

1. Sun, J.I., Golesoikhi, R. and Seed, H.B., Dynamic Moduli and Damping Ratios for Cohesive Soils, UBC/EERC-88/15, Earthquake Engineering Research Center, University of California, Berkely, CA, August, 1988.

2. Crossen, Robert S., Review of Seismicity in the Puget Sound Region from 1970 through 1978, U.S. Geological Survey Open-File Report 83-19, 1983.

3. Rasmussen, N.H., Millard, R.C., and Smith, S.W., Earthquake Hazard Evaluation of the Puget Sound Region, Washington State, Geophysics Program, University of Washington, Seattle, 1975.

4. Guide Specifications for Seismic Design of Highway Brides, American Association of State Highway and Transportation Officials, 1983.

5. Hopper, M.G., et al., A Study of Earthquake Losses in the Puget Sound, Washington, Area, U.S. Geological Survey Open-File Report 75-375, 1975.

6. Kornher, K., Design Response Spectra for Washington State Bridges, Master Thesis, Washington State University, Pullman, Washington, May, 1989.

7. Schnabel, Per B., Lysmer, J., and Seed, H.B., SHAKE, A Computer Program for Earthquake Response Analysis of Horizontally Layered Sites, EERC 72-12, Earthquake Engineering Research Center, University of California, Berkely, California, December, 1972.

8. Prevost, J.H., DYNA1D, A Complete Program for Nonlinear Seismic Site Response Analysis Technical Documentation, NCEER-89-0025, National Center for Earthquake Engineering Research, State University of New York, Buffalo, NY, September, 1989.

9. Wallis, D.M., Ground Surface Motions in the Fraser Delta Due to Earthquakes, Master Thesis, The University of British Columbia, British Columbia, Canada, April 1979.

10. Gates, J.H., "California's Seismic design Criteria for Bridges," Journal of the Structural Division, proceedings of the A.S.C.E., Vol. 102, No. st12, PP. 2301-2313, December, 1976.

11. Perkins, D.M. et al., Probalistic Estimates of Maximum Seismic Horizontal Ground Motion on Rock in the Pacific Northwest and the Adjacent outer Continental Shelf, U.S. Geological Survey Open-File Report 80-471, 1980.

12. Seed, H.B. Ugas, C., and Lysmer,J., "Site-Dependent Spectra for Earthquake

Resistant Design," Bulletin of the Seismological Society of America, Vol. 66, No. 1, pp. 221-234, February, 1976.

13. Das, B.M., Fundamentals of Soil Dynamics, The university of Texas at El Paso, Texas 1983.

14. Burns, Robert, The Shape and Form of Puget Sound, Washington SeaGrant Program, University of Washington Press, Seattle, 1985.

15. Gutenberg, B., and Richter, C.F, "Earthquake Magnitude, Intensity, Energy and Acceleration," Bulletin of the Seismological Society of America, Vol. 46(2), pp. 105-146, 1972.

16. Seed, H.B., Idriss, I.M., and Keifer, F.W., "Characteristics of Rock Motions During Earthquakes," Journal of the Soil Mechanics and Foundation Division, ASCE, Vol 95, No. SM5, September, 1969.

17. Erdik, M., Site Response Analysis, Earthquake Engineering Research Center, Middle East Technical University, Ankara, Turkey.

18. Patwardhan, A., Sadigh, K., Idriss, I.M., and Youngs, R., "Attenuation of Strong Ground Motion--Effect of Site Conditions, Transmission Path Characteristics, and Focal Depths," Bulletin of the Seismological Society of America, 1978.

19. Idriss, I.M., "Characteristics of Earthquake Ground motions," Proceedings of the ASCE Geotechnical Engineering Division Specialty Conference on Earthquake Engineering and Soil Dynamics, pp. 1151-1365, Pasadena, California, June 19-21, 1978.

20. Hayes, Walter W., Procedures for Estimating Earthquake Ground Motions, U.S. Geological Survey Professional Paper 1014, 1980.

21. Higgins, J.D., Fragaszy, R.J., and Beard L.D., Seismic Zonation for Highway Bridge Design in Washington, Washington State Department of Transportation Report, 1988.

22. Algermissen, S.T. and Perkins, D.M., A Probabilistic Estimate of Accelerations in Rock in the Contiguous United States, U.S. Geological Survey Open-File Report 76-416, 1976.

23. Applied Technology Council, Tentative Provisions for the Development of Seismic Regulations for Buildings, ATC Publication ATC 3-06, 1978.

24. Crossen, Robert S., "Small Earthquakes, Structure and Tectonics of the Puget Sound Region," Bulletin of the seismological Society of America, Vol. 62, No. 5, pp. 1133-1171, October, 1972.

25. Hardin, B.O., and Drnevich, V.P., Shear Modulus and Damping in soils: I. Measurements and Parameter Effects, II. Design Equations and Curves, Technical Reports UCY27-70-CE 2 and 3, College of Engineering, University of Kentucky, Lexington, Kentucky, July 1970.

26. Seed, H.B., and Idriss, I.M., Soil Moduli and Damping Factors for Dynamic Response Analysis, Report No. EERC 70-10, Earthquake Engineering Research Center, University of California, Berkely, California, 1970.

27. Ohsaki, Y., and Iwasaki, R., "On Dynamic Shear Moduli and Poisson's Ratio of Soil Deposits," Soils and Foundations, Japanese Society of Soil Mechanics and Foundation Engineering, Vol. 13, No.4, pp. 61-71, December, 1973.

28. Sykora, David W., and Koester, Joseph P., "Correlation Between Dynamic Shear Resistance and Standard Penetration Resistance in Soils," Earthquake Engineering and Soil Dynamics II--Recent Advances in Ground-Motion Evaluation, Geotechnical Special Publication No. 20, A.S.C.E., pp. 389-404, June, 1988.

29. Egan, J.A., and Ebling, R.M., "Variation of Small-strian Shear Modulus with undrained Shear Strength of Clay," Proceedings of Second International Conference on Soil Dynamics and Earthquake Engineering, on board the liner, the Queen Elizabeth 2, New York to Southampton, Vol. 2, pp. 27-36, June/July, 1985.

30. Joyner, W.B., and Boore, D.M. Prediction of Earthquake Response Spectra, U.S. Geological Survey Open-File Report 82-977, 1982.

31. Crouse, C.B., Byas, Y.K., and Schell, B.A., "Ground Motions from Subduction Zone Earthquakes," Bulletin of the Seismologic Society of America, Vol. 78, No. 1, pp. 1-25, February, 1988.

32. Byas, Y.K., Crouse, D.B., and Schell, B.A., "Regional Design Ground Motion Criteria for the Southern Bearing Sea," Seventh International Conference on Offshore Mechanics and Arctic Engineering, Vol. I, pp. 187-193, Houston, Texas, February, 1988.

33. Kawashima, K., Aisawa, K., and Takahashi, K., "Attenuation of Peak Ground Motion and Absolute Acceleration Response Spectra," Proceedings of the Eighth World Conference of Earthquake Engineering, Vol. II, pp. 247-264, San Francisco, California, July 21-28, 1984.

34. Crouse, C.B., and Eeri, M., "Ground-Motion Attenuation Equations for Earthquakes on the Cascadia Subduction Zone," Earthquake Spectra, Vol. 7, No. 2, pp. 201-236, May, 1991.

35. Vanmarcke, E.H. et al., SIMQUKE: A Program for Artificial Motion Generation, Department of Civil Engineering, Massachusetts Institute of Technology, November, 1976.

36. Algermissen, S. T. et al., Probabilistic Estimates of maximum Acceleration and Velocity in Rock in the Contiguous United States, USGS Open File Report 82-1033, 1982.

37. Federal Emergency Management Agency, NEHRP Recommended Provisions for the Development of Seismic Regulation for New Buildings, Building Seismic Safty Councel, Washington, D.C., 1988.

38. Mark, K.R., "Application of Linear Statistical Models of Earthquakes Magnitude Versus Fault Length in Estimating Maximum Expectable Earthquakes," Geology, Vol. 5, pp. 464-466, August 1977.

39. Hays, W. W., "Evaluation of Earthquake Hazards and Risk in the Puget Sound and Portland Areas," Proceedings of Conference XLii, U.S. Geological Survey Open File Report 88-541, 1988.

40. Schnabel, Per B. and Seed, H.B., "Acceleration in Rock for Earthquakes in the Western United States," Bulletin of the Seismologic Society of America, Vol. 63, No. 2, pp. 501-516, April 1973.

41. Perkins, D.M. et al.,"A Provisional Peak Velocity Attenuation Compatible with the Schnabel-Seed Acceleration Attenuation.", Seismic Hazard Studies in the United States, edited by S. T. Algermissen, USGS Professional Paper. Denver, 1988.

Appendix A

Soil Profiles from Washington State

The first line gives number of layers in profile, the first submerged layer, and name of profile. The subsequent lines give the layer number, soil type (1 for clay, 2 for sand, and 3 for bed rock), layer thickness in ft, maximum shear modulus in psf, and unit weight in pcf.

GROUP 1

6 3 profile 004A

1	2	5.	1700.	110.
2	2	8.	1650.	115.
3	2	7.	1650.	115.
4	2	5.	3200.	120.
5	2	10.	6250.	135.
6	3	0.	10000.	140.

11 1 profile 007A

1	2	5.	2400.	120.
2	2	5.	2400.	120.
3	2	5.	2400.	120.
4	2	5.	3070.	125.
5	2	10.	5180.	135.
6	2	5.	5800.	135.
7	2	5.	4000.	130.
8	2	5.	5560.	135.
9	2	5.	3300.	130.
10	2	15.	6000.	135.
11	3	0.	10000.	140.

4 4 profile 014A

1	2	6.	3400.	130.
2	2	5.	5800.	140.
3	2	5.	7000.	145.
4	3	0.	10000.	145.

8 8 profile 015A

1	2	5.	3200.	125.
2	2	6.	3200.	125.
3	2	7.	3200.	125.
4	2	7.	4100.	135.
5	2	6.	4100.	135.
6	2	5.	5300.	140.
7	2	14.	7000.	145.
8	3	0.	10000.	145.

5 1 profile 032A

1	2	5.	1150.	110.
2	2	5.	2650.	120.
3	2	5.	6400.	145.
4	2	5.	7000.	145.
5	3	0.	10000.	145.

7 7 profile 034A

1	2	5.	3025.	125.
2	2	5.	7500.	145.
3	2	5.	8000.	145.
4	2	10.	5800.	145.
5	2	10.	4700.	140.
6	2	5.	7000.	145.
7	3	0.	10000.	145.

7 8 profile 035A

1	2	5.	3000.	125.
2	2	5.	7500.	145.
3	2	5.	10000.	145.
4	2	5.	5340.	145.
5	2	5.	3750.	130.
6	2	5.	7000.	145.
7	3	0.	10000.	145.

7 8 profile 036A

1	2	2.	830.	110.
2	2	3.	1600.	115.
3	2	5.	2650.	125.
4	2	7.	4140.	135.
5	2	13.	4140.	135.
6	2	5.	7000.	145.
7	3	0.	10000.	145.

12 1 profile 043A

1	2	2.	500.	105.
2	2	8.	3150.	125.
3	2	5.	6400.	140.
4	2	5.	4230.	135.
5	2	5.	6100.	145.
6	2	5.	8000.	145.
7	2	5.	7000.	145.
8	2	5.	5940.	145.
9	2	5.	4050.	135.
10	2	5.	5500.	140.
11	2	5.	7000.	145.
12	3	0.	10000.	145.

9 4 profile 063A

1	2	4.	1210.	112.
2	2	6.	1880.	117.
3	2	5.	2250.	122.
4	2	7.	1800.	117.
5	2	10.	1800.	117.
6	2	5.	3650.	130.
7	2	5.	5400.	140.
8	2	8.	7000.	145.
9	3	0.	10000.	145.

8 4 profile 064A

1	2	5.	1750.	115.
2	2	5.	2280.	120.
3	2	5.	2280.	120.
4	2	5.	2280.	120.
5	2	7.	3150.	127.
6	2	8.	6070.	145.
7	2	5.	7000.	145.
8	3	0.	10000.	145.

8 3 profile 068A

1	2	5.	1300.	113.
2	2	5.	1950.	118.
3	2	7.	2450.	122.
4	2	8.	2450.	122.
5	2	5.	3350.	128.
6	2	10.	5950.	145.
7	2	5.	7000.	145.
8	3	0.	10000.	145.

11 12 profile 077A

1	2	4.	4900.	140.
2	2	4.	5700.	145.
3	2	4.	3950.	135.
4	2	5.	5170.	140.
5	2	7.	5170.	140.
6	2	4.	6130.	145.
7	2	6.	1800.	117.
8	2	6.	4600.	140.
9	2	5.	6200.	145.
10	2	5.	7000.	145.
11	3	0.	10000.	145.

9 10 profile 082B

1	2	5.	2250.	120.
2	2	5.	2250.	120.
3	2	5.	1730.	117.
4	2	5.	1400.	113.
5	2	10.	2200.	120.
6	2	15.	1800.	117.
7	2	5.	4900.	140.
8	2	5.	7000.	145.
9	3	0.	10000.	145.

9 4 profile 089A

1	2	2.	2880.	125.
2	2	4.	1650.	115.
3	2	6.	1650.	115.
4	2	6.	2150.	119.
5	2	7.	2150.	119.
6	2	10.	5750.	145.
7	2	10.	4750.	145.
8	2	5.	7000.	145.
9	3	0.	10000.	145.

10 4 profile 109A

1	2	5.	1400.	113.
2	2	5.	2200.	120.
3	2	6.	4910.	140.
4	2	4.	3800.	132.
5	2	5.	7000.	145.
6	2	5.	8600.	145.
7	2	6.	5800.	145.
8	2	9.	5800.	145.
9	2	5.	7000.	140.
10	3	0.	10000.	145.

9 8 profile 110A

1	2	5.	900.	109.
2	2	5.	4025.	133.
3	2	5.	2750.	124.
4	2	5.	4600.	137.
5	2	5.	3200.	127.
6	2	10.	2300.	122.
7	2	15.	2300.	122.
8	2	5.	7000.	145.
9	3	0.	10000.	145.

8 1 profile 141A

1	2	4.	2000.	118.
2	2	4.	5300.	140.
3	2	4.	3100.	127.
4	2	5.	4200.	133.
5	2	5.	4200.	133.
6	2	6.	5400.	140.
7	2	7.	7000.	140.
8	3	0.	10000.	145.

GROUP 2

11 4 profile 010B

1	2	4.	1200.	110.
2	2	5.	1200.	110.
3	2	3.	3170.	125.
4	2	6.	6000.	140.
5	2	7.	2570.	125.
6	2	6.	4750.	135.
7	2	14.	2400.	125.
8	2	14.	2400.	125.
9	2	26.	2200.	125.
10	2	15.	7000.	140.
11	3	0.	10000.	140.

10 1 profile 013B

1	2	5.	400.	105.
2	2	5.	400.	105.
3	2	4.	1000.	110.
4	2	7.	1980.	115.
5	3	10.	3240.	130.
6	2	16.	3900.	135.
7	2	21.	3900.	135.
8	2	15.	2300.	120.
9	2	7.	7000.	140.
10	3	0.	10000.	145.

12 13 profile 021A

1	2	5.	500.	115.
2	2	5.	3150.	110.
3	2	5.	6400.	135.
4	2	10.	4230.	125.
5	2	15.	6100.	120.
6	2	15.	8000.	120.
7	2	5.	7000.	125.
8	2	10.	5940.	135.
9	2	10.	4050.	135.
10	2	10.	5500.	130.
11	2	20.	7000.	145.
12	3	0.	10000.	145.

13 3 profile 022A

1	2	4.	1670.	115.
2	2	4.	1670.	110.
3	2	5.	1670.	115.
4	2	3.	450.	105.
5	2	6.	2360.	120.
6	2	7.	2360.	120.
7	2	4.	1550.	115.
8	2	7.	3000.	125.
9	2	12.	3000.	125.
10	2	17.	3000.	125.
11	2	21.	5700.	140.
12	2	20.	7000.	145.
13	3	0.	10000.	145.

9 1 profile 047

1	2	5.	300.	100.
2	2	5.	1100.	110.
3	2	7.	1750.	115.
4	2	8.	2400.	120.
5	2	8.	3040.	125.
6	2	16.	4130.	135.
7	2	6.	1700.	115.
8	2	5.	7000.	145.
9	3	0.	10000.	145.

14 2 profile 056A

1	2	3.	750.	105.
2	2	4.	1400.	115.
3	2	5.	1400.	115.
4	2	8.	2130.	120.
5	2	4.	1230.	115.
6	2	7.	2700.	145.
7	2	14.	2490.	120.
8	2	10.	4300.	135.
9	2	5.	5200.	145.
10	2	5.	2500.	125.
11	2	12.	4230.	135.
12	2	13.	4680.	140.
13	2	10.	7000.	145.
14	3	0.	10000.	145.

14 6 profile 066A

1	2	5.	500.	107.
2	2	5.	1500.	115.
3	2	5.	1230.	112.
4	2	5.	860.	110.
5	2	10.	2400.	120.
6	2	10.	1800.	117.
7	2	5.	2980.	125.
8	2	10.	2290.	120.
9	2	10.	2400.	122.
10	2	15.	3080.	125.
11	2	10.	3850.	132.
12	2	10.	5300.	140.
13	2	10.	7000.	145.
14	3	0.	10000.	145.

12 13 profile 069A

1	2	3.	1500.	115.
2	2	5.	3450.	128.
3	2	7.	3450.	128.
4	2	5.	5700.	145.
5	2	10.	3050.	127.
6	2	5.	2000.	118.
7	2	5.	2700.	125.
8	2	10.	1800.	118.
9	2	5.	6600.	145.
10	2	5.	4600.	140.
11	2	5.	7000.	145.
12	3	0.	10000.	145.

10 9 profile 079A

1	2	5.	1500.	115.
2	2	5.	2100.	119.
3	2	10.	3020.	127.
4	2	12.	1850.	117.
5	2	18.	1850.	117.
6	2	15.	3900.	132.
7	2	10.	6100.	145.
8	2	15.	5400.	140.
9	2	10.	7000.	145.
10	3	0.	10000.	145.

13 14 profile 082A

1	2	5.	1940.	118.
2	2	5.	1940.	118.
3	2	10.	1940.	118.
4	2	10.	225.	120.
5	2	10.	2250.	120.
6	2	15.	2550.	120.
7	2	10.	3650.	130.
8	2	10.	3650.	130.
9	2	5.	3100.	126.
10	2	10.	4500.	135.
11	2	10.	6300.	145.
12	2	10.	7000.	145.
13	3	0.	10000.	145.

9 2 profile 087

1	2	5.	1470.	114.
2	2	5.	1470.	114.
3	2	8.	1620.	115.
4	2	9.	1620.	115.
5	2	13.	2380.	122.
6	2	15.	2380.	122.
7	2	5.	5500.	145.
8	2	5.	7000.	145.
9	3	0.	10000.	145.

11 12 profile 088A

1	2	5.	1720.	116.
2	2	5.	1050.	112.
3	2	7.	3540.	130.
4	2	8.	3540.	130.
5	2	5.	1210.	112.
6	2	10.	2530.	123.
7	2	20.	2530.	123.
8	2	15.	4100.	135.
9	2	15.	4100.	135.
10	2	10.	7000.	145.
11	3	0.	10000.	145.

10 6 profile 111A

1	2	6.	3950.	133.
2	2	9.	3950.	133.
3	2	10.	3000.	126.
4	2	5.	1630.	116.
5	2	7.	3000.	127.
6	2	8.	3000.	127.
7	2	10.	3700.	132.
8	2	10.	3350.	128.
9	2	15.	4180.	135.
10	3	0.	10000.	145.

11 3 profile 112A

1	2	5.	830.	107.
2	2	5.	950.	109.
3	2	8.	1670.	117.
4	2	12.	1670.	117.
5	2	10.	2730.	124.
6	2	10.	3100.	127.
7	2	10.	3100.	127.
8	2	5.	7100.	145.
9	2	5.	4200.	137.
10	2	5.	8000.	145.
11	3	0.	10000.	145.

7 2 profile 120

1	2	6.	1300.	112.
2	2	6.	2500.	123.
3	2	12.	1670.	117.
4	2	16.	3700.	132.
5	2	20.	2830.	125.
6	2	5.	7000.	145.
7	3	0.	10000.	145.

10 2 profile 129A

1	2	3.	700.	106.
2	2	7.	1460.	115.
3	2	8.	3600.	130.
4	2	7.	2300.	122.
5	2	15.	3400.	128.
6	2	20.	4470.	137.
7	2	10.	2700.	124.
8	2	5.	6600.	140.
9	2	5.	7000.	145.
10	3	0.	10000.	145.

11 1 profile 132A

1	2	5.	4350.	135.
2	2	5.	9360.	130.
3	2	5.	2900.	125.
4	2	8.	3880.	131.
5	2	9.	3880.	131.
6	2	10.	4800.	138.
7	2	13.	4800.	138.
8	2	15.	4500.	136.
9	2	10.	5600.	140.
10	2	10.	7000.	145.
11	3	0.	10000.	145.

10 10 profile 142A

1	2	5.	1000.	110.
2	2	5.	2160.	120.
3	2	5.	2920.	125.
4	2	5.	1850.	117.
5	2	5.	4200.	132.
6	2	10.	2600.	123.
7	2	15.	4540.	136.
8	2	15.	4540.	136.
9	2	5.	7000.	140.
10	3	0.	10000.	145.

8 6 profile 143A

1	2	4.	3800.	131.
2	2	6.	3800.	131.
3	2	10.	6300.	140.
4	2	15.	3900.	132.
5	2	10.	3040.	126.
6	2	10.	6200.	140.
7	2	15.	3950.	132.
8	3	0.	10000.	140.

GROUP 3

15 1 profile 001A

1	2	5.	1800.	120.
2	2	10.	1800.	120.
3	2	5.	3240.	125.
4	2	10.	383.	130.
5	2	10.	950.	115.
6	2	15.	1960.	120.
7	2	10.	5450.	135.
8	2	10.	1700.	120.
9	2	25.	4730.	130.
10	2	20.	4730.	130.
11	2	20.	3740.	125.
12	2	30.	4800.	130.
13	2	30.	5800.	135.
14	2	30.	6700.	135.
15	3	0.	10000.	140.

13 3 profile 003A

1	2	5.	2600.	120.
2	2	5.	1400.	115.
3	2	2.	600.	110.
4	2	3.	600.	110.
5	2	10.	1800.	115.
6	2	15.	1800.	115.
7	2	15.	1800.	115.
8	2	15.	2540.	115.
9	2	30.	2540.	115.
10	2	50.	3400.	125.
11	2	60.	5650.	130.
12	2	30.	6600.	135.
13	3	0.	10000.	140.

19 1 profile 009A

1	2	5.	840.	110.
2	2	5.	840.	110.
3	2	10.	840.	110.
4	2	10.	840.	110.
5	2	10.	2200.	115.
6	2	10.	1650.	115.
7	2	13.	1650.	115.
8	2	10.	2460.	120.
9	2	12.	1720.	115.
10	2	10.	3440.	125.
11	2	15.	2200.	115.
12	2	13.	2960.	125.
13	2	27.	3360.	125.
14	2	60.	2600.	120.
15	2	20.	4750.	130.
16	2	40.	3600.	130.
17	2	30.	5300.	135.
18	2	30.	6000.	135.
19	3	0.	10000.	140.

18 3 profile 010A

1	2	5.	1600.	115.
2	2	6.	1600.	115.
3	2	9.	1600.	115.
4	2	10.	1600.	115.
5	2	12.	3300.	125.
6	2	5.	4200.	135.
7	2	5.	2520.	120.
8	2	8.	1700.	115.
9	2	15.	3200.	125.
10	2	20.	3200.	125.
11	2	25.	3200.	125.
12	2	20.	4150.	130.
13	2	10.	2200.	120.
14	2	10.	4600.	135.
15	2	20.	2205.	120.
16	2	28.	5270.	135.
17	2	12.	7000.	140.
18	3	0.	10000.	140.

12 4 profile 012A

1	2	4.	700.	110.
2	2	4.	1500.	115.
3	2	4.	1000.	115.
4	2	8.	1000.	115.
5	2	15.	2280.	120.
6	2	15.	3500.	130.
7	2	15.	3500.	130.
8	2	25.	4600.	135.
9	2	20.	5130.	135.
10	2	20.	6200.	140.
11	2	20.	7000.	140.
12	3	0.	10000.	140.

11 8 profile 016A

1	2	3.	500.	105.
2	2	7.	1640.	115.
3	2	10.	2300.	120.
4	2	10.	2300.	120.
5	2	10.	2300.	120.
6	2	10.	3380.	130.
7	2	10.	3380.	130.
8	2	20.	4160.	135.
9	2	30.	5650.	140.
10	2	10.	7000.	140.
11	3	0.	10000.	145.

15 1 profile 019A

1	2	5.	1420.	110.
2	2	5.	1540.	110.
3	2	5.	2170.	120.
4	2	10.	1700.	115.
5	2	10.	3500.	125.
6	2	10.	2200.	120.
7	2	15.	2200.	120.
8	2	15.	1800.	115.
9	2	15.	1800.	115.
10	2	20.	2700.	120.
11	2	20.	2700.	120.
12	2	18.	3900.	130.
13	2	12.	1700.	115.
14	2	10.	5300.	140.
15	3	0.	10000.	140.

19 2 profile 033A

1	2	4.	1540.	115.
2	2	6.	1540.	115.
3	2	10.	1540.	115.
4	2	10.	2160.	120.
5	2	15.	2670.	120.
6	2	10.	2320.	120.
7	2	10.	1840.	115.
8	2	10.	2300.	120.
9	2	10.	2100.	120.
10	2	19.	2100.	120.
11	2	12.	1000.	110.
12	2	10.	3500.	130.
13	2	24.	2170.	120.
14	2	10.	3100.	125.
15	2	20.	3700.	130.
16	2	20.	4500.	140.
17	2	40.	5900.	140.
18	2	20.	7000.	145.
19	3	0.	10000.	145.

11 8 profile 041A

1	2	5.	2360.	120.
2	2	10.	3800.	130.
3	2	10.	3400.	130.
4	2	10.	3700.	130.
5	2	10.	3700.	130.
6	2	15.	2640.	125.
7	2	15.	3140.	125.
8	2	25.	3880.	130.
9	2	20.	5540.	120.
10	2	10.	7000.	140.
11	3	0.	10000.	140.

13 2 profile 049A

1	2	5.	300.	105.
2	2	5.	760.	110.
3	2	10.	1730.	115.
4	2	15.	1730.	115.
5	2	10.	2330.	120.
6	2	15.	2330.	120.
7	2	15.	2330.	120.
8	2	15.	3150.	125.
9	2	10.	4420.	135.
10	2	10.	2250.	120.
11	2	20.	4800.	140.
12	2	10.	7000.	145.
13	3	0.	10000.	145.

12 2 profile 057A

1	2	8.	1200.	110.
2	2	12.	2590.	125.
3	2	12.	2590.	125.
4	2	14.	4270.	135.
5	2	19.	4900.	140.
6	2	7.	3900.	130.
7	2	23.	1700.	115.
8	2	25.	1700.	115.
9	2	30.	2800.	125.
10	2	10.	5500.	145.
11	2	10.	6700.	140.
12	3	0.	10000.	140.

15 11 profile 071A

1	2	5.	500.	105.
2	2	5.	1400.	113.
3	2	5.	1930.	118.
4	2	10.	2150.	120.
5	2	13.	2950.	125.
6	2	13.	1880.	118.
7	2	3.	4100.	135.
8	2	11.	2750.	125.
9	2	15.	3420.	129.
10	2	20.	3420.	129.
11	2	20.	3420.	129.
12	2	20.	3800.	132.
13	2	10.	4500.	140.
14	2	10.	7000.	140.
15	3	0.	10000.	145.

19 15 profile 072A

1	2	5.	900.	108.
2	2	4.	1400.	113.
3	2	4.	1400.	113.
4	2	2.	1400.	113.
5	2	8.	1400.	113.
6	2	2.	1400.	113.
7	2	8.	1400.	113.
8	2	2.	1400.	113.
9	2	8.	2250.	120.
10	2	2.	2250.	120.
11	2	5.	2550.	120.
12	2	8.	2800.	125.
13	2	2.	2800.	125.
14	2	10.	3600.	130.
15	2	20.	3375.	132.
16	2	20.	4430.	135.
17	2	10.	5560.	140.
18	2	10.	7000.	145.
19	3	0.	10000.	145.

12 1 profile 102A

1	2	5.	500.	107.
2	2	5.	500.	107.
3	2	10.	2200.	120.
4	2	10.	2200.	130.
5	2	15.	2670.	123.
6	2	10.	2140.	119.
7	2	15.	1900.	116.
8	2	15.	3200.	127.
9	2	25.	3200.	127.
10	2	10.	5100.	140.
11	2	10.	7000.	140.
12	3	0.	10000.	140.

17 2 profile 113A

1	2	5.	1130.	112.
2	2	5.	1700.	117.
3	2	5.	1420.	114.
4	2	10.	1800.	117.
5	2	15.	2200.	120.
6	2	10.	2730.	123.
7	2	10.	2230.	120.
8	2	10.	1850.	117.
9	2	14.	2200.	120.
10	2	11.	1400.	113.
11	2	15.	1400.	113.
12	2	30.	2260.	120.
13	2	30.	2750.	124.
14	2	20.	3130.	127.
15	2	10.	5020.	140.
16	2	10.	7000.	145.
17	3	0.	10000.	145.

10 3 profile 136A

1	2	4.	2400.	122.
2	2	6.	3150.	127.
3	2	8.	7000.	145.
4	2	12.	7000.	145.
5	3	15.	5520.	140.
6	2	15.	6300.	145.
7	2	20.	4700.	137.
8	2	24.	4700.	137.
9	2	6.	7000.	145.
10	3	0.	10000.	145.

GROUP 4

9 4 profile 008B

1	2	5.	4200.	130.
2	2	5.	8000.	140.
3	2	5.	6000.	140.
4	2	5.	6000.	140.
5	2	4.	3280.	125.
6	1	6.	3280.	125.
7	2	6.	1220.	110.
8	2	12.	6000.	140.
9	3	0.	10000.	145.

7 1 profile 028A

1	2	5.	1110.	110.
2	2	5.	540.	105.
3	2	5.	3170.	125.
4	2	5.	5550.	140.
5	2	5.	3940.	130.
6	2	5.	6600.	145.
7	3	0.	10000.	145.

6 4 profile 029A

1	2	8.	670.	105.
2	2	9.	1570.	110.
3	1	8.	620.	105.
4	2	10.	5620.	140.
5	2	5.	6600.	145.
6	3	0.	10000.	145.

9 4 profile 042A

1	2	5.	575.	105.
2	2	5.	575.	105.
3	2	5.	575.	105.
4	2	10.	575.	105.
5	2	15.	1820.	115.
6	2	5.	3440.	125.
7	2	5.	5200.	145.
8	2	5.	7000.	145.
9	3	0.	10000.	145.

8 2 profile 085A

1	1	6.	830.	104.
2	1	4.	830.	104.
3	1	6.	830.	104.
4	2	5.	1300.	113.
5	2	6.	1300.	113.
6	2	5.	4780.	140.
7	2	8.	7000.	145.
8	3	0.	10000.	145.

8 3 profile 108A

1	2	5.	3520.	129.
2	2	5.	4320.	135.
3	2	5.	3880.	132.
4	2	7.	5200.	140.
5	2	8.	5200.	140.
6	2	5.	7000.	145.
7	2	10.	1150.	112.
8	3	0.	10000.	145.

8 8 profile 114A

1	2	4.	3500.	129.
2	2	4.	4250.	136.
3	2	5.	4250.	136.
4	2	4.	1700.	116.
5	1	5.	1900.	112.
6	2	4.	940.	108.
7	2	5.	5300.	142.
8	3	0.	10000.	145.

9 2 profile 119A

1	2	5.	600.	107.
2	2	5.	600.	107.
3	2	5.	3050.	126.
4	2	5.	3480.	128.
5	2	5.	4270.	135.
6	2	5.	5410.	142.
7	2	10.	6300.	145.
8	2	5.	7000.	145.
9	3	0.	10000.	145.

6 6 profile 134A

1	2	5.	1450.	113.
2	2	5.	1100.	112.
3	2	5.	1560.	115.
4	2	5.	1560.	115.
5	2	5.	2740.	125.
6	3	0.	10000.	140.

6 6 profile 140A

1	2	5.	1000.	110.
2	2	6.	1000.	110.
3	1	9.	1000.	110.
4	2	10.	1820.	117.
5	2	5.	2500.	123.
6	3	0.	10000.	140.

GROUP 5

13 4 profile 003C

1	2	4.	1000.	110.
2	2	4.	1680.	115.
3	2	5.	3300.	125.
4	2	2.	6000.	135.
5	2	5.	6000.	135.
6	1	10.	1400.	110.
7	2	15.	1400.	110.
8	1	15.	1930.	115.
9	2	5.	5880.	135.
10	2	10.	7000.	135.
11	2	15.	5800.	135.
12	2	20.	7000.	135.
13	3	0.	10000.	135.

12 4 profile 008A

1	2	5.	1160.	110.
2	2	5.	2950.	125.
3	2	5.	2950.	125.
4	1	11.	1300.	110.
5	2	9.	1800.	115.
6	1	9.	1800.	115.
7	1	6.	1100.	105.
8	1	10.	1800.	115.
9	1	10.	1800.	115.
10	2	7.	2900.	125.
11	2	23.	6600.	135.
12	3	0.	10000.	140.

9 1 profile 060A

1	2	4.	700.	105.
2	2	5.	1680.	115.
3	2	6.	1680.	115.
4	2	10.	1000.	110.
5	2	15.	4550.	135.
6	2	5.	5950.	145.
7	2	11.	1970.	117.
8	2	4.	7000.	145.
9	3	0.	10000.	145.

11 4 profile 076A

1	2	2.	2700.	123.
2	2	8.	1850.	117.
3	2	3.	3050.	125.
4	2	7.	4550.	140.
5	2	10.	4550.	140.
6	2	14.	4550.	140.
7	1	11.	5380.	140.
8	1	15.	5380.	140.
9	1	15.	6560.	140.
10	1	15.	6560.	140.
11	3	0.	10000.	140.

10 6 profile 083A

1	2	5.	1400.	113.
2	2	5.	1400.	113.
3	2	10.	1400.	113.
4	2	8.	2600.	123.
5	2	10.	1210.	112.
6	2	14.	1750.	117.
7	2	5.	2250.	120.
8	2	5.	3050.	127.
9	2	6.	7000.	145.
10	3	0.	10000.	145.

8 3 profile 090A

1	2	5.	1220.	112.
2	2	5.	1720.	116.
3	2	10.	1720.	116.
4	2	10.	680.	107.
5	2	15.	2230.	120.
6	2	10.	2930.	125.
7	2	15.	2450.	122.
8	3	0.	10000.	145.

12 5 profile 091A

1	2	5.	600.	107.
2	2	5.	2480.	122.
3	2	4.	2480.	122.
4	1	4.	840.	105.
5	1	7.	1070.	106.
6	2	10.	1360.	113.
7	2	10.	1360.	113.
8	2	10.	1360.	113.
9	2	5.	3950.	132.
10	2	5.	6300.	145.
11	2	5.	7000.	145.
12	3	0.	10000.	145.

12 3 profile 094A

1	2	7.	1720.	116.
2	2	3.	1200.	112.
3	1	10.	1650.	110.
4	1	10.	1650.	110.
5	1	10.	1650.	110.
6	1	8.	2820.	122.
7	2	15.	3050.	127.
8	2	2.	2960.	120.
9	1	10.	1975.	113.
10	1	10.	1975.	113.
11	2	15.	7000.	145.
12	3	0.	10000.	145.

9 5 profile 097A

1	2	7.	3050.	127.
2	1	7.	2030.	118.
3	1	6.	2030.	118.
4	2	7.	2700.	123.
5	1	9.	1440.	113.
6	1	12.	1440.	113.
7	2	4.	3700.	132.
8	2	8.	7000.	145.
9	3	0.	10000.	145.

8 5 profile 104A

1	1	6.	230.	100.
2	1	5.	2080.	114.
3	1	5.	1120.	106.
4	1	9.	380.	100.
5	1	11.	380.	100.
6	2	5.	3030.	126.
7	2	11.	4680.	140.
8	3	0.	10000.	145.

10 2 profile 105A

1	2	4.	1580.	115.
2	2	4.	1580.	115.
3	1	9.	700.	101.
4	2	5.	8000.	145.
5	2	8.	3330.	128.
6	2	15.	2320.	120.
7	2	20.	2320.	120.
8	2	5.	5040.	140.
9	2	5.	7000.	145.
10	3	0.	10000.	145.

14 2 profile 106A

1	2	3.	1850.	117.
2	2	5.	4800.	137.
3	2	5.	4800.	137.
4	2	12.	6400.	145.
5	2	10.	2300.	120.
6	1	5.	2790.	122.
7	2	8.	2700.	124.
8	1	7.	2160.	115.
9	2	5.	3300.	128.
10	2	5.	5300.	140.
11	2	5.	4700.	137.
12	2	5.	5480.	140.
13	2	5.	7000.	145.
14	3	0.	10000.	145.

11 3 profile 107A

1	2	4.	300.	105.
2	2	4.	300.	105.
3	2	6.	2600.	123.
4	1	7.	2600.	127.
5	2	5.	2930.	125.
6	2	9.	2930.	130.
7	2	10.	5050.	140.
8	1	5.	4120.	140.
9	2	10.	5600.	142.
10	2	5.	7000.	145.
11	3	0.	10000.	145.

11 2 profile 130A

1	2	5.	600.	140.
2	2	5.	600.	135.
3	2	5.	600.	122.
4	2	5.	600.	135.
5	2	12.	600.	115.
6	2	18.	2250.	117.
7	2	10.	3900.	113.
8	2	10.	2400.	132.
9	2	5.	5170.	140.
10	2	5.	7000.	145.
11	3	0.	10000.	145.

11 4 profile 121A

1	2	5.	600.	107.
2	2	5.	600.	107.
3	2	5.	600.	107.
4	2	7.	600.	107.
5	2	8.	600.	107.
6	2	10.	2250.	121.
7	2	10.	3900.	123.
8	2	10.	2400.	122.
9	2	10.	5170.	140.
10	2	5.	7000.	145.
11	3	0.	10000.	145.

11 4 profile 131A

1	2	5.	2300.	120.
2	2	5.	2300.	120.
3	2	3.	3400.	128.
4	2	3.	1300.	113.
5	2	5.	2000.	118.
6	2	7.	2000.	118.
7	2	8.	4000.	132.
8	2	12.	4000.	132.
9	2	4.	1300.	113.
10	2	3.	7000.	145.
11	3	0.	10000.	145.

9 9 profile 125A

1	2	5.	1000.	110.
2	2	5.	1600.	115.
3	2	7.	1400.	113.
4	2	8.	1400.	113.
5	2	14.	1620.	115.
6	2	9.	6500.	140.
7	2	10.	3100.	127.
8	2	7.	5200.	140.
9	3	0.	10000.	140.

GROUP 6

17 1 profile 001B

1	2	2.	2200.	120.
2	2	8.	850.	110.
3	2	10.	1200.	110.
4	2	10.	2970.	120.
5	2	10.	200.	110.
6	2	12.	4430.	130.
7	2	11.	1800.	110.
8	2	4.	4200.	125.
9	2	8.	900.	110.
10	2	13.	1600.	115.
11	2	12.	6300.	135.
12	2	20.	2930.	120.
13	2	10.	1400.	110.
14	2	10.	3310.	120.
15	2	10.	5800.	130.
16	2	30.	6600.	135.
17	3	0.	10000.	140.

17 1 profile 013A

1	2	5.	530.	105.
2	2	7.	1800.	115.
3	2	8.	1800.	115.
4	2	7.	2700.	125.
5	2	8.	5100.	135.
6	2	7.	5100.	135.
7	1	4.	870.	105.
8	2	6.	3130.	125.
9	2	4.	1000.	110.
10	2	12.	3000.	125.
11	1	3.	1550.	115.
12	2	5.	1480.	115.
13	1	8.	1480.	115.
14	1	10.	2330.	120.
15	2	16.	5050.	135.
16	2	20.	7000.	135.
17	3	0.	10000.	135.

14 4 profile 020A

1	2	4.	1480.	110.
2	2	4.	1480.	110.
3	2	5.	1480.	110.
4	2	7.	1200.	110.
5	2	10.	1200.	110.
6	2	10.	1850.	115.
7	2	15.	1850.	115.
8	2	15.	1070.	110.
9	2	20.	2540.	120.
10	2	10.	6400.	145.
11	2	10.	5200.	140.
12	2	20.	5940.	140.
13	2	20.	7000.	145.
14	3	0.	10000.	145.

13 2 profile 037A

1	2	6.	3300.	125.
2	1	5.	300.	100.
3	2	5.	700.	110.
4	2	6.	700.	110.
5	2	13.	2650.	125.
6	2	15.	2050.	120.
7	2	20.	1870.	120.
8	2	30.	2300.	120.
9	2	40.	3000.	125.
10	2	30.	3560.	130.
11	2	30.	5250.	140.
12	2	20.	7000.	145.
13	3	0.	10000.	145.

13 1 profile 051A

1	2	6.	300.	105.
2	2	10.	1600.	110.
3	2	10.	2550.	125.
4	2	13.	2550.	125.
5	1	14.	900.	110.
6	2	8.	3700.	130.
7	2	3.	5480.	145.
8	2	11.	1250.	110.
9	2	17.	1250.	110.
10	2	18.	4040.	135.
11	2	20.	4040.	135.
12	2	10.	7000.	145.
13	3	0.	10000.	145.

15 5 profile 052A

1	2	5.	500.	105.
2	2	5.	500.	105.
3	2	11.	1400.	110.
4	2	9.	2700.	125.
5	2	10.	3150.	125.
6	2	10.	930.	110.
7	2	10.	930.	110.
8	2	10.	1430.	115.
9	1	14.	1430.	115.
10	1	16.	1800.	120.
11	2	20.	3400.	135.
12	2	10.	2800.	125.
13	2	10.	4900.	140.
14	2	10.	7000.	145.
15	3	0.	10000.	145.

13 2 profile 054A

1	2	6.	830.	110.
2	1	5.	500.	100.
3	2	5.	940.	110.
4	2	8.	940.	110.
5	2	15.	2250.	120.
6	2	11.	3530.	130.
7	2	18.	3260.	125.
8	2	14.	1960.	120.
9	2	8.	2180.	120.
10	2	10.	3410.	130.
11	2	10.	5600.	145.
12	2	10.	7000.	145.
13	3	0.	10000.	145.

12 2 profile 055A

1	2	5.	620.	105.
2	2	7.	620.	105.
3	2	8.	620.	105.
4	2	10.	1730.	115.
5	2	10.	850.	110.
6	2	15.	850.	110.
7	2	12.	1270.	110.
8	2	23.	2450.	120.
9	2	30.	1750.	115.
10	2	10.	3900.	130.
11	2	10.	7000.	145.
12	3	0.	10000.	145.

11 2 profile 058A

1	2	8.	500.	105.
2	2	6.	980.	110.
3	2	8.	980.	110.
4	2	11.	2530.	123.
5	2	11.	2530.	123.
6	2	11.	1170.	112.
7	2	11.	1170.	112.
8	2	18.	5340.	140.
9	2	26.	5340.	140.
10	2	10.	7000.	145.
11	3	0.	10000.	145.

13 2 profile 059A

1	2	7.	8000.	105.
2	2	8.	5000.	105.
3	2	9.	2300.	120.
4	2	11.	2300.	120.
5	2	10.	3250.	125.
6	2	10.	780.	105.
7	2	10.	2580.	120.
8	2	8.	860.	110.
9	2	15.	2600.	125.
10	2	22.	2600.	125.
11	2	20.	5150.	140.
12	2	10.	7000.	145.
13	3	0.	10000.	145.

14 4 profile 062

1	2	4.	1530.	113.
2	2	5.	1300.	113.
3	2	4.	2750.	123.
4	2	8.	1000.	112.
5	2	9.	1000.	112.
6	2	10.	1620.	115.
7	2	10.	1860.	117.
8	2	5.	2300.	120.
9	2	15.	1150.	112.
10	2	20.	2520.	123.
11	2	10.	6300.	145.
12	2	10.	5300.	140.
13	2	10.	7000.	145.
14	3	0.	10000.	145.

12 2 profile 065A

1	2	7.	400.	105.
2	2	6.	400.	105.
3	2	7.	950.	110.
4	2	10.	950.	110.
5	2	14.	950.	110.
6	2	11.	2000.	117.
7	2	10.	2860.	125.
8	2	5.	3470.	130.
9	2	10.	2530.	122.
10	2	15.	3790.	132.
11	2	15.	3790.	132.
12	3	0.	10000.	145.

12 2 profile 093A

1	1	7.	1385.	108.
2	2	6.	530.	107.
3	2	7.	1400.	112.
4	2	10.	1400.	112.
5	2	14.	1860.	117.
6	2	11.	1860.	117.
7	2	10.	1860.	117.
8	1	5.	3580.	129.
9	1	10.	3580.	129.
10	2	15.	3840.	132.
11	2	15.	7000.	145.
12	3	0.	10000.	145.

17 1 profile 095A

1	2	5.	850.	108.
2	1	5.	2320.	116.
3	2	10.	670.	107.
4	2	10.	1980.	118.
5	1	3.	650.	100.
6	2	3.	900.	108.
7	1	5.	650.	100.
8	2	9.	1100.	110.
9	2	10.	1740.	117.
10	2	20.	1740.	117.
11	2	20.	1740.	117.
12	2	30.	2050.	118.
13	2	20.	2650.	123.
14	2	10.	3600.	130.
15	2	10.	5600.	145.
16	2	10.	7000.	145.
17	3	0.	10000.	145.

17 3 profile 100A

1	2	2.	2300.	122.
2	2	4.	680.	107.
3	2	5.	1900.	117.
4	2	7.	1900.	117.
5	2	6.	1250.	113.
6	2	9.	300.	106.
7	2	12.	300.	106.
8	2	10.	1000.	110.
9	2	15.	600.	107.
10	2	20.	2950.	125.
11	2	10.	2420.	122.
12	2	20.	1420.	113.
13	2	30.	1420.	113.
14	2	30.	2500.	122.
15	2	20.	5550.	145.
16	2	20.	7000.	145.
17	3	0.	10000.	145.

12 5 profile 103A

1	2	5.	1020.	110.
2	1	5.	1240.	108.
3	1	5.	1240.	108.
4	1	10.	1240.	108.
5	1	10.	1240.	108.
6	2	10.	3140.	127.
7	2	15.	2610.	123.
8	2	20.	2610.	123.
9	2	20.	3900.	133.
10	2	10.	5100.	140.
11	2	10.	7000.	145.
12	3	0.	10000.	145.

17 7 profile 123A

1	2	5.	5100.	140.
2	2	7.	8600.	145.
3	2	5.	12400.	145.
4	2	5.	12400.	145.
5	2	6.	14900.	145.
6	2	8.	6300.	140.
7	2	13.	2900.	125.
8	1	9.	3370.	127.
9	2	17.	4400.	135.
10	2	15.	4400.	135.
11	2	22.	4400.	135.
12	1	10.	2200.	115.
13	1	14.	6100.	140.
14	2	32.	4550.	140.
15	1	10.	2200.	115.
16	2	10.	6150.	145.
17	3	0.	10000.	145.

15 4 profile 124A

1	2	5.	1400.	112.
2	2	6.	1400.	112.
3	2	9.	4050.	135.
4	2	15.	4050.	135.
5	2	7.	3300.	127.
6	1	6.	4400.	140.
7	2	12.	4130.	135.
8	2	25.	4130.	135.
9	1	15.	1200.	110.
10	1	10.	840.	110.
11	2	12.	2930.	125.
12	2	18.	4300.	135.
13	2	10.	5800.	140.
14	2	10.	7000.	140.
15	3	0.	10000.	140.

15 2 profile 144A

1	2	5.	1600.	115.
2	2	7.	1600.	115.
3	2	8.	1600.	115.
4	2	12.	2170.	118.
5	2	16.	1400.	113.
6	2	22.	950.	110.
7	2	20.	950.	110.
8	2	20.	950.	110.
9	2	20.	1500.	115.
10	2	30.	2190.	119.
11	2	20.	2990.	125.
12	2	20.	3700.	130.
13	2	10.	5750.	140.
14	2	10.	7000.	140.
15	3	0.	10000.	140.

GROUP 7

17 2 profile 025F

1	1	4.	4040.	135.
2	1	6.	4040.	135.
3	1	5.	2150.	115.
4	1	10.	1315.	105.
5	1	5.	3000.	125.
6	1	10.	1855.	115.
7	1	15.	4380.	140.
8	2	9.	5700.	145.
9	1	8.	3920.	125.
10	2	11.	2450.	120.
11	2	19.	3030.	125.
12	1	18.	3075.	125.
13	1	20.	3075.	125.
14	2	10.	4500.	135.
15	2	10.	5800.	140.
16	2	10.	7000.	145.
17	3	0.	10000.	145.

16 11 profile 026F

1	2	5.	1250.	110.
2	2	5.	670.	105.
3	1	5.	1350.	110.
4	1	10.	910.	105.
5	1	15.	1210.	105.
6	1	5.	1735.	110.
7	1	15.	1375.	110.
8	1	5.	1735.	105.
9	1	10.	1255.	105.
10	1	9.	1945.	115.
11	1	16.	2010.	115.
12	1	20.	1660.	125.
13	1	20.	1665.	110.
14	2	20.	5800.	145.
15	2	10.	7000.	145.
16	3	0.	10000.	145.

14 3 profile 039E

1	2	4.	800.	110.
2	2	4.	800.	110.
3	2	8.	1000.	110.
4	2	9.	1000.	110.
5	2	10.	2400.	120.
6	2	10.	3000.	125.
7	1	15.	1850.	115.
8	1	15.	1280.	115.
9	1	15.	1280.	115.
10	1	10.	1750.	115.
11	2	10.	3200.	125.
12	2	10.	5700.	145.
13	2	10.	7000.	145.
14	3	0.	10000.	145.

15 5 profile 040C

1	2	5.	2600.	120.
2	2	5.	2600.	120.
3	2	5.	2600.	120.
4	1	10.	850.	105.
5	1	10.	850.	105.
6	1	15.	950.	105.
7	1	15.	1180.	105.
8	1	15.	1405.	110.
9	1	20.	1425.	110.
10	1	20.	1135.	105.
11	2	10.	1550.	115.
12	2	20.	2730.	125.
13	2	20.	4700.	135.
14	2	10.	6700.	140.
15	3	0.	10000.	140.

17 3 profile 061A

1	2	5.	2500.	123.
2	2	5.	2500.	123.
3	2	5.	2500.	123.
4	2	10.	3520.	130.
5	2	12.	3520.	130.
6	2	15.	3520.	130.
7	2	5.	1480.	115.
8	2	9.	3420.	130.
9	2	10.	3860.	130.
10	2	10.	3860.	130.
11	2	10.	2160.	120.
12	1	10.	960.	105.
13	1	12.	960.	105.
14	2	22.	4050.	135.
15	2	20.	5500.	140.
16	2	10.	7000.	145.
17	3	0.	10000.	145.

14 5 profile 078A

1	2	5.	1640.	115.
2	2	5.	3700.	130.
3	2	6.	2570.	123.
4	1	4.	220.	100.
5	1	10.	220.	100.
6	1	10.	1730.	110.
7	1	15.	3330.	127.
8	2	12.	4700.	140.
9	1	8.	3255.	126.
10	1	15.	1690.	110.
11	1	30.	1690.	110.
12	1	10.	3000.	120.
13	1	10.	7000.	130.
14	3	0.	10000.	140.

13 2 profile 081A

1	1	4.	960.	105.
2	1	4.	1330.	108.
3	1	5.	925.	104.
4	1	3.	925.	104.
5	1	6.	1500.	110.
6	1	7.	1500.	110.
7	1	4.	970.	105.
8	1	7.	1872.	113.
9	1	12.	2200.	115.
10	1	17.	1870.	112.
11	1	21.	4000.	125.
12	1	20.	7000.	130.
13	3	0.	10000.	140.

15 8 profile 086A

1	1	5.	1905.	112.
2	1	5.	1905.	112.
3	1	5.	1905.	112.
4	1	5.	1905.	112.
5	1	5.	940.	105.
6	1	10.	940.	105.
7	1	11.	2060.	115.
8	1	6.	2065.	115.
9	2	6.	2300.	122.
10	2	9.	2880.	132.
11	1	13.	3800.	132.
12	1	16.	2800.	122.
13	1	24.	6200.	140.
14	1	10.	7000.	140.
15	3	0.	10000.	140.

19 2 profile 096A

1	2	6.	300.	105.
2	2	4.	1300.	112.
3	2	7.	2500.	123.
4	2	8.	2500.	123.
5	2	5.	640.	107.
6	1	5.	930.	105.
7	2	10.	870.	108.
8	1	5.	1210.	107.
9	2	5.	1630.	116.
10	1	5.	665.	106.
11	2	5.	520.	107.
12	1	8.	1110.	106.
13	2	7.	800.	108.
14	1	10.	460.	102.
15	1	24.	1250.	107.
16	2	12.	4080.	134.
17	1	34.	1875.	112.
18	1	10.	7000.	140.
19	3	0.	10000.	140.

13 3 profile 098A

1	2	5.	600.	107.
2	2	7.	600.	107.
3	2	8.	600.	107.
4	2	7.	1440.	113.
5	2	9.	1440.	113.
6	2	14.	2400.	122.
7	1	15.	925.	105.
8	1	30.	925.	105.
9	1	12.	990.	106.
10	1	25.	1200.	115.
11	1	27.	1200.	115.
12	1	10.	7000.	145.
13	3	0.	10000.	145.

20 2 profile 099A

1	2	5.	400.	106.
2	2	5.	400.	106.
3	2	4.	400.	106.
4	1	5.	550.	100.
5	2	11.	450.	106.
6	2	5.	1440.	115.
7	2	10.	3050.	127.
8	2	15.	3050.	127.
9	2	5.	2200.	120.
10	1	5.	910.	110.
11	2	5.	2450.	122.
12	1	5.	1350.	108.
13	2	10.	2200.	120.
14	1	20.	1610.	110.
15	2	10.	1805.	117.
16	1	20.	2120.	115.
17	2	10.	3600.	130.
18	2	20.	2400.	122.
19	2	10.	6000.	140.
20	3	0.	10000.	140.

13 2 profile 101A

1	2	7.	1430.	113.
2	2	5.	650.	107.
3	1	8.	115.	100.
4	2	13.	1700.	117.
5	2	5.	3070.	126.
6	2	10.	1200.	112.
7	2	15.	2450.	122.
8	2	17.	2450.	122.
9	2	24.	1410.	113.
10	1	20.	635.	101.
11	2	26.	2800.	124.
12	2	10.	3550.	129.
13	3	0.	10000.	145.

GROUP 8

6 1 profile 002A

1	2	5.	550.	105.
2	2	5.	550.	105.
3	2	5.	550.	105.
4	2	5.	4000.	125.
5	2	10.	6600.	130.
6	3	0.	10000.	135.

8 1 profile 011A

1	2	5.	300.	105.
2	2	5.	300.	105.
3	2	10.	300.	105.
4	2	10.	300.	105.
5	2	10.	300.	105.
6	2	7.	850.	110.
7	2	8.	6600.	140.
8	3	0.	10000.	140.

6 1 profile 90001

1	2	5.	200.	104.
2	2	5.	200.	104.
3	2	5.	200.	104.
4	2	10.	200.	104.
5	2	5.	3000.	125.
6	3	0.	70000.	145.

6 1 profile 90004

1	2	5.	400.	104.
2	2	5.	400.	104.
3	2	5.	400.	104.
4	2	10.	400.	104.
5	2	5.	3000.	125.
6	3	0.	70000.	145.

6 1 profile 90008

1	2	5.	600.	104.
2	2	5.	600.	104.
3	2	5.	600.	104.
4	2	10.	600.	104.
5	2	5.	3000.	125.
6	3	0.	70000.	145.

7 1 profile 90017

1	2	5.	200.	104.
2	2	5.	200.	104.
3	2	5.	200.	104.
4	2	10.	200.	104.
5	2	15.	200.	104.
6	2	5.	3000.	125.
7	3	0.	7000.	145.

7 1 profile 90018

1	2	5.	400.	104.
2	2	5.	400.	104.
3	2	5.	400.	104.
4	2	10.	400.	104.
5	2	15.	400.	104.
6	2	5.	3000.	125.
7	3	0.	7000.	145.

7 1 profile 90019

1	2	5.	200.	104.
2	2	5.	300.	104.
3	2	5.	400.	104.
4	2	10.	500.	104.
5	2	15.	600.	104.
6	2	5.	3000.	125.
7	3	0.	7000.	145.

GROUP 9

12 1 profile 002B

1	2	5.	700.	105.
2	2	5.	980.	105.
3	2	5.	980.	105.
4	2	10.	600.	105.
5	2	10.	600.	105.
6	2	10.	600.	105.
7	2	15.	1000.	110.
8	2	15.	1000.	110.
9	2	5.	3000.	120.
10	2	10.	5270.	130.
11	2	20.	6600.	135.
12	3	0.	10000.	135.

15 1 profile 005A

1	2	5.	350.	105.
2	2	5.	350.	105.
3	2	10.	350.	105.
4	2	10.	350.	105.
5	2	10.	350.	105.
6	2	15.	350.	105.
7	2	15.	930.	110.
8	2	20.	930.	110.
9	2	20.	930.	110.
10	2	20.	1400.	110.
11	2	20.	2240.	115.
12	2	50.	2680.	120.
13	2	20.	4730.	130.
14	2	20.	6700.	135.
15	3	0.	10000.	135.

10 1 profile 006A

1	2	5.	250.	105.
2	2	5.	250.	105.
3	2	10.	250.	105.
4	2	10.	250.	105.
5	2	10.	250.	105.
6	2	15.	250.	105.
7	2	15.	250.	105.
8	2	10.	1700.	120.
9	2	20.	6000.	130.
10	3	0.	10000.	135.

14 1 profile 007B

1	2	5.	750.	105.
2	2	5.	1400.	105.
3	2	10.	1400.	105.
4	2	10.	2130.	105.
5	2	15.	1230.	105.
6	2	15.	2700.	110.
7	2	5.	2490.	105.
8	2	10.	4300.	110.
9	2	5.	5200.	105.
10	2	10.	2500.	130.
11	2	20.	4230.	135.
12	2	30.	4680.	135.
13	2	20.	7000.	135.
14	3	0.	10000.	140.

14 4 profile 027A

1	2	6.	400.	105.
2	2	8.	400.	105.
3	2	9.	400.	105.
4	2	10.	400.	105.
5	2	9.	1000.	110.
6	2	10.	1000.	110.
7	2	7.	1350.	110.
8	1	8.	2050.	115.
9	1	8.	2050.	115.
10	2	18.	2720.	120.
11	1	10.	2720.	120.
12	2	17.	4950.	135.
13	2	10.	7000.	140.
14	3	0.	10000.	140.

11 1 profile 044A

1	2	5.	2200.	120.
2	2	5.	200.	105.
3	2	10.	300.	105.
4	2	15.	300.	105.
5	2	20.	300.	105.
6	2	17.	850.	110.
7	2	12.	300.	105.
8	2	26.	1000.	110.
9	2	30.	1860.	115.
10	2	10.	7000.	145.
11	3	0.	10000.	145.

12 2 profile 045A

1	2	5.	300.	105.
2	2	5.	300.	105.
3	2	10.	300.	105.
4	2	10.	300.	105.
5	2	10.	300.	105.
6	2	15.	650.	105.
7	2	20.	650.	105.
8	2	15.	900.	115.
9	2	30.	1550.	115.
10	2	20.	2500.	125.
11	2	10.	7000.	145.
12	3	0.	10000.	145.

11 1 profile 118A

1	2	5.	200.	105.
2	2	5.	200.	105.
3	2	10.	200.	105.
4	2	10.	200.	105.
5	2	10.	200.	105.
6	2	15.	250.	105.
7	2	15.	200.	105.
8	2	10.	900.	110.
9	2	10.	2500.	123.
10	2	10.	4250.	135.
11	3	0.	10000.	140.

14 1 profile 122A

1	2	5.	400.	106.
2	2	7.	400.	106.
3	2	7.	400.	106.
4	2	7.	400.	106.
5	2	9.	400.	106.
6	2	8.	1150.	112.
7	2	12.	1150.	112.
8	2	15.	800.	107.
9	2	20.	2400.	122.
10	2	20.	900.	110.
11	2	20.	1500.	115.
12	2	20.	1500.	115.
13	2	18.	2000.	118.
14	3	0.	10000.	140.

Appendix B

Curve Ordinates

This appendix gives the curve ordinates for the basic spectrum, the nine groups soil amplification spectra and normalized response. The curves shown in the FINDINGS AND IMPLEMENTATION OF THE RESULTS section were smoothed using spline-fitting.

BASE SPECTRUM		GROUP 1		GROUP 2		GROUP 3		GROUP 4	
Period (sec)	N Acc	S Amp	N Resp	S Amp	N Resp	S Amp	N Resp	S Amp	N Resp
0.001	1	1.10531	1.10531	1.11603	1.11603	0.79743	0.79743	1.23662	1.23662
0.05	2	1.05141	2.10282	0.71453	1.42906	0.63642	1.27084	0.86436	1.7127
0.075	2.5	1.00522	2.51305	0.75346	1.8837	0.81697	1.942425	0.86756	2.168879
0.1	3	1.02481	3.07443	0.76643	2.29929	0.66239	1.98714	0.96650	2.8995
0.125	3.01	1.01367	3.0511467	0.79734	2.3999934	0.64347	1.9368447	0.87823	2.6434623
0.15	3	1.10808	3.32424	0.84367	2.53101	0.67964	2.03892	0.91084	2.73162
0.175	2.985	1.14288	3.4105416	0.84423	2.52000885	0.68023	2.03046685	0.9144	2.728484
0.2	2.97	1.30422	3.8735334	0.86707	2.5751979	0.68999	2.0519433	1.18449	3.5179086
0.225	2.945	1.36891	4.03144085	0.88847	2.61654915	0.69152	2.0365264	1.32377	3.89850265
0.25	2.92	1.44247	4.2120124	1.05603	3.0836076	0.69014	2.0152088	1.50597	4.3974324
0.275	2.87	1.4305	4.105535	1.10138	3.1609602	0.69582	1.9969814	1.55286	4.4567082
0.3	2.82	1.43907	4.0581774	1.10888	3.1270416	0.71091	2.0047662	1.5765	4.44573
0.325	2.785	1.43422	3.9943027	1.13230	3.0987570	0.73821	2.0559149	1.55085	4.32007135
0.35	2.63	1.42272	3.7417536	1.17091	3.0794933	0.77286	2.0326218	1.62360	4.2700527
0.375	2.62	1.41513	3.6001276	1.17603	2.8636800	0.79009	1.9866512	1.61686	4.0747382
0.4	2.4	1.41381	3.393144	1.36877	3.285048	0.81604	1.958496	1.66421	3.994104
0.425	2.3	1.42169	3.270047	1.4445	3.32235	0.90536	2.082328	1.71697	3.949031
0.45	2.2	1.37481	3.024582	1.61679	3.556938	0.96237	2.117214	1.65436	3.63957
0.475	2.116	1.34673	2.84968068	1.63123	3.45168268	1.00625	2.1292250	1.60280	3.39152480
0.5	2.03	1.35648	2.7516539	1.62275	3.2941825	1.05116	2.1341548	1.62561	3.2999883
0.525	1.955	1.38042	2.6987211	1.61687	3.1609809	1.13657	2.2200439	1.71682	3.3563831
0.55	1.88	1.26539	2.3789332	1.76216	3.3128608	1.08781	2.0451628	1.53081	2.8779228
0.575	1.815	1.26341	2.2930891	1.77774	3.2265981	1.08551	1.9702006	1.52687	2.77126905
0.6	1.75	1.26743	2.2180025	1.82216	3.18878	1.12916	1.974315	1.55663	2.7241025
0.625	1.7	1.20441	2.047497	1.77036	3.009612	1.11684	1.898628	1.48662	2.527254
0.65	1.65	1.2002	1.98033	1.71089	2.823117	1.10531	1.8237615	1.44153	2.3785245
0.675	1.595	1.22079	1.94716005	1.73324	2.7645178	1.12866	1.8002127	1.47801	2.35742595
0.7	1.54	1.23129	1.8961866	1.85468	2.8562072	1.29916	2.0007064	1.56833	2.4152282
0.725	1.485	1.13082	1.6792677	1.71635	2.54877975	1.28289	1.90509165	1.44535	2.14634475
0.75	1.43	1.12031	1.6020433	1.65806	2.3710258	1.24675	1.7828525	1.3063	1.868009
0.775	1.385	1.10487	1.53024495	1.59233	2.20537705	1.22184	1.6922484	1.33481	1.84871185
0.8	1.34	1.08843	1.4585102	1.50089	2.0111926	1.1803	1.581602	1.27776	1.7121984
0.825	1.3	1.10787	1.440231	1.46084	1.899092	1.18333	1.538329	1.27623	1.659099
0.85	1.25	1.12862	1.410775	1.46762	1.834525	1.19022	1.487775	1.31377	1.6422125
0.875	1.23	1.15079	1.4154717	1.51017	1.8575091	1.21435	1.4936505	1.3469	1.656687
0.9	1.2	1.16229	1.394748	1.53048	1.836576	1.25018	1.500216	1.36863	1.642356
0.925	1.165	1.16862	1.3614423	1.53401	1.78712165	1.28316	1.4948814	1.37586	1.6028769
0.95	1.13	1.17323	1.3257499	1.54678	1.7478614	1.31741	1.4886733	1.38856	1.5690728
0.975	1.1	1.18312	1.301432	1.59217	1.751387	1.37589	1.513479	1.42034	1.562374
1	1.07	1.12484	1.2035788	1.52864	1.6356448	1.38833	1.4855131	1.35186	1.4464902
1.05	1.035	1.08081	1.11863835	1.29865	1.34410275	1.28922	1.3343427	1.17739	1.21859865
1.1	1	1.07773	1.07773	1.30836	1.30836	1.27583	1.27583	1.17429	1.17429
1.15	0.975	1.09146	1.0641735	1.35589	1.3219928	1.31584	1.282944	1.19406	1.1642085
1.2	0.95	1.0684	1.01498	1.37898	1.310031	1.36082	1.292779	1.19746	1.1375775
1.25	0.925	1.08061	0.99956425	1.38813	1.28402025	1.40084	1.295777	1.19560	1.1059300
1.3	0.9	1.04201	0.937809	1.36359	1.227231	1.46735	1.311815	1.16329	1.046961
1.35	0.875	1.0287	0.9001125	1.21387	1.06213625	1.42719	1.24879125	1.10061	0.96303375
1.4	0.85	1.05388	0.895798	1.16385	0.9892725	1.33182	1.132047	1.10825	0.9420125
1.45	0.83	1.07164	0.8894612	1.22801	1.0192483	1.37764	1.1434412	1.16433	0.9663939
1.5	0.81	1.07187	0.8682147	1.27445	1.0323045	1.42823	1.1568663	1.18125	0.9568125
1.55	0.785	1.04409	0.82261065	1.23288	0.9678108	1.38622	1.0881827	1.12673	0.88448305
1.6	0.76	1.03564	0.7870864	1.20861	0.9185436	1.38083	1.0494308	1.11186	0.8450136
1.65	0.765	1.04257	0.79756605	1.21007	0.92570355	1.40334	1.0735551	1.10789	0.84753585
1.7	0.75	1.04677	0.7850775	1.2165	0.912375	1.418	1.0635	1.10716	0.83037
1.75	0.735	1.02304	0.7519344	1.18271	0.86929185	1.38289	1.01642415	1.08136	0.7947996
1.8	0.72	1.01696	0.7322112	1.15721	0.8331912	1.38005	0.993636	1.07036	0.7706592
1.85	0.71	1.01746	0.7223966	1.13019	0.8024349	1.37646	0.9772866	1.06414	0.7555394
1.9	0.7	1.02279	0.715953	1.12468	0.787182	1.37911	0.965377	1.06031	0.742217
1.95	0.69	1.02916	0.7101204	1.12168	0.7739592	1.39363	0.9616047	1.06856	0.7373064
2	0.68	1.02128	0.6944704	1.10863	0.7538684	1.41179	0.9600172	1.05872	0.7199296
2.1	0.664	1.01484	0.67385376	1.06785	0.7090524	1.27283	0.84515912	1.03803	0.68925192
2.2	0.648	1.0166	0.6587568	1.08062	0.70024176	1.2814	0.8303472	1.0513	0.6812424
2.3	0.632	1.02083	0.64516456	1.11457	0.70440824	1.32149	0.83518168	1.05669	0.66782808
2.4	0.616	1.00485	0.6189876	1.08917	0.67092872	1.32567	0.81661272	1.03225	0.635866
2.5	0.6	1.01241	0.607446	1.05809	0.634854	1.31894	0.791364	1.03468	0.620808
2.6	0.588	1.01856	0.59891328	1.09462	0.64363656	1.32864	0.78124032	1.04808	0.61627104
2.7	0.576	1.01886	0.58686336	1.06105	0.6111648	1.31559	0.75777984	1.04412	0.60141312
2.8	0.564	1.01489	0.57239796	1.0647	0.6004908	1.28917	0.72709188	1.04700	0.5905080
2.9	0.552	1.00013	0.55207176	1.04646	0.57764592	1.23389	0.68110728	1.02432	0.56542464
3	0.54	1.00008	0.5400432	1.02808	0.5551632	1.18461	0.6396894	1.01715	0.549261
3.1	0.532	1.00182	0.53296824	1.01685	0.5409642	1.16274	0.61857768	1.01289	0.53885748
3.2	0.524	1.00016	0.52408384	1.0162	0.5324888	1.11989	0.58682236	1.01186	0.53021464
3.3	0.516	1.00789	0.52007124	1.02846	0.53068536	1.09781	0.56646996	1.01606	0.52428696
3.4	0.508	1.00803	0.51207924	1.03138	0.52394104	1.10069	0.55915052	1.01972	0.51801776
3.5	0.5	1.01006	0.50503	1.03867	0.519335	1.11139	0.555695	1.02566	0.51283
3.6	0.496	1.01196	0.50193216	1.04781	0.51971376	1.13822	0.56455712	1.03142	0.51158432
3.7	0.492	1.01076	0.49729392	1.08048	0.53159616	1.1407	0.5612244	1.03256	0.50801952
3.8	0.488	1.00016	0.48807808	1.02471	0.50005848	1.11389	0.54357832	1.01086	0.49329968
3.9	0.484	1.00129	0.48462436	1.01889	0.49314276	1.08449	0.52489316	1.00622	0.48701048
4	0.48	1.01008	0.4848384	1.03424	0.4964352	1.08274	0.5197152	1.00891	0.4842768

GROUP 5		GROUP 6		GROUP 7		GROUP 8		GROUP 9	
S Amp	N Resp	S Amp	N Resp	S Amp	N Resp	S Amp	N Resp	S Amp	N Resp
1.05123	1.05123	0.78888	0.78888	0.67473	0.67473	0.90088	0.90088	0.38679	0.38679
0.56464	1.11126	0.53443	1.08888	0.48086	0.8018	0.48843	0.97088	0.28015	0.5603
0.58846	1.481126	0.48336	1.233375	0.46109	1.152726	0.48463	1.238386	0.18864	0.49136
0.60844	1.61692	0.51880	1.56679	0.48486	1.48486	0.53080	1.58279	0.25784	0.77382
0.61301	1.8481601	0.54097	1.6083197	0.48803	1.4880403	0.54376	1.6387776	0.20814	0.6174714
0.63471	1.90413	0.58234	1.68702	0.51011	1.53033	0.56384	1.68682	0.21346	0.64038
0.69862	2.0968827	0.58037	1.78226446	0.52364	1.8827689	0.64732	1.8022802	0.21588	0.64443168
0.63731	2.4868107	0.63084	1.8738816	0.54844	1.8868886	0.63886	1.8004438	0.21834	0.6484888
0.67128	2.66864608	0.62467	1.63866316	0.68686	1.6868407	0.64737	1.80880485	0.22464	0.6812708
0.69642	2.9098684	0.65389	2.0281886	0.72204	2.1088889	0.79174	2.3888800	0.28430	0.6888436
1.00169	2.8748603	0.68667	1.8682889	0.71739	2.0888883	0.7088	2.288816	0.21889	0.6310843
1.0036	2.630152	0.71642	2.0886444	0.72084	2.0810780	0.78842	2.2348844	0.2284	0.688848
1.03636	2.8210636	0.70814	1.6842316	0.75831	2.08886475	0.78813	2.18887886	0.24042	0.6861448
1.05073	2.8786089	0.74016	1.6469724	0.80487	2.1178711	0.82146	2.1688484	0.28842	0.7088448
1.09187	2.7517644	0.78129	1.8184606	0.82218	2.0744139	0.83884	2.1008306	0.30816	0.7780832
1.26419	3.034068	0.75389	1.808886	0.8881	2.13144	0.86749	2.087876	0.38882	0.884288
1.36608	3.136636	0.82415	1.886646	0.88047	2.278081	0.88171	2.211898	0.43363	0.887809
1.52636	3.36797	0.86187	1.868114	1.04072	2.308884	1.08886	2.28808	0.46873	1.018008
1.56574	3.3115401	0.80844	1.9213606	1.08113	2.20773886	1.08887	2.23828686	0.51881	1.09728316
1.61471	3.2778813	0.88814	1.8668342	1.1742	2.358889	1.1633	2.341169	0.58888	1.1807288
1.61609	3.58438686	1.04684	2.0448127	1.20618	2.5128289	1.27714	2.4888087	0.62084	1.2133812
1.74391	3.2788608	0.97534	1.8411882	1.16889	2.2842882	1.18882	2.2868486	0.56083	1.0818804
1.78634	3.2040821	0.86376	1.7480244	1.18816	2.1288884	1.19362	2.1882388	0.57882	1.0800136
1.82676	3.20033	0.87704	1.70862	1.17832	2.08361	1.21803	2.13339	0.58133	1.0348276
1.78643	3.052231	0.88873	1.843441	1.14782	1.948884	1.18407	2.088818	0.58489	0.883873
1.74686	2.881889	0.86476	1.881864	1.13789	1.8778836	1.18708	1.988862	0.68847	0.87887784
1.78671	2.88575245	1.01218	1.8143882	1.16889	1.8814786	1.28638	2.0882888	0.68626	1.0180886
1.8867	3.087976	1.19381	1.8381684	1.34888	2.0778884	1.43638	2.2103488	0.74382	1.1440888
1.88148	2.7642881	1.18826	1.78484125	1.28889	1.8878181	1.38883	2.08888786	0.74881	1.10752786
1.80821	2.6638603	1.19137	1.7038881	1.28883	1.8883189	1.34249	1.9187807	0.7571	1.082863
1.74813	2.41638006	1.17807	1.62886886	1.27084	1.7888879	1.33379	1.84728815	0.74638	1.0384788
1.67362	2.2428608	1.14752	1.6376786	1.22816	1.6881012	1.31783	1.788882	0.72809	0.9773638
1.82182	2.108106	1.13021	1.488273	1.21347	1.577511	1.30884	1.708402	0.72002	0.808006
1.64272	2.0886272	1.1502	1.448262	1.23213	1.5834638	1.33848	1.6838848	0.73101	0.8210728
1.67574	2.0811602	1.20126	1.4775488	1.28048	1.5887504	1.38883	1.7088788	0.77880	0.8880638
1.6841	2.03282	1.27676	1.532112	1.38443	1.637316	1.44882	1.738784	0.84717	1.018804
1.7017	1.8824606	1.33811	1.56006315	1.42343	1.65428886	1.4888	1.743838	0.81088	1.0812817
1.71378	1.8086714	1.40276	1.5661076	1.4783	1.688218	1.54884	1.7510832	0.87636	1.1088488
1.74662	1.921172	1.51276	1.684085	1.58884	1.714084	1.63407	1.787477	1.08739	1.188139
1.67467	1.7818869	1.60256	1.7147382	1.6304	1.747738	1.64382	1.7888734	1.18882	1.2721444
1.37662	1.4250087	1.51086	1.5637809	1.58748	1.61200815	1.46707	1.50808746	1.07147	1.10887146
1.36647	1.36647	1.48874	1.48874	1.55433	1.55433	1.41751	1.41751	1.04138	1.04138
1.40704	1.371864	1.52886	1.48160375	1.58686	1.58686375	1.48888	1.41888275	1.08143	1.03488425
1.44346	1.371287	1.67861	1.4886646	1.64688	1.5807288	1.50849	1.4283188	1.08708	1.042228
1.47662	1.385781	1.66884	1.532577	1.73848	1.60882385	1.57057	1.46277785	1.188	1.07115
1.46306	1.307746	1.74253	1.588877	1.68316	1.678882	1.68006	1.488884	1.23006	1.107342
1.30236	1.13866625	1.74804	1.526636	1.68882	1.6882176	1.61882	1.416808	1.2837	1.1318876
1.1888	1.01888	1.62001	1.3770086	1.78077	1.4888846	1.48788	1.2844615	1.28872	1.078712
1.26482	1.0418006	1.63864	1.3606182	1.78888	1.4851107	1.48082	1.2371316	1.28872	1.0784478
1.30884	1.0802414	1.68847	1.3878807	1.8458	1.484838	1.64418	1.2887888	1.34804	1.0819124
1.27377	1.01284715	1.64781	1.30884886	1.60083	1.43173886	1.50886	1.3001161	1.33806	1.0813727
1.26433	0.9861774	1.84214	1.2808882	1.78884	1.3884182	1.51164	1.1780012	1.348	1.08144
1.27189	0.97286686	1.88615	1.28886475	1.80883	1.37847086	1.53888	1.17087786	1.3783	1.0828886
1.27889	0.8882436	1.67257	1.2844276	1.88882	1.367115	1.58844	1.16883	1.40802	1.088015
1.24389	0.91425816	1.63849	1.20808816	1.78886	1.3188353	1.53079	1.11778086	1.38838	1.02781888
1.21644	0.8781169	1.69153	1.1678016	1.77484	1.2778848	1.50849	1.0817888	1.40088	1.0086782
1.18477	0.8482887	1.61609	1.1474239	1.77641	1.2812811	1.48882	1.0821082	1.41214	1.0088184
1.17767	0.824289	1.62274	1.135816	1.78744	1.281308	1.48887	1.048888	1.43488	1.004423
1.16738	0.8084822	1.64884	1.1381616	1.61482	1.2830878	1.50782	1.0808848	1.50306	1.0071282
1.14886	0.7811024	1.67482	1.1388778	1.63882	1.2808818	1.52287	1.0388418	1.68084	1.1283712
1.08089	0.71777736	1.42863	0.94861032	1.60786	1.0874788	1.31801	0.97088184	1.57884	1.04708816
1.10878	0.71813744	1.43538	0.83008144	1.6016	1.0878884	1.38888	0.88888884	1.52788	0.88813104
1.13449	0.71888786	1.48444	0.88818808	1.66831	1.08401882	1.38828	0.88108416	1.58881	0.88143812
1.11086	0.68428876	1.61461	0.83887856	1.64787	1.01814882	1.37384	0.84818884	1.60488	0.88880888
1.07623	0.647536	1.62388	0.812886	1.64303	0.998818	1.37201	0.832808	1.68088	0.888834
1.08007	0.63808116	1.66021	0.91152348	1.68376	0.97888886	1.3848	0.814088	1.78833	1.03388804
1.07322	0.61817472	1.66709	0.88268808	1.66317	0.98888888	1.38129	0.78888204	1.58144	1.0481444
1.07862	0.60848448	1.53457	0.88848748	1.684	0.816888	1.38884	0.77088416	1.8816	1.0443024
1.06861	0.58053812	1.44786	0.78827382	1.63847	0.84381144	1.31431	0.72848812	1.77151	0.97787382
1.04324	0.5653488	1.37787	0.7438418	1.4473	0.781542	1.28188	0.6812484	1.71442	0.8887888
1.03039	0.54818748	1.33853	0.71103386	1.38886	0.7441882	1.2232	0.6807424	1.68284	0.8008446
1.02445	0.5386118	1.28037	0.67815388	1.347	0.708488	1.18463	0.63088372	1.63718	0.88788788
1.02634	0.53082344	1.25886	0.6484314	1.28848	0.68867804	1.18802	0.58808432	1.58431	0.88713838
1.03162	0.52408286	1.24142	0.63084136	1.288	0.644144	1.14638	0.58180824	1.51789	0.77113882
1.03802	0.51801	1.24815	0.624675	1.28786	0.633876	1.15228	0.57814	1.58184	0.78082
1.04646	0.51865726	1.27218	0.6308864	1.28817	0.64388838	1.17114	0.58088544	1.68864	0.63807744
1.04827	0.51674884	1.28876	0.63848182	1.32862	0.68215884	1.16837	0.58487804	1.60788	0.68833438
1.02782	0.50182486	1.24821	0.60815048	1.28888	0.61880384	1.15228	0.58231284	1.7878	0.6773284
1.02175	0.494627	1.21471	0.58791884	1.23282	0.58888808	1.13381	0.54818324	1.77838	0.68823682
1.02866	0.483704	1.21574	0.5836662	1.22732	0.5881138	1.13383	0.5442884	1.77888	0.8828084